

December 2016

The Impact of Nanomaterial Functionalization and Core Chemical Composition on Toxicity to *Daphnia Magna*

Jared S. Bozich

University of Wisconsin-Milwaukee

Follow this and additional works at: <https://dc.uwm.edu/etd>

 Part of the [Environmental Sciences Commons](#)

Recommended Citation

Bozich, Jared S., "The Impact of Nanomaterial Functionalization and Core Chemical Composition on Toxicity to *Daphnia Magna*" (2016). *Theses and Dissertations*. 1354.
<https://dc.uwm.edu/etd/1354>

This Dissertation is brought to you for free and open access by UWM Digital Commons. It has been accepted for inclusion in Theses and Dissertations by an authorized administrator of UWM Digital Commons. For more information, please contact open-access@uwm.edu.

THE IMPACT OF NANOMATERIAL FUNCTIONALIZATION AND CORE CHEMICAL
COMPOSITION ON TOXICITY TO *DAPHNIA MAGNA*

by

Jared Bozich

A Dissertation Submitted in
Partial Fulfillment of the
Requirements for the Degree of

Doctor of Philosophy
in Freshwater Sciences

at

The University of Wisconsin-Milwaukee

December 2016

ABSTRACT
THE IMPACT OF NANOMATERIAL FUNCTIONALIZATION AND CORE CHEMICAL
COMPOSITION ON TOXICITY TO *DAPHNIA MAGNA*

by

Jared Bozich

The University of Wisconsin-Milwaukee, 2016
Under the Supervision of Professor Dr. Rebecca D. Klaper

Nanomaterials (NMs) are being developed for a variety of industrial, biomedical, and environmental applications. Initially these materials consisted of simple metal oxides or carbon based NMs. More recently NMs have become increasingly complex consisting of multiple transition metals and surfaces functionalized with polymers, surfactants and ligands that have the ability to alter their physiochemical properties and enhance performance. As manufactured NM production increases, so does the concern about their release into the environment and potentially harmful effects. The focus of toxicology has largely been on first generation materials and we have comparatively less information about the potential impacts of complex NMs. In order to create environmentally friendly nanotechnologies, the properties that govern NM toxicity need to be better elucidated. In addition, understanding mechanisms for toxicity and impacts to molecular and apical endpoints will greatly aid in the rapid assessment and design of current and future nanotechnologies. In this dissertation my central hypothesis is: altering the core chemical composition and surface functionalization impacts the toxicity of nanomaterials to *Daphnia magna*. To

determine whether to accept or refute this hypothesis I used the environmentally relevant model organism, *Daphnia magna*, and chemically tailored NMs. My results indicated that acute and chronic impacts to *Daphnia* upon exposure to functionalized gold NMs are strongly dependent on initial surface charge and the ligand used in the functionalization process; depending on the ligand, negative impacts are explained by the ligand choice, however with others the NM-ligand combination are required for a negative impact indicating a nanospecific effect. Positively charged gold NMs functionalized with polyallylamine hydrochloride are more toxic than negatively charged particles functionalized with citrate or mercaptopropionic acid, impacting daphnid reproduction and mortality at low part per billion concentrations. Gene expression results from *Daphnia* acutely and chronically exposed to these same materials show that each NM-ligand combination has a unique molecular fingerprint and that for most of the genes I explored the NM-ligand combination induces similar responses in the *Daphnia* as its respective ligand. Lastly, my studies demonstrate that altering the core chemical composition of complex NMs to decrease toxicity. In addition, this study indicated a nanospecific impact, as the dissolved metals found in solution could not reproduce the chronic endpoint impacts and daphnid gene expression response. Collectively, this work assisted in the development of fundamental knowledge for the factors that regulate NM toxicity and identified novel molecular pathways and responses triggered by specific alterations to complex NM surface and core properties.

© Copyright by Jared Bozich, 2016
All Rights Reserved

TABLE OF CONTENTS

List of Figures.....	vi
List of Tables.....	vii
List of Abbreviations.....	viii
Acknowledgements.....	ix
Chapter	
1 Introduction.....	1
2 Surface chemistry, charge and ligand type impact the toxicity of gold nanoparticles to <i>Daphnia magna</i>	22
3 Gene expression response of the Gram-negative bacterium <i>Shewanella oneidensis</i> and the water flea <i>Daphnia magna</i> exposed to functionalized gold nanoparticles.....	70
4 Core chemistry influences the toxicity of multi-component metal oxide nanomaterials, lithium nickel manganese cobalt oxide and lithium cobalt oxide to <i>Daphnia magna</i>	123
5 Discussion and conclusion.....	168
Curriculum Vitae.....	192

LIST OF FIGURES

Figure 2.1 Schematic representation of functionalized AuNPs used in the toxicology study.....	57
Figure 2.2 Agglomerated vs. aggregated AuNPs.....	58
Figure 2.3 Effects of AuNPs, free ligands and impurities on daphnid acute mortality..	59
Figure 2.4 Effects of AuNPs, free ligands and impurities on daphnid reproduction in chronic assays.....	60
Figure 2.5 Effects of AuNPs on daphnid body size after 21-day chronic exposure.....	61
Figure 2.6 Nanoparticles adhered to daphnid exoskeleton.....	62
Figure 3.1 Nanoparticle toxicity to <i>D. magna</i> and <i>S. oneidensis</i>	115
Figure 3.2 Gene expression heat map.....	116
Figure 3.3 Selected gene responses in <i>S. oneidensis</i> upon AuNP/ligand exposure..	117
Figure 3.4 <i>S. Oneidensis</i> 16s and sodB gene expression.....	118
Figure 3.5 Selected gene responses in <i>D. magna</i> upon AuNP/ligand exposure.....	119
Figure 4.1 ICPMS results for metal dissolution in daphnid media at 72 hours.....	152
Figure 4.2 Avg. chronic daphnid survival rate over 21 days compared to controls....	153
Figure 4.3 Avg. chronic daphnid reproduction over 21 days compared to controls...	154
Figure 4.4 Avg. chronic daphnid survival rate over 21 days compared to controls.....	155
Figure 4.5 Avg. chronic daphnid reproduction over 21 days compared to controls...	157
Figure 4.6 Fold change gene expression.....	159

LIST OF TABLES

Table 2.1 AuNP characterization as synthesized.....	55
Table 2.2 AuNP characterization in daphnid media.....	56
Table 2.3 AuNP ligand density determined by XPS.....	56
Table 3.1 Target genes, corresponding functions, and their primers for qPCR.....	113
Table 3.2 Nanoparticle characterization based on TEM analysis.....	114
Table 4.1 Genes explored, primer sequence information, gene description and accession number.....	151
Table 4.2 Nanomaterial characterization.....	151

LIST OF ABBREVIATIONS

AuNP Gold nanoparticle

Cit Citrate

CTAB Cetyltrimethylammonium bromide

DNA Deoxyribonucleic acid

ICPMS Inductively coupled plasma mass spectrometry

ICPOES Inductively couples plasma optical emission spectrometry

LCO Lithium cobalt oxide

MPA Mercaptopropionic acid

NM Nanomaterial

NMC Nickel manganese cobalt oxide

NP Nanoparticle

PAH Polyallylamine hydrochloride

PXRD Powder x-ray diffractometer

RNA Ribonucleic acid

ROS Reactive oxygen specie

SEM Scanning electron microscopy

TEM Transmission electron microscopy

UV Ultraviolet

XPS X-ray photon spectroscopy

ACKNOWLEDGEMENTS

There is no single person who has been more influential and important to me than my advisor, Dr. Rebecca Klaper. The first time I met Dr. Klaper was in a class she taught on environmental health. Her passion for science and the environment instantly showed. When I first started graduate school I had only a few strengths and many more weaknesses. Dr. Klaper helped me work on those weaknesses and turn them into strengths. Dr. Klaper is not only a great advisor and scientist but she is a great role model, person, and friend. Without her willingness to let me pursue what I wanted to pursue I don't know if I could say I would be in the place I am today. I am forever grateful to have her as an advisor.

I also owe a great deal to my research center, The Center for Sustainable Nanotechnology, founded by Dr. Robert Hamers and funded by the NSF. This center, and all of the brilliant people within, humbled me greatly. Each person within the center helped me grow as a scientist and person. I not only consider them my colleagues but also my friends. Without them I would not be the multi-disciplinary scientist I am today.

Lastly, I would like to thank my amazing lab and committee. My lab in particular helped me get through the tough times and always lent their expertise whenever I asked. My committee and their willingness to be flexible were greatly appreciated. They consistently provided me with great feedback and advised me through the most difficult time of my life. Thank you all.

CHAPTER 1: INTRODUCTION

Nanomaterials and Nanotechnology

Industry annually produces tens of thousands of tons of nanomaterials (NMs) to be incorporated in a variety of industrial applications such as water treatment⁴ and sustainable energy production² and commercial products such as cosmetics and medical therapeutics³. Nanomaterials are broadly defined as materials that have one or more dimensions on the order of 100 nanometers or less. Engineers are developing NMs to be enhanced and more complex by enriching them with a variety of surface ligands, surfactants, polymers and core materials that have the ability to alter their physiochemical properties such as surface charge, reactivity and energy storage capacity⁴. The nanotechnology industry as a whole has seen substantial growth with the NM market estimated at a value of US \$4.4 trillion by the year 2018⁵. Increased production has led to a growing concern for unintended environmental impacts as these materials are expected to reach the environment through intentional and unintentional disposal⁶. One study estimates that 63-91% of 260,000-309,000 metric tons of global nanomaterial production in 2010 ended up in landfills of which up to 7% entered the aquatic environment⁷. Concern for unintended impacts have been exacerbated by claims of NMs causing adverse outcomes in a wide range of cells and organisms⁸.

The Impact of Nanomaterial Surface and Core Modification on Toxicity

Initial studies of NM induced *in vivo* impacts have been largely focused on NMs such as carbon nanomaterials⁹⁻¹¹, silver nanoparticles¹²⁻¹⁴, silica¹⁵⁻¹⁷ and single

component metal oxides¹⁸⁻²⁰ with the majority having been investigated in acute exposures. These NMs are mainly chosen due to their commercial use, availability and relative simplicity. However, the applications that rely on NMs that have complex core structures and surface functionalities are growing. Little emphasis has been given to studying the long-term *in vivo* impacts linked to specific properties of complex multicomponent and surface functionalized NMs. Understanding the impact of modifying specific core and surface properties (e.g. core chemistry, ligand composition, charge, charge density, hydrophobicity, etc.) and the combination of these properties on toxicity is vital to the sustainable production of these complex NMs²¹.

Literature indicates that NM surface functionalization plays an important role in nanomaterial-biological interactions, bioavailability and biocompatibility²². It is well known that NM surface coatings increase commercial and industrial applications. However, it is these altered surfaces that interact with endogenous molecules, cell organelles, cells, tissues and whole organisms. Nanomaterial surface charge and degree of hydrophobicity can increase NM-protein interactions and reduce NM dissolution and toxicity²³⁻²⁵. It has been established that NM surface charge dictates cellular uptake, subcellular localization and cytotoxicity^{26, 27}. For example, positively charged particles have a high affinity towards the negative charged phospholipid bilayer and exhibit greater cellular uptake and cytotoxicity than negative or neutral charged particles in various cell lines^{27, 28}. The charge dependent subcellular localization also influences their toxicity profile²⁷. While the majority of studies that highlight charge as a factor for NM toxicity are *in vitro* studies, whole organism studies

have also showed deleterious effects dependent upon initial surface charge, with positively charged particles showing greater uptake and toxicity in a variety of aquatic and soil dwelling invertebrates and fish^{29, 30}. Some of the effects include decreased body size, lifespan and increased developmental abnormalities^{31, 32}. In rare cases, negatively charged particles have been show to be more cytotoxic than positively charged particles^{33, 34}. This effect is thought to be specific to cell type and role. For example, phagocytic cells may have a higher affinity towards negatively charged particles as they mimic the negatively charged surfaces of bacteria²⁶. Furthermore, differences can be seen even among NMs with the same charge^{35, 36}. This indicates that toxicity is not only solely dependent on the charge of the NM but also the functional group in question and suggests that potential structure-activity relationships of the NM bound chemical may be equally important in determining NM toxicity though the toxicity of ligand itself is often not examined.

Significant differences in NM toxicity have been attributed to the chemical composition of the core material therefore the core material is expected to be an important predictor of NM toxicity. For example, many studies have compared the toxicity of various similar sized single component metal oxide NMs such as ZnO, FeO, and CuO³⁷⁻³⁹. These materials show various levels of toxicity that can only be attributed to their differences in core chemical composition. Most often, the toxicity of the free metal ion predicts the toxicity of the metal oxide NM, where toxic metal ions produce NMs with greater toxicity³⁸. In addition, metal oxide NMs elicit effects equal to that of the effects from the metals dissolved in suspension indicating that there is no nanospecific effect^{37, 40, 41}. Mortality has been observed in cells, bacteria and whole

organisms at low concentrations for NMs containing toxic metals and high concentrations for NMs containing benign metals. Surface coatings on metallic NMs reduces their dissolution and therefore toxic effects²³. Less commonly reported is the toxicity of bimetallic and multicomponent core/shell particles (e.g. Au-Ag and CdSe/ZnS core/shell NMs). These materials are more complex and contain multiple metals in their core structures but at different ratios. While these materials are more complex, studies have begun to show that core chemical substitution or mixing toxic metals with less toxic metals at different ratios has been proven to effectively reduce NM toxicity^{42, 43}. For example CdSe/ZnS was replaced with InP/ZnS, which has comparable chemical and morphological properties. It was concluded that, the substitution of CdSe with InP as the core material significantly reduced toxicity⁴³.

Crystalline phase of the core of a NM can also have an impact on toxicity. Silver nanoparticle toxicity is influenced by crystal defects, which make the surfaces more reactive and may explain studies that cannot contribute observed toxicity solely to ion shedding⁴⁴. The toxicity of TiO₂ for example is dependent on its crystal structure with anatase being more toxic than rutile⁴⁵. Anatase has been shown to be more photoreactive with ultraviolet (UV) radiation and in the presence of water, produces free radicals that lead to toxic effects in aquatic organisms⁴⁶. Other studies suggest that without UV radiation present in the exposure crystalline phase may not be as important as properties such as charge and shape which cause greater uptake and particle-organism interactions⁴⁷.

In order to fully understand the importance of surface functionalization and core modification to NM toxicity more studies are needed that incorporate multiple surface

chemistries and core chemistries within a given study. Identifying trends in properties that make NMs harmful has been difficult as the use of a wide range of organisms, experimental conditions and NM synthesis and delivery techniques in experiments lead to contradictory results⁴⁸. Since most of the work has been scattered with few studies comparing multiple functionalized NMs let alone multiple NMs with complex core materials, more studies are needed that assess the specific alterations to surface and core chemistry of technologically relevant complex NMs with comparable physical and chemical properties. In addition, more studies are needed that address the impact of surface and core modifications in long-term *in vivo* exposures, as they are the more environmentally realistic scenarios. While studies have critically improved our baseline understanding of which starting materials might be inherently toxic and what general NM properties are of concern, it remains unclear as to what combination of NM properties may be used to predict toxicity^{21, 49}. Nevertheless, addressing these needs will enable us to better understand how we might avoid unwanted impacts from the production of future NMs.

Mechanisms for Toxicity and Cellular and Organism Molecular Response to Nanomaterial Exposures

The current and future assessment of NM toxicity may benefit from a molecular level understanding of toxicity linked to individual and population level impacts⁵⁰. Historically, environmental monitoring and chemical screening programs for several classes of chemicals such as estrogenic mimicking compounds and legacy contaminants have benefited from an understanding toxicity at the molecular level^{51, 52}.

Molecular biomarkers have enhanced these programs as they provide an early indication of organism exposure and a way to determine potential impacts prior to their occurrence. In addition, molecular biomarkers provide a way to examine mechanisms of impact^{51, 21, 50, 52}. Defining the ability of a NM to react with various biological receptors (e.g. proteins, enzymes, and DNA) and trigger molecular pathways will provide opportunities to develop biomarkers for high-throughput screening assays that inform the NM design process⁵¹. However, the molecular and mechanistic information describing NM perturbations to cells and organisms is still in its infancy³. A unique mechanism for toxicity that would unite all NMs has yet to be discovered, rather several mechanisms have been proposed dependent upon the NM physiochemical properties^{3, 48, 49, 53}. The NMs explored in this scope do not represent the actual complexity of future NMs.

The primary mechanism for NM toxicity is believed to be directly or indirectly related to oxidative stress⁵³⁻⁵⁷. Oxidative stress from NMs may be manifested in several ways³. For example, UV activation of electron hole pairs in the crystal structure of photoactive chemicals produces reactive oxygen species (ROS) that are then able to damage cells and organisms⁴⁶. NMs containing redox active materials undergo redox cycling and continually produce ROS. Unsatisfied electron donor/acceptor chemical groups from crystal defects can create free radicals inside the cell³. Redox inactive groups can inactivate biological antioxidants leading to the accumulation of free radicals⁵⁸. When the generated ROS overwhelms the cellular mechanisms for coping, oxidative damage occurs. One consequence of the generation of ROS may be lipid peroxidation, which results in even greater production of free radical species that

have the potential to damage proteins and DNA^{57, 58}. However, NM exposures that have demonstrated oxidative stress have largely been high concentration exposures over acute periods of time^{50, 59}. In addition, oxidative stress is a natural response to aging⁶⁰ and is a natural product of exposure to chemical stressors and xenobiotic metabolism which makes this a nonspecific response. While oxidative stress might be a good indicator of exposure to stressors, such as heavy metals⁵⁸, it is often a poor indicator for environmentally relevant health effects. Several studies have documented other potential mechanisms for NM toxicity⁵⁰ such as endocrine disruption⁶¹, metabolic impairment⁶² and pH induced lysosomal swelling⁶³. Understanding which properties impact pathways involved in reproduction, for example, would help predict potential population and ecosystem level impacts of functionalized NMs. More studies are needed that explore mechanisms and modes of action other than oxidative stress. Identifying sensitive pathways will greatly improve our ability to predict early impacts of NMs at low-level, chronic exposures⁶⁴.

Gene expression studies have demonstrated that organisms respond uniquely to different NM-ligand combinations and core compositions and have the potential to identify nanospecific impacts⁶⁵. For instance, Griffitt et al. (2009) assessed the global transcriptional responses of zebrafish gills upon exposure to sub-lethal concentrations of CuO, Ag and TiO₂. They determined that each particle type and their respective soluble metal had a distinct molecular fingerprint or transcriptional pattern with many more genes down regulated than up regulated⁶⁶. Other studies demonstrate nanospecific impacts to organisms by comparing the organism's gene expression response after exposure to NM-ligand combinations and their respective unbound

ligands⁶⁷. When organisms are exposed to different functionalized NMs with similar cores, comparing their gene expression patterns show that genes may be triggered to a greater extent when an organism is exposed to one NM type versus another⁶⁸. For example, positively charged quantum dots induced the up regulation of genes associated with metal contamination more so than neutral or negatively charged quantum dots⁶⁹. Examining molecular pathways triggered when organisms are exposed to NMs containing specific properties and their respective metal ions or free ligands may make it possible to identify novel NM specific effects. This may offer insight for uncovering new mechanisms for NM toxicity.

Studies have covered many different cell lines and organisms, time points and exposures and a wide range of doses which further complicates our understanding of the molecular response²¹. The molecular level response of an organism may strongly depend on the concentration of the chemical. In toxicology studies of NMs, cells or organisms are often exposed to high concentrations of NMs that may trigger pathways involved in cellular apoptosis and oxidative stress attenuation where if they were exposed at lower concentrations they may reveal an entirely different response⁵⁰. For example, organisms exhibit biphasic dose responses where low concentrations may be stimulatory and high concentrations may be inhibitory^{70, 71}. Long-term stimulation at low concentrations of chemicals may be simply due to a beneficial aspect of that chemical at low concentrations, such as increased metabolism⁷². However, it also may be a maladaptive approach that eventually may cause negative impacts to organism health. Therefore it is important that we examine molecular perturbations when organisms are exposed at low concentrations, which is the more environmentally

realistic scenario. Time dependent molecular responses upon organism exposure to NMs have also been observed⁵⁰. ROS for example, are short lived, are important in cell signaling in organisms and organisms defense mechanisms rapidly respond to oxidative stress. Therefore, depending on duration of the exposure, this effect may be captured or not⁷³. The majority of molecular level research has been largely focused on *in vitro* studies, which do not represent the complexities associated with whole organisms. Although they enable mechanistic studies, they often do not provide clear extrapolation of effects to whole organisms. Therefore, when considering the environmental impacts of NMs, assessing the changes in molecular pathways most relevant to the environment using environmental model organisms in long-term low dose exposures is critical. This will better enable the development of high-throughput molecular approaches and inform models to assess NM toxicity and design.

Difficulties in Nanomaterial Hazard Assessment

Nanomaterial physiochemical properties and toxicity may be regulated by environmental factors in experiments and the chemical composition of the media, which may explain the wide variation that exists in organism response across laboratory experiments⁵³. The toxicity of certain classes of chemicals such as dissolved metals and polymers may be influenced by factors such as water hardness and presence of natural organic matter^{74, 75}. Experimental media in standard toxicity tests with NMs may vary greatly across labs, with different water hardness levels, ionic strength, and varying amounts and sources of natural organic matter or proteins. Nanomaterials may aggregate and fall out of suspension or stay stable depending on

the chemical characteristics of the media⁷⁶. Nanomaterial surfaces may form protective coronas and their effective surface charge or chemistry and subsequent biological impacts may flip as they adsorb organic molecules⁷⁶⁻⁷⁸. In addition NMs may undergo dissolution with a change in pH or ionic strength making it difficult to determine whether the observed effects in cells or organisms are nanospecific. While out of the scope of this project, understanding the impact these variables will have on NM toxicity in standard toxicity experiments will increase the transparency of the hazard assessment being performed and identify causes for variation when comparing results from one lab to another⁸.

Conclusions about which NM properties are important for toxicity also has been complicated by the presence of experimental artifacts, confounding factors (e.g. synthesis impurities, byproducts, free ligand contamination, etc.) and inadequate NM characterization^{79, 80}. Nanomaterials may contain impurities, reagents and byproducts from synthesis and dispersion that interfere with biological assays or result in misinterpretations of toxicity⁸¹. Previous examples of this may be found in the early studies of fullerenes and the use of the chemical dispersant tetrahydrofuran (THF). Fullerenes dispersed with THF were originally seen as a chemical of toxicological concern capable of negatively effecting fish at low concentrations⁸¹. When THF was identified as a potential artifact the studies were corrected. Fullerenes were then mixed with water and tested and the observed effects were minimal⁸². Inadequate NM characterization can also lead to both misinterpretations and increased experimental uncertainty, as less information is known about the physical and chemical properties of the NM being tested^{79, 81}. Therefore, controlling for experimental artifacts and using

well characterized NMs will increase the robustness of the data generated and enables us to make sound conclusions regarding what properties are most important for NM toxicity^{79, 81}.

Project Scope

The central hypothesis of this dissertation was: nanomaterial core chemistry and surface functionalization impact the toxicity of nanomaterials to *Daphnia magna*.

Three sub hypotheses were developed to better define the central hypothesis.

These hypotheses were:

- 1) Positively charged AuNPs and ligands cause greater impacts to daphnid survival and reproduction.
- 2) Daphnids exposed to positively charged particles will express a greater molecular response at lower concentrations than daphnids exposed to negatively charged particles.
- 3) Replacing known toxic metals in multicomponent metal NMs with less toxic counterparts will reduce their impacts to molecular and apical endpoints.

In order to appropriately address these hypotheses I performed three studies using a suite of NMs and *Daphnia magna* as a model organism in acute and/or chronic exposures. The first of the three experiments explored the acute and chronic apical endpoint impacts of two positively and two negatively charged AuNPs to *Daphnia* (Hypothesis 1). The second experiment builds off of the first experiment in that it explored the gene expression response of *Daphnia* upon acute and chronic exposure to these same functionalized AuNPs (Hypothesis 2). The third experiment explored

how alterations in the core chemistry of two lithium based NMs of technological importance impact acute and chronic toxicity and the gene expression response in *Daphnia* (Hypothesis 3).

Daphnia magna are chosen as a model as they are abundant freshwater invertebrates that are key organisms to the proliferation of higher and lower trophic levels and form the base of aquatic food webs⁸³. *Daphnia* have also been designated by the U.S. EPA and OECD as a model organism and are widely used for assessing the toxicity of environmental contaminants. *Daphnia* are sensitive to xenobiotic stressors⁸⁴ and environmental changes⁸⁵ and experience reduced reproduction, growth and increased mortality with exposure to toxic substances or substandard food items⁸⁶⁻⁸⁸. Studies have demonstrated their ability to accumulate and respond to NMs and some suggest that these materials may be further incorporated in *Daphnia* tissues⁸⁹⁻⁹¹. In addition, *Daphnia* spp. has emerged as a model for toxicological genomics since they have the ability to perform clonal reproduction and maintain a static genotype that minimizes genetic drift that would otherwise interfere with toxicological studies⁹². This allows *Daphnia* to be used as a model to assess the gene expression level impacts of NMs. Collectively, these traits make *Daphnia* an ideal model organism to be used to assess the environmental impact of engineered NMs.

The first part of this dissertation seeks to better understand how variations in NM surface properties and functionalization impact *Daphnia magna* acute and chronic apical endpoints. Specifically, I examined daphnid survival in acute 48-hour static exposures and chronic 21-day semi-static renewal exposures. Chronic studies examined impacts to daphnid reproduction, survival and body size. NMs I tested in this

study were two positively charged AuNPs functionalized with a cationic polymer, polyallylamine hydrochloride (PAH-AuNP), and with a cationic surfactant, cetyltrimethylammonium bromide (CTAB-AuNP), and two negatively charged AuNPs functionalized with an anionic molecule, citrate (Cit-AuNP) and an anionic ligand, mercaptopropionic acid (MPA-AuNP). In addition, I tested their respective agents used in the functionalization process or what I herein will refer to as “free ligands” (i.e. free PAH, CTAB, Cit and MPA) and their respective AuNP supernatants to determine if toxicity is attributed to the ligand itself or the byproducts in solution from the synthesis process. Lastly, I explored AuNP aggregation using transmission electron microscopy (TEM) and their uptake, ingestion and adherence in daphnids using inductively coupled plasma mass spectrometry (ICPMS). It was anticipated that positively charged AuNPs would be more toxic and accumulate/adhere in daphnids to a greater extent than negatively charged AuNPs as positively charged substances have a higher affinity towards negatively charged components of biological systems. This research improved our understanding of how variations in NM charge and ligand composition influence individual and population relevant endpoints and biological uptake in an environmentally relevant organism.

The second part of this dissertation expanded on part one as it attempted to better understand how changes in AuNP surface properties impact molecular pathways important in cellular processes and population level impacts in daphnids. This part explored changes in gene expression levels of oxidative stress, reproduction, cell maintenance and xenobiotic metabolism related genes upon acute chronic exposure to PAH-AuNPs and MPA-AuNPs and their respective free ligands used in

part one. I expected that the molecular fingerprint for these two particle types would vary greatly due to their inherently different surface properties and surface chemical composition. I hypothesized that daphnids would respond similarly to the NM and their respective ligands revealing overlap in their gene expression response. The knowledge obtained from this study will help us better understand important linkages along the adverse outcome pathway for NM apical endpoint toxicity. In addition, this study will help identify novel molecular level indicators for exposure and health effects of functionalized NMs that are conserved across multiple organisms. This work addresses critical knowledge gaps in the nanotoxicological field.

The last part of this dissertation examined how subtle alterations in the core chemical composition of multicomponent metal oxide NMs elicit impacts to molecular and apical endpoints in *Daphnia*. For this study, two lithium intercalation cathode materials, lithium cobalt oxide (LCO) and lithium nickel manganese cobalt oxide (NMC), used in energy storage devices were assessed in *daphnia* acute and chronic exposures. To determine if there is a nanospecific impact or if the impact is due solely to dissolved metals in solution I assessed the acute and chronic impacts of their respective free metal ions and NM supernatants. For NMC, a body burden experiment was performed to differentiate the amount of NMs adhered to the daphnid carapace compared to the amount ingested/internalized. In addition, I determined the gene expression response of a suite of genes involved in metal detoxification, oxidative stress and cellular maintenance. I hypothesized that, based on the literature; LCO will be more toxic than NMC because it contains significantly more cobalt, which is found to be toxic to daphnids at low concentrations compared to the other metals present in

these materials. I also hypothesized that genes involved in oxidative stress and metal toxicity attenuation will be significantly up regulated upon daphnid exposure to the battery materials. This study will add fundamental knowledge as to how core chemistry alterations change the toxicity of complex multicomponent metal oxide. This study intended to identify potential environmental impacts of these materials, mechanisms for their impacts and whether they can or cannot be mitigated. It is anticipated that study will greatly inform the battery industry, as toxicity is not currently a part of the battery design process and little information exists on these novel materials.

Previous groups have indicated the need to develop a molecular understanding for long-term NM impacts to living organisms linked to their inherent core and surface properties and the need to rectify known nanotoxicology experimental issues^{21, 50, 79, 80}. The proposed work in this dissertation is innovative in that this work addresses known nanotoxicological experimental design problems, responds to the need for more molecular based information from long-term low dose exposures and describes the impacts of specific alterations of NM properties of technologically relevant materials. Specifically, this work provides information to begin to identify: 1.) Trends across different NM core types and surface properties, that cause NMs to have the greatest environmental impact; and 2) Molecular pathways triggered upon NM exposure which are indicative of NM exposure and pathways that are important links in environmentally relevant adverse outcome pathways for NM toxicity. While the studies performed herein will not be definitive and represent all NM types and environmental situations, these studies in addition to others will add to our fundamental knowledge base to help answer critical questions regarding NM toxicity. Therefore, this project is

expected to help advance our understanding of pathways for adverse outcomes underlying toxicity and describe the potential environmental implications of specific alterations of NM core and surface chemistries.

REFERENCES:

1. N. Savage and M. S. Diallo, *J Nanopart Res*, 2005, **7**, 331-342.
2. M. Pumera, *Energy & Environmental Science*, 2011, **4**, 668-674.
3. A. Nel, T. Xia, L. Mädler and N. Li, *science*, 2006, **311**, 622-627.
4. W. Stark, P. Stoessel, W. Wohlleben and A. Hafner, *Chemical Society Reviews*, 2015, **44**, 5793-5805.
5. H. Flynn, *Lux research*, 2014.
6. B. Nowack, J. F. Ranville, S. Diamond, J. A. Gallego - Urrea, C. Metcalfe, J. Rose, N. Horne, A. A. Koelmans and S. J. Klaine, *Environmental Toxicology and Chemistry*, 2012, **31**, 50-59.
7. A. Keller, S. McFerran, A. Lazareva and S. Suh, *J Nanopart Res*, 2013, **15**, 1-17.
8. S. J. Klaine, P. J. Alvarez, G. E. Batley, T. F. Fernandes, R. D. Handy, D. Y. Lyon, S. Mahendra, M. J. McLaughlin and J. R. Lead, *Environmental Toxicology and Chemistry*, 2008, **27**, 1825-1851.
9. E. Oberdörster, S. Zhu, T. M. Blickey, P. McClellan-Green and M. L. Haasch, *Carbon*, 2006, **44**, 1112-1120.
10. C. J. Smith, B. J. Shaw and R. D. Handy, *Aquatic toxicology*, 2007, **82**, 94-109.
11. M. S. Hull, A. J. Kennedy, J. A. Steevens, A. J. Bednar, J. Weiss, Charles A and P. J. Vikesland, *Environmental science & technology*, 2009, **43**, 4169-4174.
12. E. Navarro, F. Piccapietra, B. Wagner, F. Marconi, R. Kaegi, N. Odzak, L. Sigg and R. Behra, *Environmental Science & Technology*, 2008, **42**, 8959-8964.
13. F. Seitz, R. R. Rosenfeldt, K. Storm, G. Metreveli, G. E. Schaumann, R. Schulz and M. Bundschuh, *Ecotoxicology and environmental safety*, 2015, **111**, 263-270.
14. D. L. Starnes, J. M. Unrine, C. P. Starnes, B. E. Collin, E. K. Oostveen, R. Ma, G. V. Lowry, P. M. Bertsch and O. V. Tsyusko, *Environmental Pollution*, 2015, **196**, 239-246.
15. K. Fent, C. J. Weisbrod, A. Wirth-Heller and U. Pieleas, *Aquatic toxicology*, 2010, **100**, 218-228.
16. K. Fujiwara, H. Suematsu, E. Kiyomiya, M. Aoki, M. Sato and N. Moritoki, *Journal of Environmental Science and Health, Part A*, 2008, **43**, 1167-1173.
17. S.-W. Lee, S.-M. Kim and J. Choi, *Environmental Toxicology and Pharmacology*, 2009, **28**, 86-91.
18. H. Ma, A. Brennan and S. A. Diamond, *Environmental Toxicology and Chemistry*, 2012, **31**, 2099-2107.
19. A. García, R. Espinosa, L. Delgado, E. Casals, E. González, V. Puentes, C. Barata, X. Font and A. Sánchez, *Desalination*, 2011, **269**, 136-141.
20. X. Zhu, S. Tian and Z. Cai, *PLoS One*, 2012, **7**, e46286.
21. C. J. Murphy, A. M. Vartanian, F. M. Geiger, R. J. Hamers, J. Pedersen, Q. Cui, C. L. Haynes, E. E. Carlson, R. Hernandez and R. D. Klaper, *ACS central science*, 2015, **1**, 117-123.
22. A. Verma and F. Stellacci, *Small*, 2010, **6**, 12-21.
23. K. M. Newton, H. L. Puppala, C. L. Kitchens, V. L. Colvin and S. J. Klaine, *Environmental Toxicology and Chemistry*, 2013, **32**, 2356-2364.

24. A. Gessner, R. Waicz, A. Lieske, B.-R. Paulke, K. Mäder and R. Müller, *International journal of pharmaceutics*, 2000, **196**, 245-249.
25. M. S. Ehrenberg, A. E. Friedman, J. N. Finkelstein, G. Oberdörster and J. L. McGrath, *Biomaterials*, 2009, **30**, 603-610.
26. E. Fröhlich, *Int J Nanomedicine*, 2012, **7**, 5577-5591.
27. A. Asati, S. Santra, C. Kaittanis and J. M. Perez, *ACS nano*, 2010, **4**, 5321-5331.
28. Y. Qiu, Y. Liu, L. Wang, L. Xu, R. Bai, Y. Ji, X. Wu, Y. Zhao, Y. Li and C. Chen, *Biomaterials*, 2010, **31**, 7606-7619.
29. B. Collin, E. Oostveen, O. V. Tsyusko and J. M. Unrine, *Environmental science & technology*, 2014, **48**, 1280-1289.
30. L. M. Skjolding, M. Winther-Nielsen and A. Baun, *Aquatic Toxicology*, 2014, **157**, 101-108.
31. S.-K. Jung, X. Qu, B. Aleman-Meza, T. Wang, C. Riepe, Z. Liu, Q. Li and W. Zhong, *Environmental Science & Technology*, 2015.
32. R. Vankayala, P. Kalluru, H.-H. Tsai, C.-S. Chiang and K. C. Hwang, *Journal of Materials Chemistry B*, 2014, **2**, 1038-1047.
33. Y. Tomita, A. Rikimaru-Kaneko, K. Hashiguchi and S. Shirotake, *Immunopharmacology and immunotoxicology*, 2011.
34. A. Petushkov, J. Intra, J. B. Graham, S. C. Larsen and A. K. Salem, *Chemical research in toxicology*, 2009, **22**, 1359-1368.
35. R. Klaper, J. Crago, J. Barr, D. Arndt, K. Setyowati and J. Chen, *Environmental Pollution*, 2009, **157**, 1152-1156.
36. Z.-J. Zhu, P. S. Ghosh, O. R. Miranda, R. W. Vachet and V. M. Rotello, *Journal of the American Chemical Society*, 2008, **130**, 14139-14143.
37. M. Heinlaan, A. Ivask, I. Blinova, H.-C. Dubourguier and A. Kahru, *Chemosphere*, 2008, **71**, 1308-1316.
38. R. J. Griffitt, J. Luo, J. Gao, J. C. Bonzongo and D. S. Barber, *Environmental Toxicology and Chemistry*, 2008, **27**, 1972-1978.
39. D. R. Hristozov, S. Gottardo, A. Critto and A. Marcomini, *Nanotoxicology*, 2012, **6**, 880-898.
40. M. Horie, K. Fujita, H. Kato, S. Endoh, K. Nishio, L. K. Komaba, A. Nakamura, A. Miyauchi, S. Kinugasa and Y. Hagihara, *Metallomics*, 2012, **4**, 350-360.
41. N. M. Franklin, N. J. Rogers, S. C. Apte, G. E. Batley, G. E. Gadd and P. S. Casey, *Environmental Science & Technology*, 2007, **41**, 8484-8490.
42. T. Li, B. Albee, M. Alemayehu, R. Diaz, L. Ingham, S. Kamal, M. Rodriguez and S. W. Bishnoi, *Analytical and bioanalytical chemistry*, 2010, **398**, 689-700.
43. V. Brunetti, H. Chibli, R. Fiammengo, A. Galeone, M. A. Malvindi, G. Vecchio, R. Cingolani, J. L. Nadeau and P. P. Pompa, *Nanoscale*, 2013, **5**, 307-317.
44. S. George, S. Lin, Z. Ji, C. R. Thomas, L. Li, M. Mecklenburg, H. Meng, X. Wang, H. Zhang and T. Xia, *Acs Nano*, 2012, **6**, 3745-3759.
45. C. Jin, Y. Tang, F. G. Yang, X. L. Li, S. Xu, X. Y. Fan, Y. Y. Huang and Y. J. Yang, *Biological trace element research*, 2011, **141**, 3-15.
46. P.-C. Maness, S. Smolinski, D. M. Blake, Z. Huang, E. J. Wolfrum and W. A. Jacoby, *Applied and environmental microbiology*, 1999, **65**, 4094-4098.

47. A. Simon-Deckers, S. Loo, M. Mayne-L'hermite, N. Herlin-Boime, N. Menguy, C. Reynaud, B. Gouget and M. Carrière, *Environmental science & technology*, 2009, **43**, 8423-8429.
48. A. B. Djurišić, Y. H. Leung, A. Ng, X. Y. Xu, P. K. Lee and N. Degger, *Small*, 2015, **11**, 26-44.
49. M. R. Wiesner, G. V. Lowry, K. L. Jones, J. Hochella, Michael F, R. T. Di Giulio, E. Casman and E. S. Bernhardt, *Environmental Science & Technology*, 2009, **43**, 6458-6462.
50. R. Klaper, D. Arndt, J. Bozich and G. Dominguez, *Analyst*, 2014, **139**, 882-895.
51. G. T. Ankley, R. S. Bennett, R. J. Erickson, D. J. Hoff, M. W. Hornung, R. D. Johnson, D. R. Mount, J. W. Nichols, C. L. Russom and P. K. Schmieder, *Environmental Toxicology and Chemistry*, 2010, **29**, 730-741.
52. J. Ryan and L. Hightower, in *Stress-Inducible Cellular Responses*, Springer, Editon edn., 1996, pp. 411-424.
53. A. E. Nel, L. Mädler, D. Velegol, T. Xia, E. M. Hoek, P. Somasundaran, F. Klaessig, V. Castranova and M. Thompson, *Nature materials*, 2009, **8**, 543-557.
54. A. Manke, L. Wang and Y. Rojanasakul, *BioMed research international*, 2013, **2013**.
55. A. A. Shvedova, A. Pietroiusti, B. Fadeel and V. E. Kagan, *Toxicology and applied pharmacology*, 2012, **261**, 121-133.
56. E.-J. Park and K. Park, *Toxicology Letters*, 2009, **184**, 18-25.
57. P. P. Fu, Q. Xia, H.-M. Hwang, P. C. Ray and H. Yu, *Journal of food and drug analysis*, 2014, **22**, 64-75.
58. N. Ercal, H. Gurer-Orhan and N. Aykin-Burns, *Current topics in medicinal chemistry*, 2001, **1**, 529-539.
59. J. Wang, M. F. Rahman, H. M. Duhart, G. D. Newport, T. A. Patterson, R. C. Murdock, S. M. Hussain, J. J. Schlager and S. F. Ali, *Neurotoxicity*, 2009, **30**, 926-933
60. T. Finkel and N. J. Holbrook, *Nature*, 2000, **408**, 239-247.
61. I. Iavicoli, L. Fontana, V. Leso and A. Bergamaschi, *International journal of molecular sciences*, 2013, **14**, 16732-16801.
62. S. Sharifi, S. Daghighi, M. Motazacker, B. Badlou, B. Sanjabi, A. Akbarkhanzadeh, A. Rowshani, S. Laurent, M. Peppelenbosch and F. Rezaee, *Scientific reports*, 2013, **3**.
63. S. T. Stern, P. P. Adisheshaiah and R. M. Crist, *Part Fibre Toxicol*, 2012, **9**, 1.
64. F. Gottschalk, T. Sonderer, R. W. Scholz and B. Nowack, *Environmental science & technology*, 2009, **43**, 9216-9222.
65. J.-Y. Roh, Y.-K. Park, K. Park and J. Choi, *Environmental toxicology and pharmacology*, 2010, **29**, 167-172.
66. R. J. Griffitt, K. Hyndman, N. D. Denslow and D. S. Barber, *Toxicological Sciences*, 2009, **107**, 404-415.
67. G. A. Dominguez, S. E. Lohse, M. D. Torelli, C. J. Murphy, R. J. Hamers, G. Orr and R. D. Klaper, *Aquat Toxicol*, 2015, **162**, 1-9.
68. H. C. Poynton, J. M. Lazorchak, C. A. Impellitteri, B. J. Blalock, K. Rogers, H. J. Allen, A. Loguinov, J. L. Heckman and S. Govindasmawy, *Environmental science & technology*, 2012, **46**, 6288-6296.
69. Y. Yang, J. Wang, H. Zhu, V. L. Colvin and P. J. Alvarez, *Environmental science & technology*, 2012, **46**, 3433-3441.

70. E. J. Calabrese and L. A. Baldwin, *Annual review of pharmacology and toxicology*, 2003, **43**, 175-197.
71. E. J. Calabrese, L. A. Baldwin and C. D. Holland, *Risk Analysis*, 1999, **19**, 261-281.
72. J. K. Stanley, E. J. Perkins, T. Habib, J. G. Sims, P. Chappell, B. L. Escalon, M. Wilbanks and N. Garcia-Reyero, *Environmental science & technology*, 2013, **47**, 9424-9433.
73. M. Husain, A. T. Saber, C. Guo, N. R. Jacobsen, K. A. Jensen, C. L. Yauk, A. Williams, U. Vogel, H. Wallin and S. Halappanavar, *Toxicology and applied pharmacology*, 2013, **269**, 250-262.
74. M. S. Goodrich, L. H. Dulak, M. A. Friedman and J. J. Lech, *Environmental toxicology and chemistry*, 1991, **10**, 509-515.
75. G. K. Pagenkopf, *Environmental Science & Technology*, 1983, **17**, 342-347.
76. D. P. Stankus, S. E. Lohse, J. E. Hutchison and J. A. Nason, *Environmental science & technology*, 2010, **45**, 3238-3244.
77. D. Docter, D. Westmeier, M. Markiewicz, S. Stolte, S. Knauer and R. Stauber, *Chemical Society reviews*, 2015, **44**, 6094-6121.
78. A. M. Alkilany, P. K. Nagaria, C. R. Hexel, T. J. Shaw, C. J. Murphy and M. D. Wyatt, *small*, 2009, **5**, 701-708.
79. R. M. Crist, J. H. Grossman, A. K. Patri, S. T. Stern, M. A. Dobrovolskaia, P. P. Adisheshaiah, J. D. Clogston and S. E. McNeil, *Integrative Biology*, 2013, **5**, 66-73.
80. E. J. Petersen, S. A. Diamond, A. J. Kennedy, G. G. Goss, K. Ho, J. Lead, S. K. Hanna, N. B. Hartmann, K. Hund-Rinke and B. Mader, *Environmental science & technology*, 2015, **49**, 9532-9547.
81. E. J. Petersen, T. B. Henry, J. Zhao, R. I. MacCuspie, T. L. Kirschling, M. A. Dobrovolskaia, V. Hackley, B. Xing and J. C. White, *Environmental science & technology*, 2014, **48**, 4226-4246.
82. T. B. Henry, E. J. Petersen and R. N. Compton, *Current opinion in biotechnology*, 2011, **22**, 533-537.
83. K. Jürgens, *Marine Microbial Food Webs*, 1994, **8**, 295-324.
84. Z. Ren, J. Zha, M. Ma, Z. Wang and A. Gerhardt, *Environmental monitoring and assessment*, 2007, **134**, 373-383.
85. E. Michels, M. Leynen, C. Cousyn, L. De Meester and F. Ollevier, *Water research*, 1999, **33**, 401-408.
86. W. S. Baldwin, D. L. Milam and G. A. Leblanc, *Environmental Toxicology and Chemistry*, 1995, **14**, 945-952.
87. K. E. Biesinger and G. M. Christensen, *Journal of the Fisheries Board of Canada*, 1972, **29**, 1691-1700.
88. M. Sundbom and T. Vrede, *Freshwater Biology*, 1997, **38**, 665-674.
89. K. Tervonen, G. Waissi, E. J. Petersen, J. Akkanen and J. V. Kukkonen, *Environmental Toxicology and Chemistry*, 2010, **29**, 1072-1078.
90. S. B. Lovern, H. A. Owen and R. Klaper, *Nanotoxicology*, 2008, **2**, 43-48.
91. X. Zhu, J. Wang, X. Zhang, Y. Chang and Y. Chen, *Chemosphere*, 2010, **79**, 928-933.
92. J. R. Shaw, M. E. Pfrender, B. D. Eads, R. Klaper, A. Callaghan, R. M. Sibly, I. Colson, B. Jansen, D. Gilbert and J. K. Colbourne, *Advances in Experimental Biology*, 2008, **2**, 165-328.

CHAPTER 2

Surface chemistry, charge and ligand type impact the toxicity of gold nanoparticles to *Daphnia magna*

Published in:

Royal Society of Chemistry, Environmental Science: Nano

DOI: 10.1039/C4EN00006D

Jared S. Bozich^a, Samuel E. Lohse^b, Marco D. Torelli^c, Catherine J. Murphy^b, Robert J. Hamers^c, Rebecca D. Klaper^{a*}

^a School of Freshwater Sciences, University of Wisconsin Milwaukee, 600 E. Greenfield Ave, Milwaukee, WI 53204

^b Department of Chemistry, University of Illinois at Urbana-Champaign, 600 S. Mathews Ave, Urbana, IL 61801

^c Department of Chemistry, University of Wisconsin-Madison, 1101 University Ave, Madison, WI 53706

*Corresponding Author

rklaper@uwm.edu, Phone (work): 414-382-1713, Fax: 414-382-1705

(Received 16 Jan 2014, Accepted 26 Mar 2014)

Abstract

Nanoparticles (NPs) are the basis of a range of emerging technologies used for a variety of industrial, biomedical, and environmental applications. As manufactured NP production increases, so too does the concern about their release into the environment and potentially harmful effects. Creating nanomaterials that have minimal negative environmental impact will heavily influence the sustainability of nanomaterials as a technology. In order to create such NPs, the mechanisms that govern NP toxicity need to be better elucidated. One aspect of NP structure that may influence toxicity is the identity and charge of ligand molecules used to functionalize the NP surface. These surface chemistries have the potential to increase or decrease negative biological impacts, yet their impacts are poorly understood. In this study, the toxicity of three types of functionalized ~4-5 nm gold NPs (AuNPs), polyallylamine hydrochloride (PAH-AuNPs), citrate (Cit-AuNPs) and mercaptopropionic acid (MPA-AuNPs) as well as cetyltrimethylammonium bromide-functionalized gold nanorods (CTAB-AuNRs) were evaluated in the toxicological model species, *Daphnia magna*. In order to get the most detailed information on NP toxicity in *D. magna*, both acute and chronic toxicity assays were performed. Acute exposure toxicity assays show that overall the negatively-charged AuNPs tested are orders of magnitude less toxic than the positively-charged AuNPs. However, chronic exposure assays show that both positively and negatively-charged particles impact reproduction but potentially through

different mechanisms and dependent upon functional group. In addition, while select ligands used in NP functionalization (such as CTAB) that are toxic on their own can contribute to observed NP toxicity, our acute toxicity assays indicate that minimally toxic ligands (such as PAH) can also cause significant toxicity when conjugated to NPs. This research demonstrates that surface chemistry plays a pivotal role in NP toxicity and that surface chemistry has the potential to affect the sustainability of these materials.

Introduction

In the U.S. alone, the engineered nanoparticle (NP) industry is a multibillion-dollar industry and is predicted to increase to a one-trillion-dollar industry by 2015¹. One study estimates that 63-91% of over 260,000-309,000 metric tons of the world NP production in 2010 entered our environment through landfills². As production increases, there is a concern about the potential environmental and health effects of NP exposures. The surfaces of NPs are typically modified with surface functional groups that control properties such as NP stability³⁻⁵. To create NPs that are less toxic and more environmentally sustainable there is a need to understand which NPs may cause harm to the environment and what physiochemical properties determine their impacts on organisms. This involves: 1) understanding the interaction of NPs with an organism; 2) which physiochemical properties of a NP best predict toxicity; and 3) how alterations in NP surface chemistry can alleviate toxic impacts. To better understand these factors, experiments are needed that use fine-scale alterations in NP surface chemistry to probe the interactions of NPs with cells, tissues and organisms. In

addition, it is necessary to create NPs that have specific and well-defined bulk and surface chemistries to determine how their chemical composition and structure of the NP and surface functional groups may influence toxicity.

Although many studies on toxicity of NPs have been conducted to date, the mechanisms that govern NP toxicity are still in question as experimental artifacts and the design of experiments can impede understanding of the fine scale interactions of NPs with biological entities⁶. For example, the charge of the NP surface has been implicated as a major factor in toxicity⁷⁻¹². Yet the initial charge of a particle may be altered during an experiment due to interactions with media¹³⁻¹⁶. Particle size and surface chemistry have also been suggested to impact NP toxicity¹⁷⁻²³ as both particle size and surface chemistry can influence particle uptake and partitioning in organelles and tissues²⁴⁻²⁹. The density of ligands on the NP surface is often poorly characterized, however it may also have an impact on toxicity^{30, 31}. Aggregation over time in experimental media or in the environment, can either increase or decrease NP toxicity and may have a significant impact on toxicity³²⁻³⁴. Byproducts from particle synthesis or the ligands alone may cause toxicity³⁵. Few studies attempt to include controls for several of these factors, which can complicate conclusions of properties associated with toxicity. Finally, many studies that have been conducted to date have been carried out using *in vitro* systems and only over short time periods, which may not accurately reflect real world whole organismal interactions with NPs^{8, 36, 37}.

To examine the specific interactions of NPs with differing surface functionalization in a whole organism model, we evaluated the *in vivo* toxicity of a library of well-characterized gold NPs (AuNPs) with differing surface functionalities to

the aquatic toxicity model *Daphnia magna*. AuNPs were chosen as a model NP as they can be synthesized with very fine control of size and shape, are readily altered with well-know surface chemistries, have a low environmental background level (so they can be easily tracked within an organism), and have many potential commercial applications due to their unique optical properties and their benign nature.

Furthermore, unlike other functionalized metal and metal oxide NPs, AuNPs are resistant to dissolution or significant changes in size or shape under typical environmental and biological conditions³⁸⁻⁴¹. Applications where these particles have been used range from cellular imaging⁴², bio-chemical sensing⁴³, drug and gene delivery^{44, 45}, to medical therapeutics⁴⁶. The successful implementation of AuNPs in these applications depend strongly upon appropriate particle functionalization⁴⁷.

In this study, acute and chronic assays were carried out in order to measure both short term and full life cycle effects of various functionalized AuNPs on *Daphnia magna*. Particles were characterized after synthesis and within exposure media to better untangle the biological effects caused by particle stability and aggregation. Controls were designed to take into account the toxicity and other adverse impacts due to free ligands, supernatants containing reagents and NP synthesis byproducts and impurities in reagents. This study begins to address the molecular properties of NPs that influence their toxicity and interactions with aquatic organisms.

Materials and Methods

Nanoparticle synthesis and functionalization.

All materials were used as received, unless otherwise noted. Gold tetrachloroaurate trihydrate ($\text{HAuCl}_4 \cdot 3\text{H}_2\text{O}$), 3-mercaptopropionic acid (MPA), sodium borohydride (NaBH_4), polyallylamine hydrochloride (PAH; M_w 15, 000 g/mol), and silver nitrate (AgNO_3) were obtained from Sigma Aldrich. Hexadecyltrimethyl ammonium bromide (CTAB), L-ascorbic acid, and trisodium citrate were obtained from Sigma. Deionized water was prepared using a Barnstead NANOPURE water filtration system. PALL Minimate tangential flow filtration capsules for AuNP purification, with 50 kD pore size was obtained from VWR. TEM grids, SiO on copper mesh (PELCO) were used for transmission electron microscopy studies. Functionalized AuNPs were synthesized using previously reported methods in a millifluidic reactor, which enabled high-throughput NP synthesis. The millifluidic reactor for NP synthesis was assembled (as previously described) from commercially available components: a peristaltic pump (Cole-Palmer Masterflex L/S), Tygon polyvinyl tubing (ID = 2.79 mm), polyethylene Y-mixers (ID = 1.79 mm), and polyethylene joints⁴⁸. AuNPs were synthesized in the reactor at an overall flow rate of 50.0 mL/min, and experienced a residence time of 3.0 min for the spherical AuNP syntheses, and 20.0 min for the gold nanorod synthesis.

NPs stabilized with four different surface chemistries were synthesized: (1) Citrate-functionalized NPs (“CIT-AuNPs”), (2) Poly(allylamine) hydrochloride (“PAH-AuNPs”), (3) mercaptopropionic acid-functionalized NPs (“MPA-NPs”) and (4) Cetyl trimethylammonium bromide -functionalized gold nanorods (“CTAB-AuNRs”) (Fig. 1).

Cit-AuNPs (5.0 nm). 5.0 nm Citrate AuNPs were synthesized using previously reported procedures⁴⁹. In a typical synthesis, 4.0 L of a growth solution, consisting of aqueous gold tetrachloroaurate (HAuCl_4 , 10.0 mM) and 10.0 mM sodium citrate_(aq), as

well as a 4.0 L of an aqueous solution of sodium borohydride (5.0 mM) were prepared. The two solutions were flowed together in a millifluidic synthesis reactor at a flow rate of 50.0 mL/min, and experienced a residence time of 3.0 min. The combined solutions rapidly change color to a deep brown, and then red-brown prior to exiting the reactor. The AuNP solution was collected in an *aqua regia*-cleaned 4.0 L bottles and stirred for 3.0 hours. The Cit-AuNPs were then concentrated and purified by diafiltration (5.0 volume equivalents)⁵⁰.

PAH-AuNPs (5.0 nm). Cit-AuNPs were wrapped with polyallylamine hydrochloride (PAH) to prepare 4.0 PAH-Functionalized AuNPs, as previously described⁵¹. Briefly, Cit-AuNPs were dissolved in 20.0 mL of a 1.0 mM aqueous sodium chloride solution to give a final AuNP concentration of approximately 20.0 nM. To each 20.0 mL of polyelectrolyte wrapping solution, 500.0 μ L of PAH (10.0 mg/mL) dissolved in 1.0 mM NaCl was added. The wrapping solution was then mixed at vortex briefly and left to stand for 16 h. The PAH-AuNPs were subsequently purified by centrifugation and washing (55 min. at 8000 rcf), in nanopure deionized water. The PAH-AuNPs were then concentrated in a diafiltration membrane.

MPA-AuNPs (4.0 nm). Thiol-stabilized AuNPs were prepared by direct synthesis with sodium borohydride according to previously reported methods^{50, 52}. Briefly, two 4.0 L aqueous solutions (a growth solution and a reducing agent solution) were prepared. The growth solution contained HAuCl₄ (3.0 mM) and MPA(6.0 mM) dissolved in nanopure deionized water. The pH of the growth solution was adjusted to approximately 8.5 by the addition of sodium hydroxide. The other 4.0 L solution consisted of 5.0 mM-aqueous NaBH₄. The two solutions were flowed together in a

millifluidic reactor at 50.0 mL/min. and experienced a residence time of 3.0 min. The combined solutions rapidly change color to a deep orange-brown. The AuNP solution was collected in an *aqua regia*-cleaned 4.0 L bottle and stirred for 3.0 hours. The thiol-stabilized AuNPs were then concentrated and purified by diafiltration (40.0 volume equivalents of nanopure deionized water in a 50 kD membrane).

CTAB-Stabilized Gold Nanorods (AuNRs). CTAB-stabilized Gold nanorods with aspect ratio (length/width) 4.0 were synthesized using our previously reported seeded growth procedures⁵³. Two solutions were prepared: a growth solution and a “Seed” solution. For the growth solution, 10.0 mL HAuCl₄ (0.1M), 16.0 mL AgNO₃ (0.01M), and 11.0 mL of ascorbic acid (0.1M) were added to 1.0 L of a 0.1 M aqueous CTAB solution. For the seed solution, 2.4 mL of a previously prepared gold NP seed dispersion (aged 2 hours) was added to 998.0 mL of a 0.1 M CTAB solution. The solutions were mixed within the flow reactor (flow rate = 50.0 mL/min), and the AuNR growth solution experienced a residence time of approximately 15.0 min in the reactor before being deposited into an *aqua regia*-cleaned 4.0 L bottle. AuNRs were purified and concentrated by centrifugation and washing (two times, 20 min. at 11 000 rcf) with nanopure deionized water.

Functionalized gold nanoparticle characterization and analysis.

Gold NP solutions were analyzed using a combination of UV-vis absorption spectroscopy, transmission electron microscopy (TEM), ζ -potential analysis, Dynamic Light Scattering (DLS) and x-ray photoelectron spectroscopy (XPS). UV-vis absorbance spectroscopy analysis was performed using a Cary 500 Scan UV-vis-NIR

Spectrophotometer. For transmission electron microscopy analysis, a small aliquot of the purified AuNP solution was dropcast onto a SiO/Cu mesh/formvar TEM grid (Ted Pella), and examined using a JEOL 2100 Cryo TEM. Size distributions for the AuNPs were determined using ImageJ analysis, according to previously reported procedures⁵⁴. For XPS analysis, purified AuNP solutions were dropcast onto indium foil and analyzed using a custom-designed, ultrahigh vacuum Physical Electronics XPS system with a monochromated Al X-ray source. DLS and ζ -potential (Malvern Instruments, model #ZEN3600) of the functionalized NPs were obtained in both nanopure deionized water ([AuNP] = 10 nM, pH = 5.8) and daphnid media ([AuNP] = 10 nM, pH = 6.8) to determine aggregate sizes and stability of particles in MHRW prior to and during the experiment.

Ligand densities for particles at the beginning of the experiment were determined using XPS. Detailed procedures for XPS sample preparation and analysis are presented in the Supporting Information. Briefly, NP solutions were dripped onto Si wafers, and XPS features characteristic for each molecule were measured and normalized against gold as an internal standard. A quantitative numerical modeling procedure was validated and used to correct for NP curvature and scattering effects. These measurements are presented in Table 3.

***Daphnia magna* toxicity assays.**

Daphnia magna are freshwater invertebrates that selectively filter feed in both benthic and pelagic regions of the aquatic environment. Important to aquatic food webs and designated by the U.S Environmental Protection Agency (U.S. EPA) as a

model organism, *Daphnia magna* are widely accepted as a model organism for assessing the toxicity of environmental contaminants and experience reduced reproduction, growth and increased mortality with exposure to toxic substances or substandard food items⁵⁵.

Daphnids were bred in the Klaper lab at UWM-School of Freshwater Sciences and cultures were maintained in tanks of moderately hard reconstituted water (MHRW) at 20°C on a 16:8 light/dark cycle (per OECD and EPA protocols)^{56, 57}. Daphnids were fed a diet composed of freshwater algae (*Selenastrum capricornutum*) with an algal density of 400,000 algal cells/mL and the supernatant of 405 mg of alfalfa (*Medicago sativa*) suspended in 50 mL ultrapure water after 20 min of stirring and 10 min of settling.

D. magna were exposed to concentrations of four types of functionalized AuNPs, described above, over a concentration range of 0.001-25 mg/L (see particle descriptions, and synthesis methods). In addition, the corresponding ligands (Cit, MPA, PAH and CTAB) were tested at 0.001-25 mg/L. These concentrations were chosen to be far in excess of the total ligand present in the NP suspension. The supernatants and filtrates were collected from the particle purification process and then the supernatant and filtrate stocks were diluted to a concentration of 0.001-25 mg/L (based on the estimated total ligand concentration in the supernatant). AuNP stock solutions were prepared at a maximum concentration of 2000 mg/L^{58, 59}. Accordingly, daphnids were exposed to functionalized AuNPs at a maximum concentration of 25 mg/L in the acute and chronic exposure studies.

For 48 hour acute studies five female daphnid neonates less than 48 hours old were placed in 100 mL of MHRW (control) or NPs in MHRW (experimental) totaling 100 mL in volume. A minimum of three replicates was carried out for each concentration and the mortality of daphnids were assessed per beaker by calculating the remaining percentage of daphnids alive.

For chronic exposures, daphnids less than 48 hours old were exposed to NPs for 21 days below the concentrations that were found to be acutely toxic. Five neonates were placed in 94 mL of MHRW (control) or NPs in a static renewal exposure where 100% media exchange occurred three times per week. *Daphnia magna* were fed 4 mL of algae (*Selenastrum capricornutum*) and 2 mL of alfalfa (*Medicago sativa*) at each exchange period to bring the total beaker volume to 100 mL. Mortality and reproduction were measured during the media changes and daphnid size was measured at the end of the exposure. Size was measured on day 21 of the exposure as the length of the daphnid from the top of the helmet to the base of the spine.

Exposures adhered to the mortality and reproduction guide lines designated by the OECD guidelines for the Testing of Chemicals⁶⁰. Alterations were done to the exposures to account for discrepancy introduced by changes in population density through the exposure²³. Daphnids were held at a concentration of one daphnid per 20 mL of media. Reproduction was calculated for the number of remaining individuals at the time of measurement and stated as the mean number of neonates generated per remaining individual.

ICP-MS determination of AuNP uptake by *Daphnia magna*.

In order to determine how the surface chemistry of the AuNPs influenced NP uptake by daphnids as well as the external adsorption onto the daphnid carapace, gold content both inside and outside of the daphnids were quantified by ICP-MS analysis. For the ICP studies, *D. magna* were exposed to AuNPs at a concentration of 5.0 ppb for a period of 6 h, under the standard acute toxicity conditions. After 6 h, five daphnids were removed from each of the AuNP-containing media and either treated with or without a 100 mM iodide etchant solution for 5 min to differentiate the particles adsorbed onto the daphnid carapace vs. particles ingested. Daphnids were then individually digested in 1.0 mL of freshly prepared *aqua regia* for 2 h. Afterwards, the digest solutions were diluted to a final volume of 10.0 mL with nanopure water. The digested *Daphnia magna* samples were analyzed by ICP-MS (Perkin-Elmer SCIEX Elan DRCe) to determine the total gold concentration. The total Au concentration was then converted to the number of AuNPs taken up/adsorbed by each daphnid using the density of bulk gold and the volume of each AuNP in order to determine the number of Au atoms per NP.

Statistical Analysis

D. magna body size and reproduction were normalized to control averages to account for changes in daphnid populations over time. Some of the data failed to meet the assumptions of normality for the independent *t* test analysis. Therefore, the effects of NP exposures on daphnid fecundity, mortality and body size were weighed against controls by the nonparametric Mann-Whitney U test for two-independent samples.

Values were considered significant at $p < 0.05$. SPSS (IBM 2013) was the program chosen to carry out statistical analysis.

Gold NP uptake in *D. magna* (see Supporting Information Fig. S6) was analyzed using the independent t test in Microsoft Excel 2013. Values were considered significant at $p < 0.05$.

Results

Gold nanoparticle characterization.

AuNPs were characterized using TEM, UV-vis absorbance spectroscopy, and dynamic light scattering in order to rigorously determine AuNP size. The size and surface chemistry characterization data for the AuNPs is presented in detail in Table 1. Representative TEM images and size analysis for the spherical AuNPs are provided in the Supporting Information (Fig. S1 and S2, respectively). The CTAB-stabilized AuNRs had a longitudinal diameter of ~ 50 nm, and a transverse diameter of ~ 12 nm. PAH-AuNPs had a mean diameter of 4.7 ± 1.4 nm (1σ). Cit-AuNPs had a mean core diameter of 4.9 ± 1.4 nm. MPA-AuNPs had a mean core diameter of 3.8 ± 1.1 nm. Here, the polydispersity in the sample is given as a single standard deviation from the mean core diameter. The surface charge of the AuNPs was determined using ζ -potential analysis (Table 1).

The ligand density of the AuNP library was determined using XPS and with the exception of CTAB-AuNR Table 3 shows that the ligand densities for Cit-AuNP and MPA-AuNP are nearly the same and are also nearly identical to values previously reported for densely-packed self-assembled monolayers on planar gold surfaces⁶¹.

Because CTAB-AuNR is a rod shaped particle, a max/min range based on the assumption of a planar and spherical particle has been provided. As the rods still possess a significant amount of curvature the ligand density should be closer to the lower density estimate. Though there are physically more CTAB molecules, CTAB coats the AuNR in a bilayer^{62, 63}. Thus, the increased number of CTAB ligands is not due to a higher packing density. The number of ligands on the outer leaflet of CTAB-AuNR is comparable to the other functionalized particles in this study. For PAH-AuNP, the polymeric nature of the PAH ligand makes it difficult to determine an equivalent molecular density.

Stability of AuNPs in daphnid media.

In order to better connect the physiochemical properties of the AuNPs tested with their acute mortality in *Daphnia magna*, we monitored the changes in the AuNP physiochemical properties the AuNPs undergo following dispersion in daphnid media using UV-vis absorption spectroscopy, DLS, and ζ -potential analysis. The positively-charged AuNPs (the CTAB-AuNRs and the PAH-AuNPs) showed no evidence of changes in size, shape, or aggregation state (based on their UV-vis spectra, Fig. S3, and DLS analysis, Table 2). In contrast, the negatively-charged AuNPs show evidence of aggregation following dispersion in daphnid media. This aggregation is evidenced by broadening of the Surface Plasmon Resonance (SPR) absorbance (~520 nm) in the UV-vis spectra, and a significant increase in their hydrodynamic diameter over the course of the 48 h exposure time (D_h , see Table 2). Interestingly, the structure of the aggregated Cit-AuNPs appears to be different from the MPA-AuNP aggregates. TEM analysis of the AuNP aggregates shows significant fusion of the Cit-AuNP cores to

form larger AuNPs and wire-like structures after 48 h, while the MPA-AuNP aggregates appear to consist primarily of large, loosely bound networks of AuNPs with an ~4 nm primary particle size (Fig. 2). The MPA-AuNPs could be re-suspended from their aggregated state by gentle agitation, while the Cit-AuNPs could not, which would be consistent with the structure of the aggregates observed in the TEM images (Fig. S5).

Effects of AuNPs on daphnid acute mortality.

Particle surface chemistry and stability played an important role in daphnid survival, with positively-charged particles, CTAB-AuNRs and PAH-AuNPs, being orders of magnitude more toxic than the negatively-charged particles, Cit-AuNPs and MPA-AuNPs. CTAB and PAH-AuNPs significantly affected daphnid mortality (93% mortality, $U = 0$, $p < 0.05$; and 40% mortality, $U = 0$, $p < 0.05$, respectively) at concentrations as low as 10 $\mu\text{g/L}$ (Fig. 3). However, PAH and CTAB-AuNPs demonstrated similar toxicity at 5 $\mu\text{g/L}$, showing 13% mortality. Cit and MPA-AuNPs did not significantly affect *Daphnia magna* mortality at all concentrations tested ($p > 0.05$), which reached an order of magnitude higher than the positively charged particle. Positively-charged particles were also more stable in the MHRW media (Table 2).

Of the four ligands tested, CTAB was the only ligand that by itself significantly affected *D. magna* mortality compared to control daphnids (Fig. 3). CTAB ligand caused the same daphnid mortality as CTAB-AuNR acute exposure, causing 13% mortality at 5 $\mu\text{g/L}$, 93% mortality at 10 $\mu\text{g/L}$ and 100% mortality at 50 $\mu\text{g/L}$ (Fig. 3). The PAH ligand, unlike the PAH-AuNP, did not affect daphnid mortality at the

concentrations that were significantly impacting daphnid mortality in the PAH-AuNP acute assay (Fig. 3). Citrate and MPA free ligands, like Cit and MPA-AuNPs, had no impact on daphnid mortality.

When comparing toxicity to that of supernatants and filtrates (collected from the particle purification process), only the supernatants significantly impacted daphnid survival with PAH-AuNP supernatant being the more toxic of the two positively-charged supernatants (Fig. 2). PAH-AuNP supernatant significantly affected daphnid mortality up to 5 µg/L causing 73% mortality ($U = 0, p < 0.05$) and 100% mortality at 10 and 50 µg/L ($U = 0, p < 0.05$). UV-vis and TEM analysis of the PAH-AuNP supernatant indicated that, unlike the other supernatants used tested in this study, the PAH-AuNP supernatant contained a low concentration of very small ($d_{\text{core}} < 4.0$ nm) AuNPs. The UV-vis spectrum of the PAH-AuNP supernatant and a representative TEM image are provided in the Supporting Information as Figure S7. CTAB-AuNR supernatant significantly caused mortality at 50 µg/L, eliciting 100% mortality in *D. magna* exposures ($U = 0, p < 0.05$).

Effects of chronic AuNP exposures on daphnid survival, reproduction, and body size.

PAH (positively charged) and Cit-AuNPs (negatively charged) were the only functionalized AuNPs that significantly decreased daphnid reproduction over the 21-day chronic exposure (Fig. 4a and 4b). PAH-AuNPs significantly decreased reproduction at 5 µg/L (12% decrease, $U = 10, p < 0.05$)(Fig. 4a). In contrast, the free ligand PAH, significantly increased reproduction in daphnids (10% increase, $U = 7, p <$

0.05; and 13% increase, $U = 8$, $p < 0.05$) at both 1 $\mu\text{g/L}$ and 5 $\mu\text{g/L}$ concentrations. Daphnid exposed to the CTAB free ligand also experienced increased reproduction by 20% in 5 $\mu\text{g/L}$ exposures ($U = 3$, $p < 0.05$) but the CTAB supernatant decreased reproduction by 18% at 1 $\mu\text{g/L}$ ($U = 9.5$, $p < 0.05$). For negatively charged particles, Cit-AuNPs significantly decreased daphnid reproduction (97% decrease, $U = 0$, $p < 0.05$) at 25 mg/L averaging only 3 *D. magna* neonates per individual compared to 83 neonates per individual control daphnids (Fig. 4b). MPA-AuNPs had no impact yet at 5 mg/L the MPA free ligand increased reproduction by 14% ($U = 4$, $p < 0.05$).

Daphnia magna exposed to 25 mg/L Cit-AuNPs and MPA-AuNPs exhibited a significant reduction in adult body size as compared to control daphnids ($U = 0$, $p < 0.05$; and $U = 0$, $p < 0.05$)(Fig. 5), while daphnids exposed to CTAB and PAH showed no significant reduction in daphnid body size. At 25 mg/L, Cit-AuNPs reduced daphnid growth by 15% compared to control daphnids, having an average length of 3.36 mm compared to 3.85 mm, respectively and exposure to MPA-AuNPs elicited a 7% reduction in daphnid body size, averaging 3.57 mm body length. Since chronic exposures were conducted at sub lethal levels as determined by acute exposures we did not observe any significant mortality for any of the chronic NP exposures.

Effects of surface chemistry on AuNP uptake in *Daphnia magna*.

The surface chemistry of the AuNPs was found to have minimal influence on NP uptake by daphnids in this study (Fig. S6), as ICP-MS analysis indicated that all the AuNPs tested were found to be taken up by daphnids in similar amounts (on a per mass basis). However, MPA-AuNPs were significantly taken up ($p < 0.05$) to a greater

extent when compared to PAH-AuNPs and Cit-AuNPs even though it is still relatively comparable throughout treatments. Additionally, there was no significant difference in the quantity of NPs on the daphnid carapace and minimal accumulation across all treatments when iodide treated samples were compared to samples without the iodide treatment.

Discussion

Initial particle charge significantly impacted overall toxicity observed in this study, with positively-charged particles being more toxic than their negatively-charged counterparts. Positively-charged particles, PAH and CTAB-AuNPs, were orders of magnitude more toxic than negatively-charged citrate and MPA-AuNPs, significantly eliciting mortality in *Daphnia magna* down to a concentration of 10 µg/L. In addition, PAH-AuNPs significantly affected daphnid reproduction at 5 µg/L whereas Cit-AuNPs affected *Daphnia magna* reproduction at 25 mg/L (Fig. 4a and 4b). Toxicity caused by imparting positive charge to NPs has been shown with other cells, mammals and aquatic organisms such as algae, bivalves and fish^{7, 10, 64-67}. One study in particular, demonstrated a charge dependent response when exposing zebrafish to AuNPs. When 0.8 nm and 1.5 nm AuNPs functionalized with a cationic surface group, trimethylammoniummethanethiol (TMAT), were more toxic than anionic 2-mercaptoethanesulfonate (MES) or neutral charged 2-(2-mercaptoethoxy)ethanol (MEE) surface groups, affecting mortality, morphology, behavior and developmental endpoints to a greater extent⁶⁵.

One possible reason that PAH and CTAB-AuNPs were more toxic than their negatively-charged counterparts is potentially due to these particles having a high affinity towards the negative charged surfaces of cellular membranes⁶⁸. The high level of attraction that positive charged particles have with cellular membranes increases cellular uptake of these particles through mechanisms such as phagocytosis, pinocytosis and membrane disruption, which creates holes in the membrane due to the densely populated charge on the NP surface^{69, 70}. This allows the positive charged particles to enter the intracellular matrix and potentially damage cell organelles integral to cellular functions. Lovern et al. (2008)⁷¹ and Garcia-Camero et al. (2013)⁷² observed the uptake of gold NPs *in vivo* with minimal evidence of AuNPs ability to cross the *Daphnia magna* digestive tract. However, these studies were not focused on positively-charged particles, which have a greater potential to be further incorporated into the organism. The lack of tissue accumulation of negatively-charged NPs could be one of the potential mechanisms that caused the positively charged NPs to be more toxic and could explain the low toxicity observed with the negatively charged particles.

Another potential explanation for the difference seen in toxicity between the differentially charged particles in our experiment may be due to particle stability and aggregation in our media (MHRW). Positively charged particles, PAH and CTAB-AuNPs, did not aggregate significantly in the media (as can be seen in the UV-vis spectra of these AuNPs, provided in the Supporting Information, Fig. S3), while negatively charged particles, MPA and Cit-AuNPs, underwent greater aggregation during in our experiments (Table 2). Stable particles, PAH-AuNP and CTAB-AuNP, remained less than 100 nm in size (55.9 ± 4.1 and 17.5 ± 0.2 , respectively) and the

unstable particles, MPA-AuNP and Cit-AuNP, aggregated or agglomerated to a large extent, drastically increasing their size over the period between media exchanges (750.6 ± 8.2 and 90.8 ± 5.9 , respectively) (see Fig. 6 and Fig. S3-S5). Aggregation-dependent toxicity has been seen in other studies using zebrafish embryos, leading us to believe that aggregation can affect NP toxicity^{73, 74}. Although daphnids clearly ingested all functionalized particles (Fig. S6) the aggregation size may cause a difference in their interactions with daphnid, potentially affecting the surface area of the particle available for interaction with the cells within the organism, as well as the potential uptake into cells.

The smaller size of the positively-charged particles in our study may have increased their toxicity by enabling them to cross the gut lumen of the daphnids, potentially further interacting with *D. magna* cells and organelles vital to daphnid homeostasis and other functions. This could account for the high mortality seen at low concentrations, especially because the PAH-AuNP supernatant exposure produced high mortality and TEM images revealed a small amount of < 4 nm PAH-AuNPs present in the supernatant suspension (Fig. S7). Small, 10 nm positively-charged amine coated AuNPs have been shown to enter a freshwater bivalve's branchial and digestive epithelial cells, entering the cytoplasm where the particles were then able to penetrate the cells nucleus and lysosomal vesicles⁶⁴. AuNPs with core diameters less than 50 nm (15 and 50 nm AuNPs) have also been shown to affect inner organs of rats to a greater extent than larger particles (160 nm)^{24, 75, 24}. Similar size dependent toxicity has been shown in aquatic organisms with various NP types¹⁷. Negatively-charged particles aggregating to a large size have fewer mechanisms to enter the cell,

reducing the ability to cross the cellular membrane and damage cell organelles. Main routes of entry of larger particles are through macropinocytosis, phagocytosis and clathrin mediated endocytosis⁶⁹. Other studies have shown that larger particles and aggregates are less toxic than their smaller, monodispersed counterparts^{21, 32, 34}. For example, increasing the extent of aggregation therefore increase particle size of MPA-AuNPs, also reduced toxicity to zebrafish embryos^{73, 74}.

MPA and Cit-AuNPs did impact reproduction (at high concentrations of Cit-AuNP, Fig. 4b) and body size (Fig. 5), however we observed unusual aggregation in the chronic exposures for these two particles. Cit-AuNPs, the more toxic of the two negatively-charged particles, formed agglomerates as appose to aggregates (Fig. 2). These agglomerates could not be re-suspended and formed a film on the bottom of the beaker. TEM imaging of the AuNP aggregates confirms that the Cit-AuNPs form extended wires and larger spherical AuNPs as a result of their aggregation process as appose to the MPA-AuNPs, which remain ~4.0 nm particles, but form large networks of closely associated AuNPs. We hypothesize that these agglomerates could cause an impact on the energy budgets of these organisms either through blocked nutrient absorption or a decrease in food consumption⁷⁶ or due to an impact on swimming and molting as these particles were found to adhere to the exoskeleton, adding mass to the swimming organism (Fig. 6). Lee and Ranville (2012)⁷⁷ while conducting a 48-hour acute assay using *D. magna*, found that organisms exposed to aggregated Cit-AuNPs shed their exoskeletons while the controls did not. The increased molting observed in the Cit-AuNP exposed daphnids demonstrates that *Daphnia magna* may use this tactic

to avoid any unwanted effects caused by the adhered Cit-AuNPs, however, the increased molting requires energy, leaving less for daphnid growth and reproduction.

Certain ligands used to alter the surface chemistry of NPs are more toxic than others, which could also explain the increased toxicity of CTAB-AuNRs in particular in our study. For the CTAB ligands, the acute ligand toxicity exactly matched the acute toxicity of the CTAB-AuNR, while the PAH ligand was only toxic when paired with the gold NP (Fig. 3). For CTAB-AuNRs, it is widely accepted that improper purification or ligand desorption can result in free-floating CTAB ligands in NP suspensions, which leads to this functionalized particle being highly toxic¹³. This potentially downplays the effect of charge on toxicity for this functionalized AuNP, However, both ligand concentrations in the particle suspensions were much lower than what we tested in the free ligand control experiments implying that there is another mechanism that causes the ligands as well as the particles to become more toxic. We hypothesize that the increase in PAH and CTAB toxicity when attached to the gold NPs may be due to an increase in the concentration of PAH and CTAB inside the daphnids gut due to their ingestion with the NP and localization of ligand on or in daphnid cells. There were some indications of an increase in the reproduction of daphnids in the presence of the free ligand of CTAB, PAH and MPA. This may be due to some physiological use for the daphnids of these functional groups but may also be due to a hormesis effect of the ligands where a small amount of these chemicals is stimulatory to the organism's biochemical mechanisms that deal with toxins and therefore an up-regulation of other pathways dealing with reproduction. This may be a life history strategy for the organism to increase reproduction in a time of stress, as seen by others^{78, 79}.

Lastly, in this experiment, the effects of ligand density and gold dissolution on NP toxicity are thought to be minimal. The similarity in ligand densities determined by XPS results (Table 3) for these ligands demonstrates that the differences in subsequent biological interaction are not likely to be associated with differences in ligand density. Additionally, it should be noted that while functionalized AuNPs may be susceptible to aggregation under specific environmental conditions, AuNPs are not readily susceptible to dissolution or oxidation under typical environmental conditions (which is in contrast to many functionalized silver or metal oxide NPs)³⁸⁻⁴¹. As a consequence, when we considered how AuNP stability influences toxicity in this discussion, we focused primarily on the stability of AuNPs against aggregation, rather than dissolution or oxidation.

The results of this study are important, because it identifies mechanisms for AuNP toxicity by examining NP toxicity with different charges using an environmentally relevant organism. The present study and our previous work²³ demonstrate the need for functionalized NPs to be evaluated in chronic exposures, as acute exposures do not explain the full adverse affects of NPs on aquatic organisms, as seen with Cit-AuNPs. This study also demonstrates that characterization of NP size after exposure to media as well as accounting for free ligand and synthesis impurity toxicity are important in determining the mechanism for NP toxicity.

Conclusion

NPs have the potential to be highly beneficial to society, however in order to create NPs that are beneficial, while minimizing the environmental implications of

these materials, the mechanisms that govern the toxicity of NPs need to be better elucidated. We found that surface chemistry plays a significant role in NP toxicity; not only does the charge of the ligand on the AuNP surface influence both acute and chronic toxicity, but the identity of the ligand itself can influence toxicity. Interestingly, ~4.0 nm AuNPs functionalized with a non-toxic ligand (PAH) showed significant acute and chronic toxicity. In addition, the smallest particles (< 4 nm) as seen in the PAH-AuNP supernatant exposures, could potentially be much more harmful to *Daphnia magna* than comparatively larger sized PAH-AuNPs (> 4 nm). Furthermore, the chronic toxicity assays performed in this study indicate that AuNPs that show minimal acute toxicity can induce significant long-term effects, impacting daphnid reproduction. Therefore, chronic toxicity studies are essential for elucidating potential long-term exposures of manufactured NPs. Testing libraries of NPs with a variety of surface chemistries with different effective charges and functionalities in a given study will help discover trends in NP toxicity and translate these experiments to predictions for other types of NPs.

ACKNOWLEDGEMENTS

This work was funded by the National Science Foundation Center for Chemical Innovations Grant CHE-1240151: Center for Sustainable Nanotechnology to R. Hamers, R. Klaper, and C. Murphy.

Supporting Information

Nanoparticle ligand density measurement and analysis: Nanoparticle suspensions were centrifuged (14.5 kxg, minimum 60 min) to pellet particles, and the supernatant was removed and the particles were re-suspended and sonicated in a small amount of 18 M Ω cm deionized water (Barnsted Nanopure). Particles were dripped onto pre-cleaned highly conductive (<1 milliohm-cm) silicon wafers and dried in at least two iterations. The nanoparticle layers were sufficiently thick that the underlying Si wafer was not detectable in subsequent XPS measurements. In order to validate the procedures used to correct the data for electron scattering, we also prepared “ligand-free” samples by gently removing the ligands by photo-oxidation. XPS measurements were performed using a custom-built, ultra-high vacuum Physical Electronics XPS system equipped with an aluminum K α source (~ 1487 eV x-ray energy), a quartz-crystal X-ray monochromator, a hemispherical electron energy analyzer, and a 16-channel array detector. This system is ion-pumped with a base pressure of 2×10^{-10} torr. For each ligand, XPS spectra were obtained, and initial experiments were used to determine which specific peaks provided the best quantitative data free of extraneous contamination. Subsequent experiments involved measuring and quantitatively analyzing these peaks. For CTAB and PAH-modified nanoparticles, the C(1s) /Au peak area ratio was used for quantitative primary analysis. For MPA, the S(2p) peak was used because the C(1s) signal from this small molecule is otherwise difficult to separate unambiguously from potential background

contamination. For citrate, we used the high binding-energy carbon peak near 290 eV that is characteristic of carboxylic acid groups; typical contamination shows little or no signal in this region.

Nanoparticle shape and inelastic scattering within the Au and within the inorganic layer accounted for using direct finite-element analysis to model the creation and scattering of electrons within ligand-coated spherical nanoparticles¹ To account for the electron scattering within the organic layers, values for the inelastic mean free paths (IMFP) measured by Laibinis, et al² for Au photoelectrons propagating through self-assembled alkyl monolayers of different thicknesses, yielding values for the IMFP of ~ 1400 eV for Au photoelectrons propagating through the organic monolayers $\lambda_{Au,C}$. The IMFP of the ~ 1200 eV C(1s) electrons scattering within the organic film were then obtained using the well-known energy scaling laws,³ and these values were used as inputs into the finite-element analysis program to model the experimentally observed XPS peak ratios as a function of ligand coverage. As a check, we also compared the absolute intensity of the Au XPS peaks from ligand-covered and the “ligand-free” samples prepared by ozone oxidation of the ligand-covered samples, as described above. Measuring the absolute Au peak areas from the ligand-free sample ($A_{\text{ligand-free}}$) and ligand-bearing samples ($A_{\text{ligand-bearing}}$) with identical sample geometry and alignment yields a direct measure of the $t/\lambda_{Au,C}$ via

$$\frac{A_{\text{ligand-bearing}}}{A_{\text{ligand-free}}} = \exp^{-t/\lambda_{Au,C}}$$

where t is the thickness of the film and the $\lambda_{Au,C}$ is the inelastic mean free path of Au electrons in the organic layer. In all cases where a direct comparison could be made,

we found that the finite-element modeling yielded results consistent with the experimental data.

REFERENCES

1. R. J. Aitken, M. Q. Chaudhry, A. B. A. Boxall and M. Hull, *Occupational Medicine*, 2006, **56**, 300-306.
2. A. A. Keller, S. McFerran, A. Lazareva and S. Suh, *Journal of Nanoparticle Research*, 2013, **15**.
3. E. V. Rogozhina, D. A. Eckhoff, E. Gratton and P. V. Braun, *Journal of Materials Chemistry*, 2006, **16**, 1421-1430.
4. B. G. Trewyn, Slowing, II, S. Giri, H. T. Chen and V. S. Y. Lin, *Accounts of Chemical Research*, 2007, **40**, 846-853.
5. Y. Zhang, N. Kohler and M. Q. Zhang, *Biomaterials*, 2002, **23**, 1553-1561.
6. R. M. Crist, J. H. Grossman, A. K. Patri, S. T. Stern, M. A. Dobrovolskaia, P. P. Adisshaiah, J. D. Clogston and S. E. McNeil, *Integrative Biology*, 2013, **5**, 66-73.
7. C. M. Goodman, C. D. McCusker, T. Yilmaz and V. M. Rotello, *Bioconjugate Chemistry*, 2004, **15**, 897-900.
8. N. Lewinski, V. Colvin and R. Drezek, *Small*, 2008, **4**, 26-49.
9. Z.-J. Zhu, R. Carboni, M. J. Quercio, B. Yan, O. R. Miranda, D. L. Anderton, K. F. Arcaro, V. M. Rotello and R. W. Vachet, *Small*, 2010, **6**, 2261-2265.
10. A. M. El Badawy, R. G. Silva, B. Morris, K. G. Scheckel, M. T. Suidan and T. M. Tolaymat, *Environmental Science & Technology*, 2010, **45**, 283-287.
11. K. Isoda, T. Hasezaki, M. Kondoh, Y. Tsutsumi and K. Yagi, *Die Pharmazie - An International Journal of Pharmaceutical Sciences*, 2011, **66**, 278-281.
12. K. L. Aillon, Y. Xie, N. El-Gendy, C. J. Berkland and M. L. Forrest, *Advanced Drug Delivery Reviews*, 2009, **61**, 457-466.
13. A. M. Alkilany, P. K. Nagaria, C. R. Hexel, T. J. Shaw, C. J. Murphy and M. D. Wyatt, *Small*, 2009, **5**, 701-708.
14. D. P. Stankus, S. E. Lohse, J. E. Hutchison and J. A. Nason, *Environ Sci Technol*, 2011, **45**, 3238-3244.
15. M. P. Monopoli, D. Walczyk, A. Campbell, G. Elia, I. Lynch, F. Baldelli Bombelli and K. A. Dawson, *Journal of the American Chemical Society*, 2011, **133**, 2525-2534.
16. I. Lynch and K. A. Dawson, *Nano Today*, 2008, **3**, 40-47.
17. O. Bar-Ilan, R. M. Albrecht, V. E. Fako and D. Y. Furgeson, *Small*, 2009, **5**, 1897-1910.
18. C. Grabinski, N. Schaeublin, A. Wijaya, H. D' Couto, S. H. Baxamusa, K. Hamad-Schifferli and S. M. Hussain, *ACS Nano*, 2011, **5**, 2870-2879.
19. R. J. Griffitt, L. Jing, G. Jie, J.-C. Bonzongo and D. S. Barber, *Environmental Toxicology & Chemistry*, 2008, **27**, 1972-1978.
20. Y. Pan, S. Neuss, A. Leifert, M. Fischler, F. Wen, U. Simon, G. Schmid, W. Brandau and W. Jahnen-Dechent, *Small*, 2007, **3**, 1941-1949.
21. Y. S. Chen, Y. C. Hung, I. Liao and G. S. Huang, *Nanoscale research letters*, 2009, **4**, 858-864.
22. R. Klaper, J. Crago, J. Barr, D. Arndt, K. Setyowati and J. Chen, *Environmental Pollution*, 2009, **157**, 1152-1156.

23. D. A. Arndt, M. Moua, J. Chen and R. Klaper, *Environmental science & technology*, 2013.
24. G. S. Terentyuk, G. N. Maslyakova, L. V. Suleymanova, B. N. Khlebtsov, B. Y. Kogan, G. G. Akchurin, A. V. Shantrocha, I. L. Maksimova, N. G. Khlebtsov and V. V. Tuchin, *Journal of Biophotonics*, 2009, **2**, 292-302.
25. J. F. Hillyer and R. M. Albrecht, *Journal of Pharmaceutical Sciences*, 2001, **90**, 1927-1936.
26. K. Yin Win and S.-S. Feng, *Biomaterials*, 2005, **26**, 2713-2722.
27. C. Foged, B. Brodin, S. Frokjaer and A. Sundblad, *International Journal of Pharmaceutics*, 2005, **298**, 315-322.
28. M. S. Cartiera, K. M. Johnson, V. Rajendran, M. J. Caplan and W. M. Saltzman, *Biomaterials*, 2009, **30**, 2790-2798.
29. O. F. Karatas, E. Sezgin, O. Aydin and M. Culha, *Colloids and surfaces. B, Biointerfaces*, 2009, **71**, 315-318.
30. A. Albanese, P. S. Tang and W. C. W. Chan, *Annual Review of Biomedical Engineering*, 2012, **14**, 1-16.
31. A. E. Nel, L. Mädler, D. Velegol, T. Xia, E. M. V. Hoek, P. Somasundaran, F. Klaessig, V. Castranova and M. Thompson, *Nature Materials*, 2009, **8**, 543-557.
32. L. Truong, T. Zaikova, E. K. Richman, J. E. Hutchison and R. L. Tanguay, *Nanotoxicology*, 2012, **6**, 691-699.
33. A. Albanese and W. C. W. Chan, *ACS Nano*, 2011, **5**, 5478-5489.
34. S. B. Lovern and R. Klaper, *Environmental Toxicology and Chemistry*, 2006, **25**, 1132-1137.
35. A. M. Alkilany and C. J. Murphy, *Journal of nanoparticle research : an interdisciplinary forum for nanoscale science and technology*, 2010, **12**, 2313-2333.
36. A. Ostrowski, T. Martin, J. Conti, I. Hurt and B. Harthorn, *Journal of Nanoparticle Research*, 2009, **11**, 251-257.
37. A. Kroll, M. H. Pillukat, D. Hahn and J. Schnekenburger, *European Journal of Pharmaceutics and Biopharmaceutics*, 2009, **72**, 370-377.
38. C. J. Murphy, A. M. Gole, J. W. Stone, P. N. Sisco, A. M. Alkilany, E. C. Goldsmith and S. C. Baxter, *Accounts of Chemical Research*, 2008, **41**, 1721-1730.
39. K. Kenison Falkner and J. M. Edmond, *Earth and Planetary Science Letters*, 1990, **98**, 208-221.
40. K. B. Krauskopf, *Economic Geology*, 1951, **46**, 858-870.
41. A. M. Alkilany, S. E. Lohse and C. J. Murphy, *Accounts of Chemical Research*, 2012, **46**, 650-661.
42. J. Aaron, E. de la Rosa, K. Travis, N. Harrison, J. Burt, M. JosÈ-Yacamòn and K. Sokolov, *Opt. Express*, 2008, **16**, 2153-2167.
43. Calander, *Current analytical chemistry*, 2006, **2**, 203-211.
44. G. F. Paciotti, L. Myer, D. Weinreich, D. Goia, N. Pavel, R. E. McLaughlin and L. Tamarkin, *Drug Delivery*, 2004, **11**, 169-183.
45. D. Pissuwan, T. Niidome and M. B. Cortie, *Journal of Controlled Release*, 2011, **149**, 65-71.
46. C. Corti and R. Holliday, *Gold Bull*, 2004, **37**, 20-26.

47. N. Khlebtsov and L. Dykman, *Chemical Society reviews*, 2011, **40**, 1647-1671.
48. S. E. Lohse, J. R. Eller, S. T. Sivapalan, M. R. Plews and C. J. Murphy, *ACS Nano*, 2013, **7**, 4135-4150.
49. N. R. Jana, L. Gearheart and C. J. Murphy, *Langmuir*, 2001, **17**, 6782-6786.
50. S. F. Sweeney, G. H. Woehrle and J. E. Hutchison, *Journal of the American Chemical Society*, 2006, **128**, 3190-3197.
51. A. Gole and C. J. Murphy, *Chemistry of Materials*, 2004, **16**, 3633-3640.
52. C. J. Ackerson, P. D. Jadzinsky and R. D. Kornberg, *Journal of the American Chemical Society*, 2005, **127**, 6550-6551.
53. T. K. Sau and C. J. Murphy, *Langmuir*, 2004, **20**, 6414-6420.
54. G. H. Woehrle, J. E. Hutchison, S. Özkar and R. G. Finke, *Turkish Journal of Chemistry*, 2006, **30**, 1-13.
55. J. W. McMahon and F. H. Rigler, *Limnology and Oceanography*, 1965, **10**, 105-113.
56. EPA, *Standard operating procedure for moderately hard reconstituted water*, SoBran, Dayton, OH, USA, 2003.
57. U. S. E. P. Agency, in *SoBran*, Dayton, OH, USA, Editon edn., 2003.
58. W. Haiss, N. T. K. Thanh, J. Aveyard and D. G. Fernig, *Analytical Chemistry*, 2007, **79**, 4215-4221.
59. C. J. Orendorff and C. J. Murphy, *The Journal of Physical Chemistry B*, 2006, **110**, 3990-3994.
60. in *211*, OECD/OCDE, USA, Editon edn., 1998, pp. 1-21.
61. W. P. Wuelfing, S. M. Gross, D. T. Miles and R. W. Murray, *Journal of the American Chemical Society*, 1998, **120**, 12696-12697.
62. C. J. Orendorff, T. M. Alam, D. Y. Sasaki, B. C. Bunker and J. A. Voigt, *ACS Nano*, 2009, **3**, 971-983.
63. B. Nikoobakht and M. A. El-Sayed, *Langmuir*, 2001, **17**, 6368-6374.
64. S. Renault, M. Baudrimont, N. Mesmer-Dudons, P. Gonzalez, S. Mornet and A. Brisson, *Gold Bull*, 2008, **41**, 116-126.
65. S. Harper, C. Usenko, J. E. Hutchison, B. L. S. Maddux and R. L. Tanguay, *Journal of Experimental Nanoscience*, 2008, **3**, 195-206.
66. A. Asati, S. Santra, C. Kaittanis and J. M. Perez, *ACS Nano*, 2010, **4**, 5321-5331.
67. Y. Yang, J. Wang, H. Zhu, V. L. Colvin and P. J. Alvarez, *Environmental Science & Technology*, 2012, **46**, 3433-3441.
68. E. C. Cho, J. Xie, P. A. Wurm and Y. Xia, *Nano Letters*, 2009, **9**, 1080-1084.
69. S. D. Conner and S. L. Schmid, *Nature*, 2003, **422**, 37.
70. A. Verma and F. Stellacci, *Small*, 2010, **6**, 12-21.
71. S. B. Lovern, H. A. Owen and R. Klaper, *Nanotoxicology*, 2008, **2**, 43-48.
72. J. P. García-Camero, M. Núñez García, G. D. López, A. L. Herranz, L. Cuevas, E. Pérez-Pastrana, J. S. Cuadal, M. R. Castellort and A. C. Calvo, *Chemosphere*.
73. E. Ying and H.-M. Hwang, *Science of The Total Environment*, 2010, **408**, 4475-4481.

74. M. W. Katrina, M. M. Lisa, C. Z. Richard, J. T. Barbara, J. K. Norman, D. Q. Ryan, B. Somnath, G. T. Justin, G. P. Joel and D. T. Brian, *Toxicological Sciences*, 2009, **107**, 553-553.
75. W. H. De Jong, W. I. Hagens, P. Krystek, M. C. Burger, A. J. A. M. Sips and R. E. Geertsma, *Biomaterials*, 2008, **29**, 1912-1919.
76. D. Ebert, 2005.
77. B.-T. Lee and J. F. Ranville, *Journal of Hazardous Materials*, 2012, **213–214**, 434-439.
78. C. M. Flaherty and S. I. Dodson, *Chemosphere*, 2005, **61**, 200-207.
79. M. Knops, R. Altenburger and H. Segner, *Aquatic Toxicology*, 2001, **53**, 79-90.

SUPPORTING INFORMATION REFERENCES

1. Y. Tan, S. Jin and R. J. Hamers, *Journal of Physical Chemistry C*, 2013, **117**, 313-320.
2. P. E. Laibinis, C. D. Bain and G. M. Whitesides, *Journal of Physical Chemistry*, 1991, **95**, 7017-7021.
3. S. Tanuma, C. J. Powell and D. R. Penn, *Surface and Interface Analysis*, 1993, **20**, 77-89.

CHAPTER 2 TABLES

Table 1. AuNP characterization as synthesized.

AuNP Sample	SPR λ max (nm)	dcore (nm)	Dh (nm)	ζ -Potential (mV)
CTAB -AuNRs	512, 778	50 x 14	20.7 \pm 0.5	16.7 \pm 1.5
PAH-AuNPs	524	4.7 \pm 1.2	17.9 \pm 0.9	17.9 \pm 0.9
Cit-AuNPs	518	4.9 \pm 1.4	12.8 \pm 1.2	-15.3 \pm 1.5
MPA-AuNPs	512	3.8 \pm 1.1	8.0 \pm 1.2	-18.5 \pm 1.3

Table 2. AuNP characterization in daphnid media.

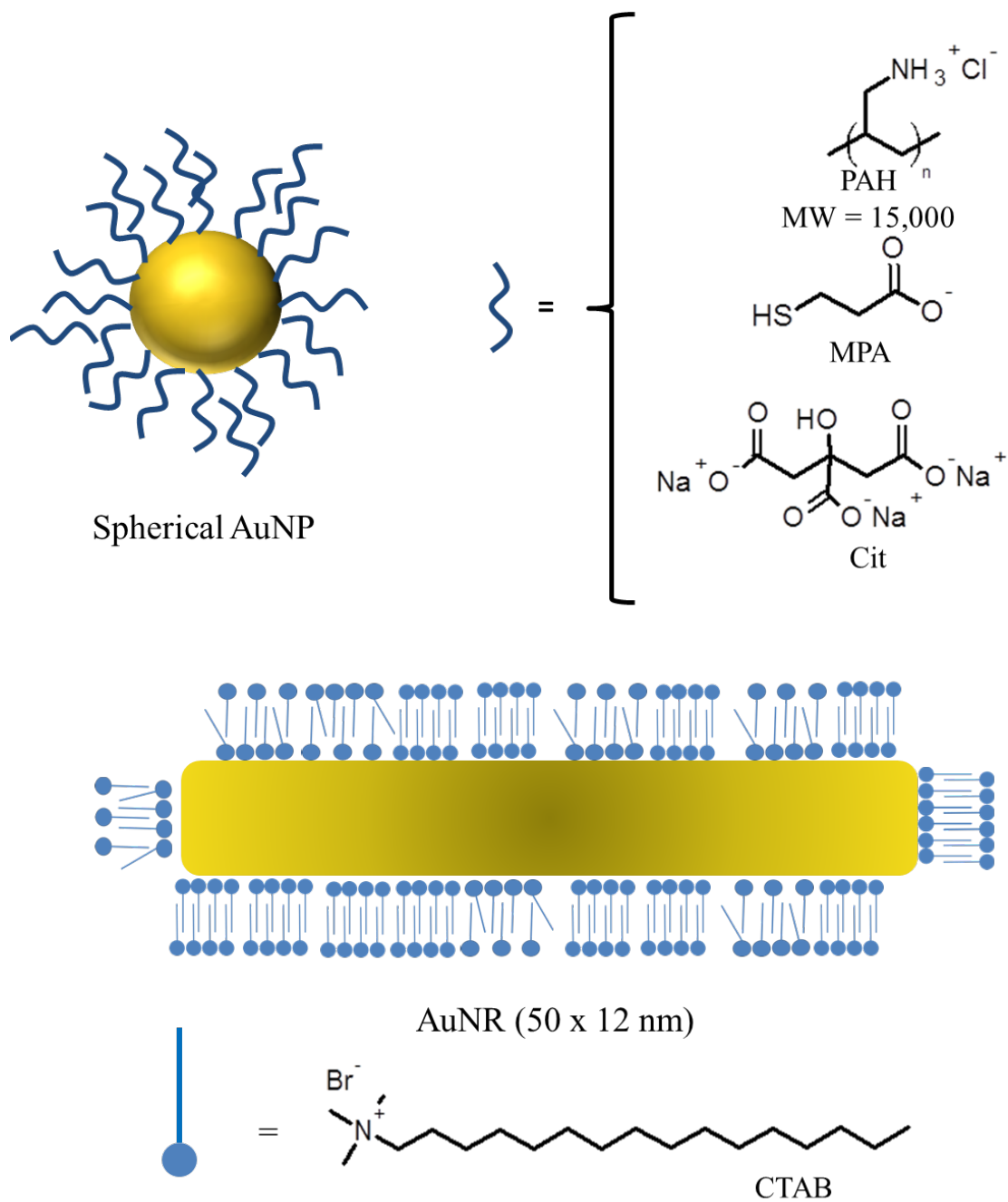
AuNP Sample	Time (h)	Dh (nm)	Z-Potential (mV)
CTAB-AuNRs	0	16.6 ± 2.0	28.1 ± 1.6
CTAB-AuNRs	48	17.5 ± 0.2	27.7 ± 1.8
PAH-AuNPs	0	52.8 ± 1.7	11.8 ± 5.2
PAH-AuNPs	48	55.9 ± 4.1	20.4 ± 0.4
Cit-AuNPs	0	21.9 ± 0.9	-15.3 ± 1.5
Cit-AuNPs	48	90.8 ± 5.9	-5.6 ± 0.2
MPA-AuNPs	0	50.7 ± 1.1	-9.1 ± 5.3
MPA-AuNPs	48	750.6 ± 8.2	-11.0 ± 1.0

Table 3. AuNP ligand density determined by XPS.

AuNP Sample	Measured density
CTAB-AuNR	7.6 x 10¹⁴ and 1.39 x 10¹⁵ molecules/cm²
PAH-AuNP	1.12 x 10¹⁵ formula units/cm²
Cit-AuNP	4.7 x 10¹⁴ molecules/cm²
MPA-AuNP	5.6 x 10¹⁴ molecules/cm²

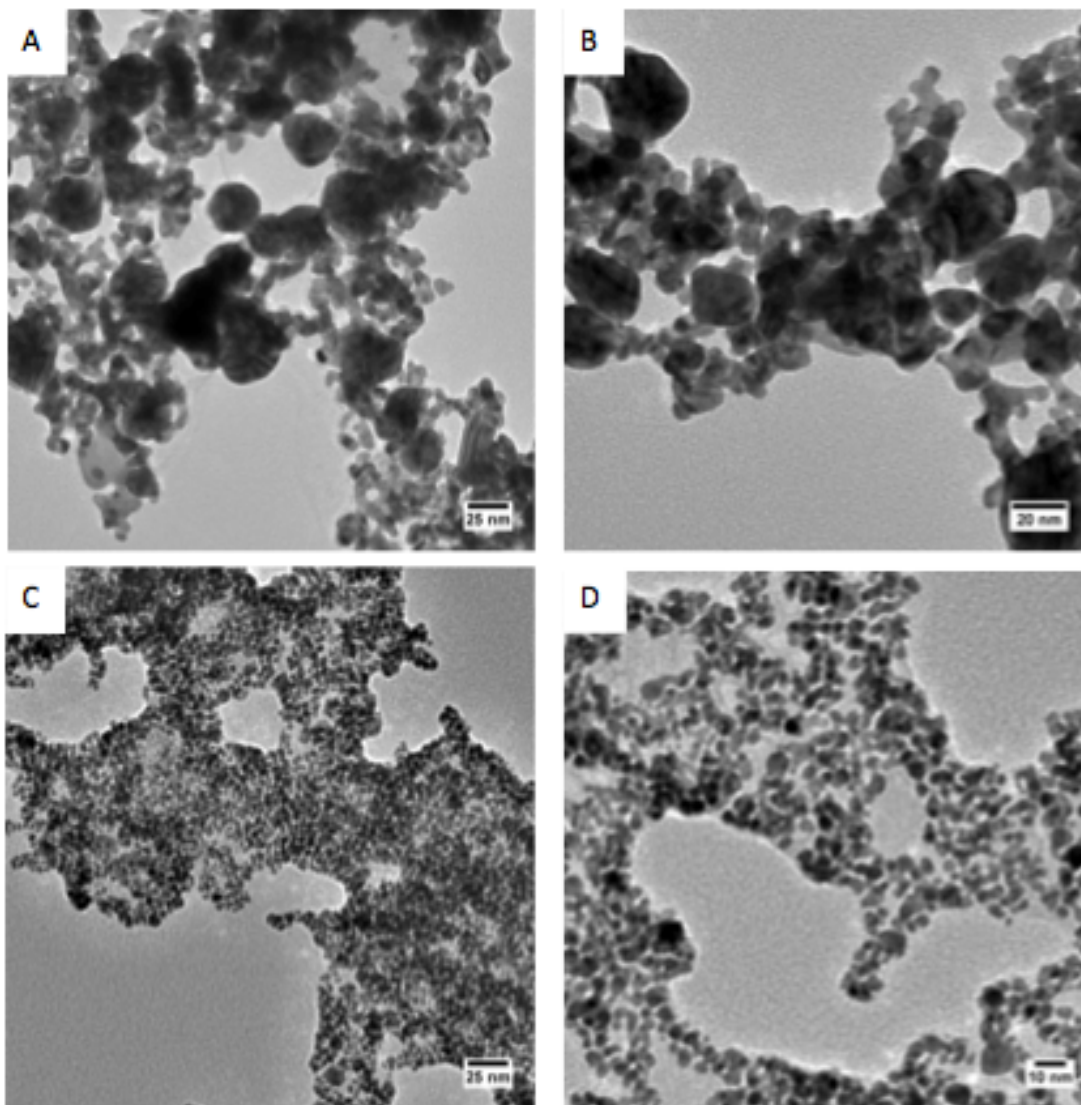
CHAPTER 2 FIGURES

Figure 1



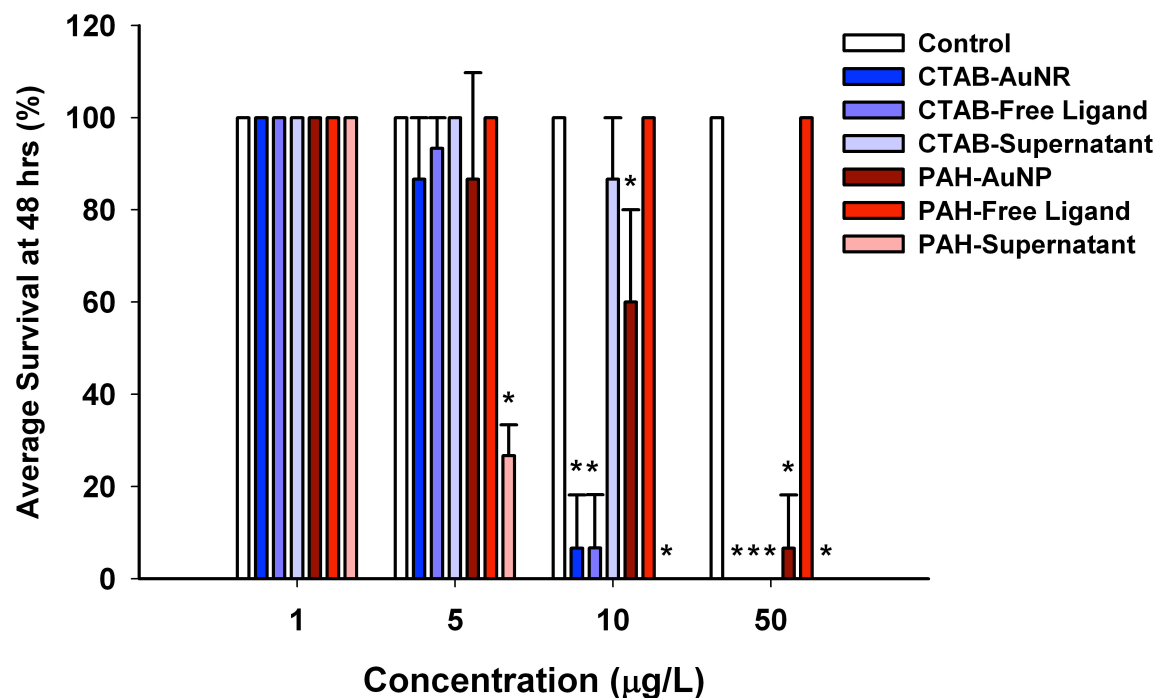
Schematic representation of functionalized AuNPs used in the toxicology study.

Figure 2



Agglomerated vs. aggregated AuNPs. TEM images of 4.0 nm Cit-AuNPs (A,B) and MPA-AuNPs (C,D) immersed in daphnid media for 48 h. Close examination of the aggregated Cit-AuNPs reveal that the AuNPs have formed extended networks of irregular nanowires and large particles. In contrast, the MPA-AuNPs remain dispersed, but closely associated individual AuNPs. Scale bar in (A) and (C) is 25 nm. Scale bar in (B) is 20 nm. Scale bar in (D) is 10 nm.

Figure 3



Effects of AuNPs, free ligands and impurities on daphnid acute mortality. Effects of AuNP exposure on (a) daphnid mortality after 48-hour exposure to 1, 5, 10 and 50 µg/L CTAB or PAH-AuNPs, free ligands and supernatants. Acute mortality evaluated by Mann-Whitney U test for two independent samples. Asterix indicate significant difference from control ($p < 0.05$).

Figure 4a

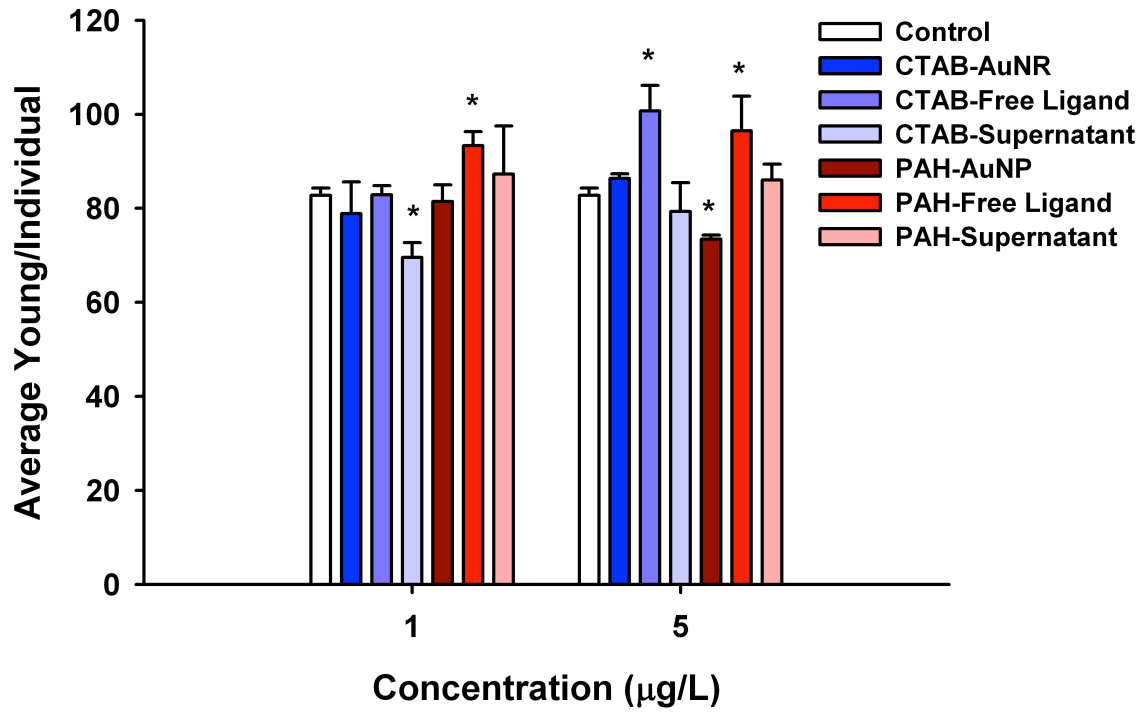
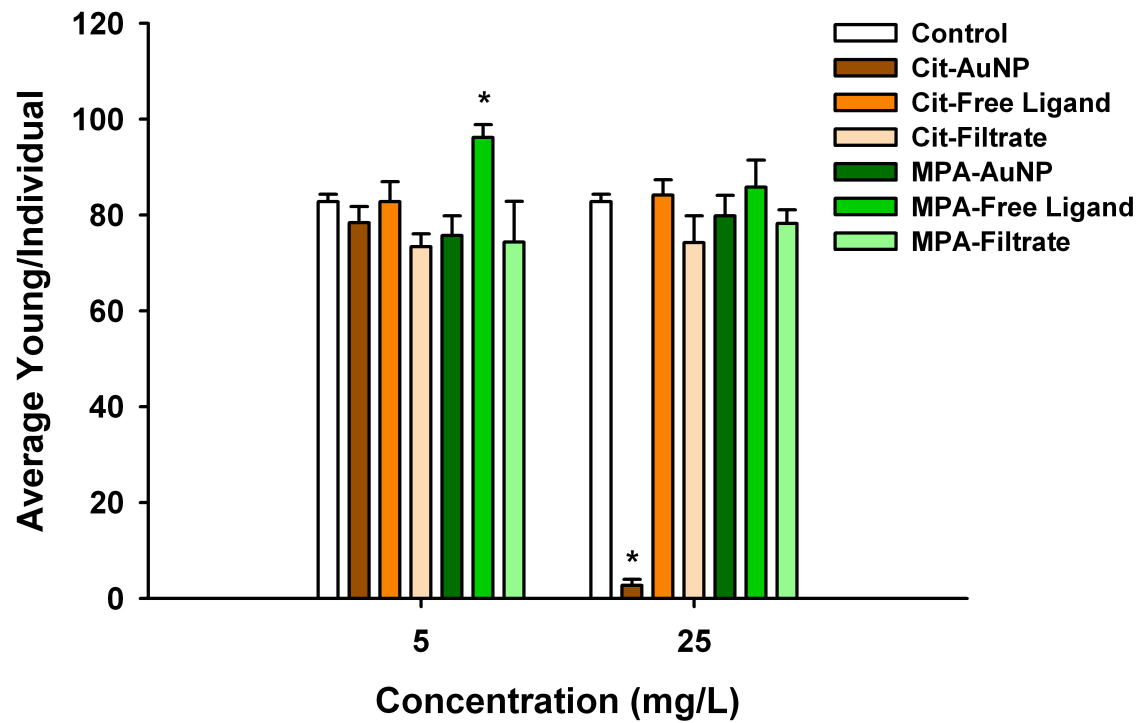
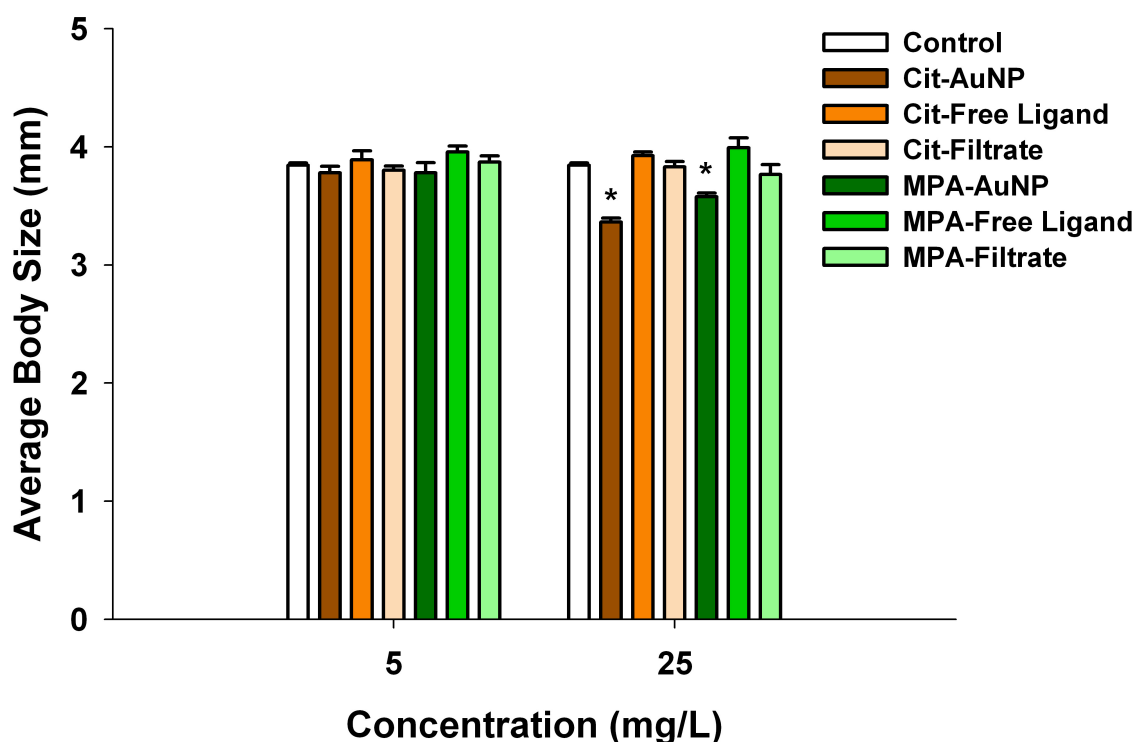


Figure 4b



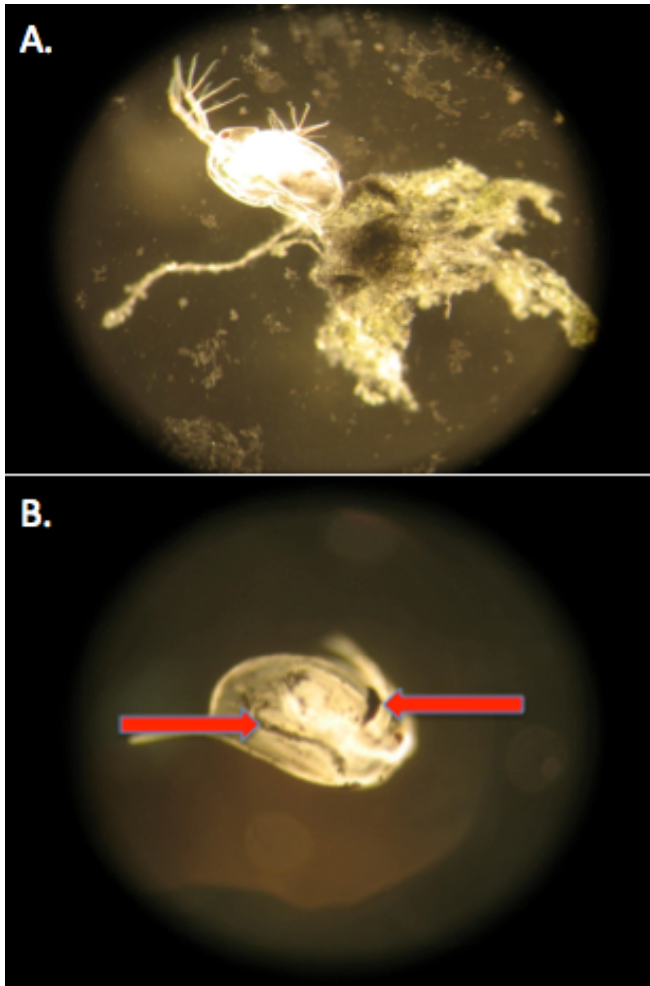
Effects of AuNPs, free ligands and impurities on daphnid reproduction in chronic assays. Effects of AuNP exposure on (a) daphnid reproduction after 21-day exposure to 1 and 5 $\mu\text{g/L}$ CTAB or PAH-AuNPs, free ligands and supernatants and (b) daphnid reproduction after 21-day exposure to 5 and 25 mg/L Cit or MPA-AuNPs, free ligands and filtrates. Reproduction evaluated by Mann-Whitney U test for two independent samples. Asterix indicate significant difference from control ($p < 0.05$)

Figure 5



Effects of AuNPs on daphnid body size after 21-day chronic exposure. Effects of AuNP exposure on daphnid body size after 21-day exposure to 5 and 25 mg/L of Cit or MPA AuNPs. Body size evaluated by Mann-Whitney U test for two independent samples. Asterix indicate significant difference from control ($p < 0.05$).

Figure 6



Nanoparticles adhered to daphnid exoskeleton. Cit-AuNPs adhered to a daphnid carapace. (a) Cit-AuNP algal-agglomerate adhering to daphnid carapace. (b) Cit-AuNPs are ingested by daphnids but may also be found on the outside of the daphnids.

CHAPTER 2 SUPPORTING INFORMATION

Surface chemistry, charge and ligand type impact the toxicity of gold nanoparticles to

Daphnia magna

Number of supporting information pages: 10

Number of Figures: 7

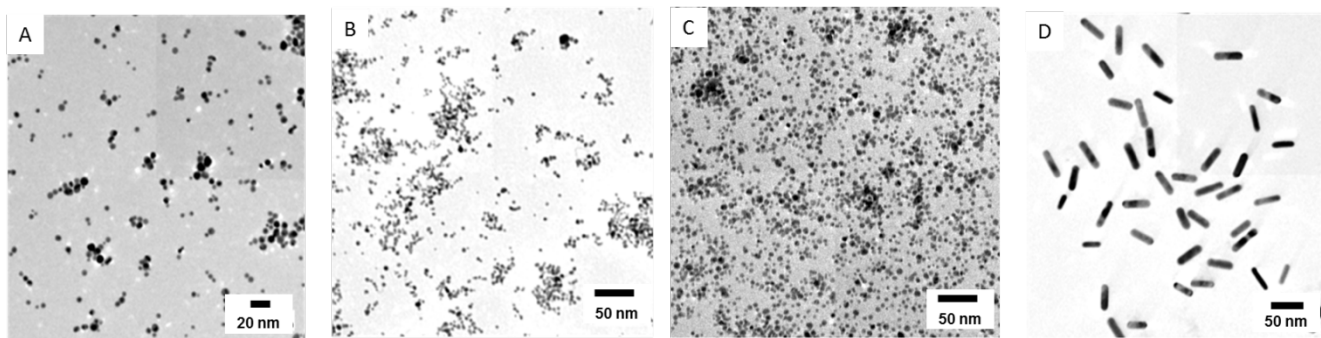


Figure S1. Representative TEM images of functionalized AuNPs used in this study.

(A) 4.7 nm PAH-AuNPs, scale bar 20 nm. **(B)** 4.9 nm Cit-AuNPs, scale bar 50 nm. **(C)** 3.8 nm MPA-AuNPs, scale bar 50 nm. **(D)** 50x12 nm CTAB-AuNRs, scale bar 50 nm.

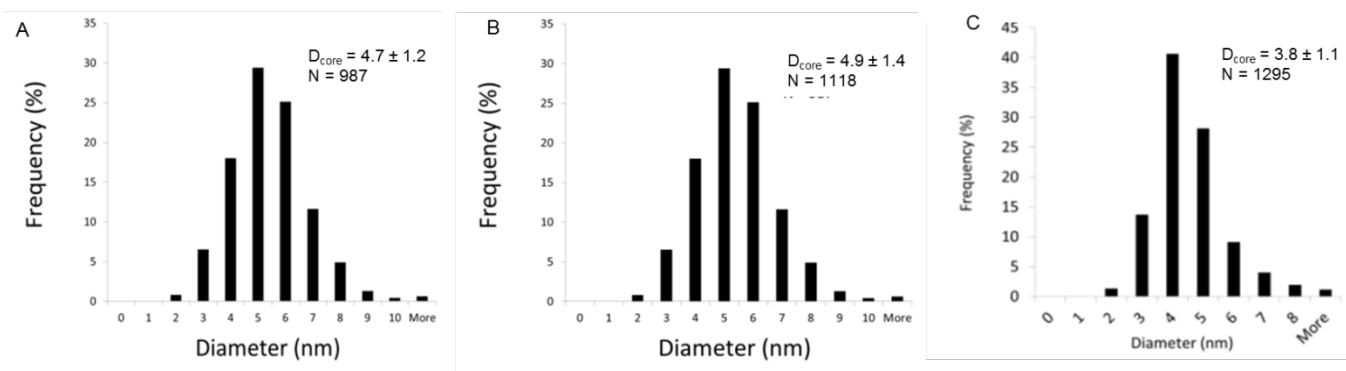


Figure S2. Size distribution data for the spherical AuNPs used in the study. **(A)** 4.7 nm PAH-AuNPs. **(B)** 4.9 nm Cit-AuNPs. **(C)** 3.8 nm MPA-AuNPs.

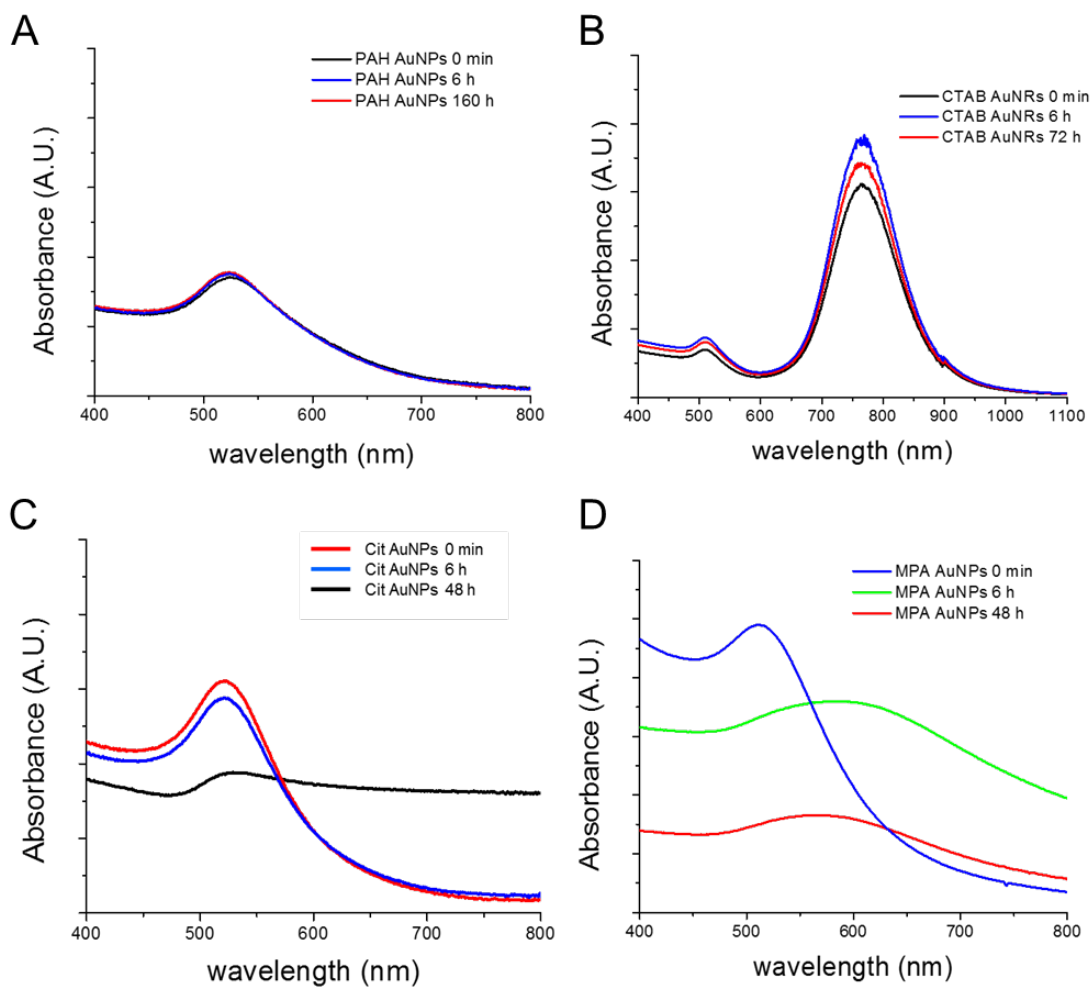


Figure S3. UV-vis spectroscopy analysis of AuNP stability in *Daphnia* media over an extended period of time. Exposure conditions mirror the acute toxicity exposures. **(A)** PAH-AuNPs, **(B)** CTAB-AuNRs, **(C)** Cit-AuNPs, and **(D)** MPA-AuNPs. [AuNP] = 10.0 nM, [CTAB-AuNR] = 2.0 nM.

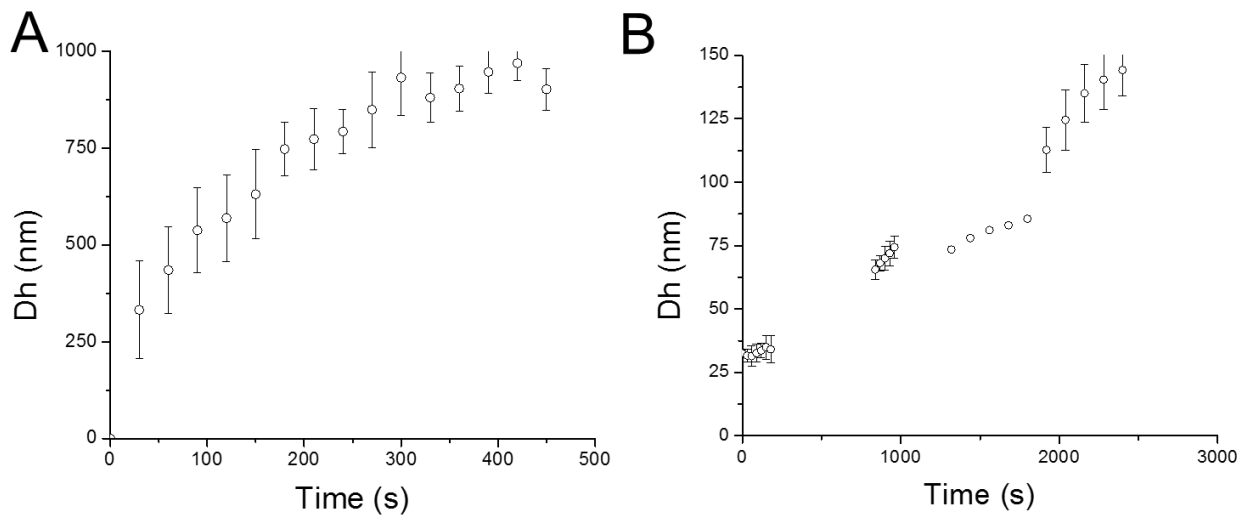


Figure S4. DLS analysis of **(A)** MPA-AuNP aggregation and **(B)** Cit-AuNP aggregation in *Daphnia* media over various incubation times. Incubation conditions mirrored the acute toxicity exposures. [AuNP] = 10.0 nM.

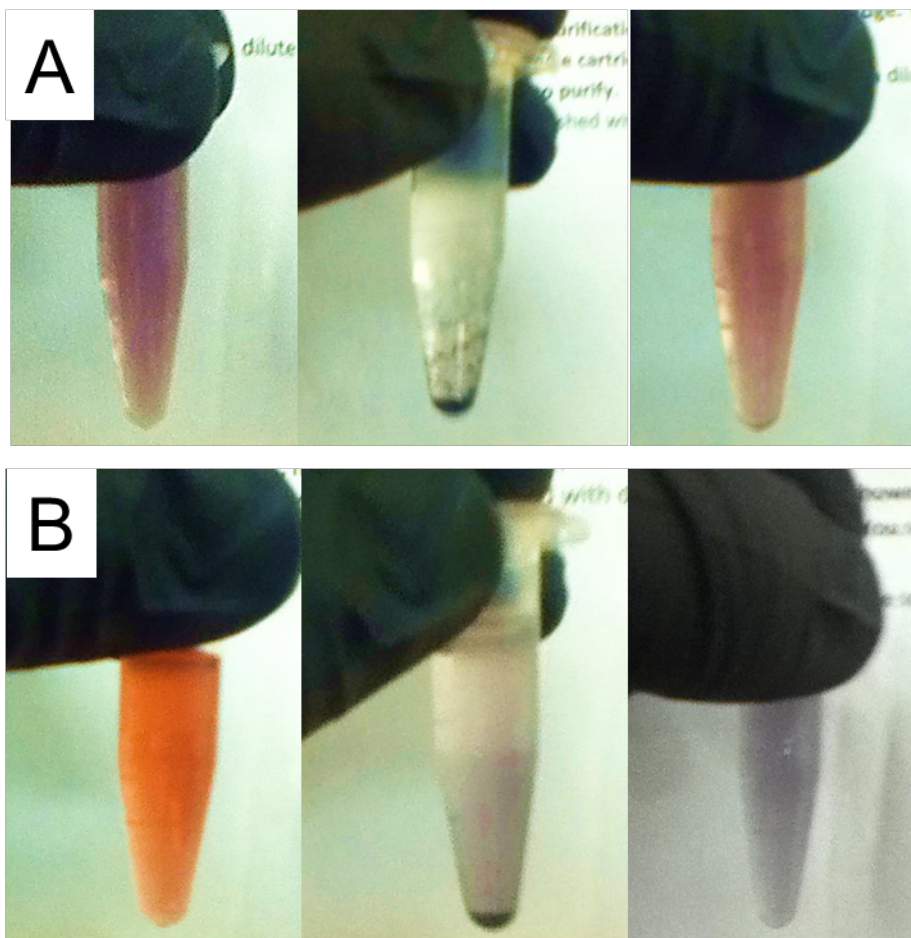
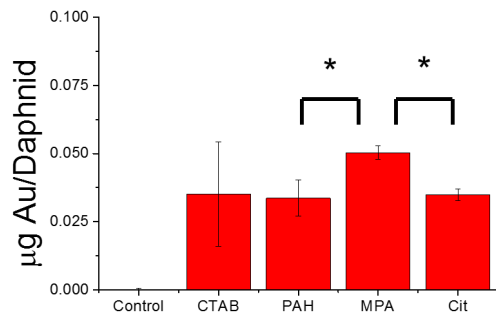
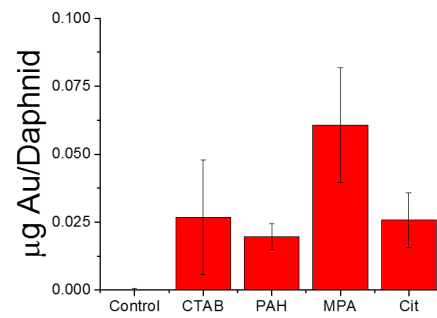
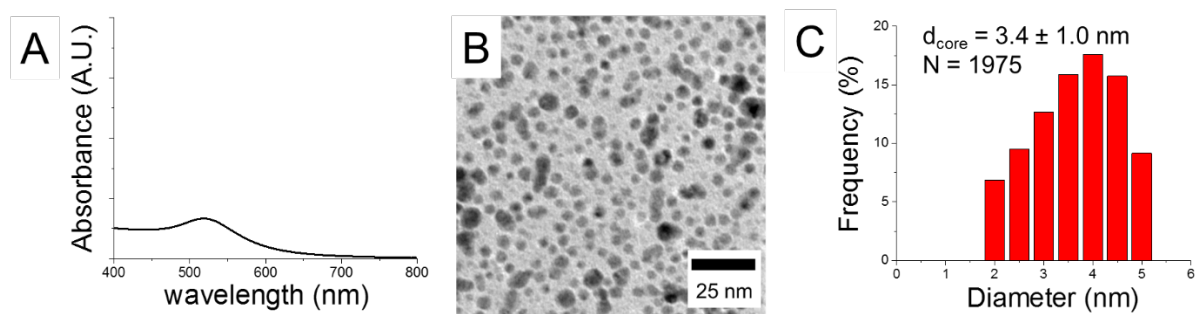


Figure S5. Negatively-charged AuNPs (Cit, MPA-AuNPs) aggregate over 48 h in Daphnia media, however the MPA-AuNPs and the Cit-AuNPs show different aggregation behaviors. (A) MPA-AuNPs aggregate reversibly. After 48 hours, the initial red-brown solution (left) gives way to black clumps of aggregated AuNPs (middle), but after gentle agitation, the red-brown solution color is restored (right). (B) In contrast, Cit-AuNPs aggregate irreversibly. The red-orange solution (left) gives way to a black-blue aggregate (middle). Even after vortex mixing and sonication, the solution remains blue-black; the AuNPs have not re-suspended.

A**B**

Daphnia ICP-MS uptake data for AuNPs used in the study. Difference between the AuNP uptake in *Daphnia* (A) vs the uptake after iodide etching with a 100mM iodide solution (B). Asterix indicate significant difference ($p < 0.05$) between treatments marked by bracket.

Figure S7



UV-vis absorption spectrum **(A)** of the PAH-AuNP supernatant. Representative TEM image **(B)** of the concentrated PAH-AuNP supernatant, and the corresponding size distribution analysis **(C)**.

CHAPTER 3

Gene expression response of the Gram-negative bacterium *Shewanella oneidensis* and the water flea *Daphnia magna* exposed to functionalized gold nanoparticles

Published in:

Royal Society of Chemistry, Environmental Science: Nano

DOI: 10.1039/C5EN00037H

Bozich, J. S.^{a,†}, Qiu, T. A.^{b,†}, Lohse, S. E.^c, Vartanian, A. M.^c, Jacob, L. M.^c, Meyer, B. M.^a, Gunsolus, I. L.^a, Niemuth, N. J.^b, Murphy, C. J.^c, Haynes, C. L.^b, Klaper, R. D^{a*}.

^a School of Freshwater Sciences, University of Wisconsin Milwaukee, 600 E.

Greenfield Ave, Milwaukee, WI 53204

^b Department of Chemistry, University of Minnesota, 207 Pleasant St SE, Minneapolis,

MN 55455

^c Department of Chemistry, University of Illinois at Urbana-Champaign, 600 S.

Mathews Ave, Urbana, IL 61801

*Corresponding Author

rklaper@uwm.edu, Phone (work): 414-382-1713, Fax: 414-382-1705

(Received 07 Mar 2015, Accepted 02 Aug 2015)

Abstract

Nanoparticle (NP) physiochemical properties have been shown to be important determinants of NP interactions with biological systems. Due to both nanomaterial diversity and environmental complexity, a mechanistic understanding of how physiochemical properties affect NP/organism interactions will greatly aid in the accurate assessment and prediction of current and emerging NP-induced environmental impacts. Herein, we investigated key biological apical endpoints, such as viability, growth, and reproduction and the expression of genes associated with related molecular pathways in response to exposure gold nanoparticles (AuNPs) functionalized with either positively charged ligands, polyallylamine hydrochloride, or negatively charged with mercaptopropionic acid ligands, in two model organisms, the bacterium *Shewanella oneidensis* MR-1 and the water flea *Daphnia magna*. By linking changes in molecular pathways to apical endpoints, potential biomarkers for functionalized AuNP impacts were identified in both organisms. Specifically, *act* was identified as a potential biomarker in *D. magna* and 16S as a potential biomarker in *S. oneidensis*. We also revealed that changes in molecular pathways induced by ligand-NP combination were strongly dependent upon the type of ligand on NP surface and the effects from their respective ligand alone might predict these effects from the ligand-NP combination. Lastly, we identified that it is possible to identify similar pathways provoked upon NP exposure across organisms. This study shows that molecular pathways will help elucidate mechanisms for NP toxicity that are predictive of adverse environmental outcomes.

Introduction

Engineered nanoparticles (NPs) are being produced to enhance a wide range of societally beneficial applications, from energy storage capacities and material durability to medical therapeutics and water treatment devices¹⁻³. These applications are possible because of the novel physiochemical properties NPs display, such as high surface area and reactivity as well as distinct surface chemistries, composition and size distributions. It is, however, these same size-dependent physiochemical properties that may influence their biocompatibility⁴⁻⁸. For example, size, shape and core composition have been thought to mediate receptor-ligand binding rates, cellular phagocytosis, exocytosis and cytotoxicity⁹⁻¹². Other studies suggest that NP surface charge is the main determinant of biological interactions, with positively charged particles being more toxic than negatively or neutrally charged particles¹³⁻¹⁸.

These classifications of critical features that determine biological impact all focus on the NPs themselves. The differences in response across organisms or cell types is less often considered despite the fact that toxicological evaluations of the biological impacts caused by engineered NPs have revealed a wide range in responses across cell types or organisms considered¹⁹⁻²³. For example, Sohaebuddin et al. (2010)²⁴ demonstrated that cell type determines the extent of response to nanomaterials with different composition and size. In another study using ZnO NPs, the EC₅₀ differed by orders of magnitude for *V. fischeri*, *D. magna* and *T. platyurus*²⁵. Variation across cell systems and organisms makes it difficult to develop a common understanding of the properties of nanomaterials that may determine toxicity. Even for well-studied chemicals, such as pesticides, models that use general acute endpoint

data to predict impacts often inaccurately estimate concentrations that cause effects across similar chemicals, and rarely are applicable across organisms^{26, 27}. These studies have shown that a more mechanistic understanding of the impacts of chemicals at sublethal doses provides a more accurate description of impacts and better data for modeling these effects across species. The goal of this project is to achieve a more mechanistic understanding of NP/organism interactions to facilitate efficient prediction of the impact nanotechnology will have on environmental health. Linking specific molecular mechanisms that are impacted by NPs across organisms will not only greatly aid in assessing the potential environmental impact of these materials but is also crucial to informing NP design for safe and sustainable development of nanotechnologies.

Currently, the major proposed molecular mechanism for NP toxicity is oxidative stress^{4, 28-31}. However, the exposures that produce oxidative stress in many studies are well above what is estimated to be the current or future environmental concentrations; long-term low dose exposures are the more likely scenario^{32, 33}. In addition, the molecular mechanisms responsible for coping with oxidative stress are triggered upon exposure to a wide range of chemical species^{34, 35} and are a natural biological response that does not necessarily lead to an adverse outcome³⁶. The focus on oxidative stress and lethal dose exposures makes it difficult to uncover other mechanisms that may have a greater predictive power for the environmental impact of NPs. Sublethal concentration-based exposures allow the cell to have a more natural perturbation by the contaminant that triggers subtle, but potentially specific, molecular

responses^{37, 38}. It is these more realistic exposure scenarios that will uncover more mechanism-based information to predict meaningful impacts across species.

Molecular biomarkers provide a sensitive indicator of the response of an organism to stressors such as exposure to a toxicant in addition to providing information on the mechanisms that are impacted by exposure^{37, 38}. Mechanistic information that can be tied to larger impacts on reproduction for example enhance the possibility of predicting negative outcomes where standardized toxicological tests, although valuable, have limited the ability to accurately predict the impact of emerging contaminants. Overreliance on these methods has led to risk assessment failures³⁹. Developing such candidates for molecular biomarkers for NP toxicity will greatly aid in the rapid assessment and impact prediction for current and emerging nanomaterials across a wide range of organisms. Previously developed biomarkers, for example, vitellogenin, have been used for the successful determination of adverse outcomes of some classes of endocrine disruptors and their impacts on vertebrate reproduction⁴⁰⁻⁴². Metallothioneins are biomarkers used in organisms to detect toxic metal ion exposure, and they are known to respond to a wide range of metal-based contaminants associated with environmental pollution⁴³. Heat shock proteins, indicative of proteotoxic stressors, indicate sublethal cellular damage and respond in a dose-dependent manner to environmental stressors⁴⁴. Molecular biomarkers that provide mechanistic insight for grouping nanomaterials by their molecular level interactions, especially if they apply to effects seen across species, would provide insight for grouping nanomaterials by their molecular level interactions. Furthermore, they may

indicate both nonspecific and specific modes of action as well as underlying mechanisms for toxicity of NPs with particular physiochemical properties.

In this study, we examined several candidate biomarkers in two model species, the bacterium *Shewanella oneidensis* and the invertebrate *Daphnia magna*, that are associated with pathways of importance in these two species and determined how their expression related to the biological impacts of exposure to gold NPs (AuNPs) with positively or negatively charged surfaces. *Shewanella oneidensis* (MR-1) is an environmentally beneficial gram-negative bacterium with a unique metal-reducing capability to respire heavy metals; *S. oneidensis* plays an important role in the cycling of metal elements in the ecosystem as well as the bioremediation of toxic elements⁴⁵. *Daphnia magna* is a designated toxicology and toxicogenomics model organism by multiple agencies (OECD, NIH and EPA), and is an environmentally relevant freshwater invertebrate that composes an integral part of freshwater food webs⁴⁶. AuNPs were chosen as a model NP in this study due to the chemical inertness of the gold core and our ability to readily control size⁴⁷, shape⁴⁸ and surface functionalization⁴⁹. Two ligands were used for AuNP functionalization, positively charged polyallylamine hydrochloride (PAH) and negatively charged mercaptopropionic acid (MPA).

We explored genes in various molecular pathways in our two model organisms. Pairs of genes selected from each organism were selected to represent pathways encoding for similar cellular functions in two organisms, including oxidative stress, xenobiotic detoxification, protein folding, cellular electron transport, and cellular maintenance. In addition, genes in pathways related to reproduction in *D. magna* and

to cell division, DNA repair and extracytoplasmic stress in *S. oneidensis* were also investigated. The goal was to determine 1) how the exposure to NPs with differing surface properties impacted each organism and how this differed from their respective ligand controls 2) if gene expression for these pathways were an indication of impacts seen in each organism 3) if exposure duration altered effects and gene expression measurements and if acute measurements of gene expression would provide an indication of chronic impacts 4) if gene expression for similar pathways across organisms would provide biomarkers that were predictive across species. The NPs used in this study were quantitatively and qualitatively characterized prior to and after exposure to assay media to aid us in understanding how alterations in NP physical properties may impact molecular pathways. Overall, this work aims to link molecular pathways to NP characteristics in two distinct environmentally relevant organisms.

Methods

Functionalized AuNP synthesis and characterization

All materials were used as received, unless otherwise noted. Gold tetrachloroaurate trihydrate ($\text{HAuCl}_4 \cdot 3\text{H}_2\text{O}$), sodium borohydride (NaBH_4), trisodium citrate, 3-mercaptopropionic acid (MPA), and polyallylamine hydrochloride (PAH; M_w 15, 000 g/mol) were obtained from Sigma Aldrich. Ultrapure deionized water was prepared using a Barnstead NANOPURE water filtration system. PALL Minimate tangential flow filtration capsules for AuNP purification with 50 kD pore size was obtained from VWR. Transmission electron microscopy grids were obtained from PELCO (SiO on copper mesh).

The 4.7 (\pm 1.5)-nm-diameter PAH-AuNPs were prepared by polyelectrolyte wrapping of \sim 4-nm-diameter citrate-coated AuNPs. The (4.3 \pm 1.3)-nm-diameter MPA-AuNPs were prepared by direct synthesis. After synthesis, measuring and counting using TEM images determined size distributions. Detailed descriptions of the AuNP syntheses are given below.

PAH-AuNPs (4.7 \pm 1.5 nm). As a first step in synthesis of PAH-AuNPs citrate AuNPs were synthesized using previously reported procedures^{47, 47, 47, 47}. In an *aqua regia*-cleaned round-bottomed flask, 5.0 mL of aqueous gold tetrachloraurate hydrate (HAuCl₄•3H₂O, 10.0 mM) was combined with 1.5 mL of aqueous 0.1M sodium citrate and diluted to a final volume of 400 mL with ultrapure deionized water. The reaction mixture was stirred vigorously for 10 min. An aqueous solution of ice-cold 10.0 mM sodium borohydride (30.0 mL) was then added to the reaction mixture, while stirring continued. Following borohydride addition, the solution rapidly changed color to a deep brown, and then red-orange over the course of the first 10 minutes of stirring. The resulting AuNP solution was then stirred for a further 3.0 hours. The crude 4 nm Cit-AuNPs were then concentrated using a diafiltration apparatus, prior to polyelectrolyte wrapping⁵⁰. Cit-AuNPs were then wrapped with polyallylamine hydrochloride (PAH) to prepare 4 nm PAH- AuNPs, as previously described⁵¹. Briefly, the concentrated Cit-AuNP solution was dispersed in 20.0 mL of a 1.0 mM aqueous sodium chloride solution to give a final AuNP concentration of approximately 20.0 nM . To each 20.0 mL of polyelectrolyte wrapping solution, 500 μ L of 15 000 M_w PAH (10.0 mg/mL) dissolved in 1.0 mM NaCl was then added. The wrapping solution was briefly mixed at

vortex briefly and left to stand for 16 h. The PAH-AuNPs were subsequently purified by centrifugation and washing (55 min. at 18,894 rcf), in ultrapure deionized water. The purified PAH-AuNPs were then concentrated in a diafiltration membrane⁵⁰.

MPA-AuNPs (4.3 ± 1.3 nm). MPA-stabilized AuNPs were prepared by direct synthesis with sodium borohydride according to previously reported methods⁵². Briefly, a 500 mL aqueous solution of HAuCl₄ (1.5 mM) and MPA (3.0 mM) was prepared using ultrapure deionized water in aqua regia-cleaned round-bottomed flask. The pH of the growth solution was adjusted to approximately 8.5 by the addition of dilute aqueous sodium hydroxide, and stirred at vortex for 10 min. 10.0 mL of a 0.1 M aqueous sodium borohydride solution was then added to the reaction mixture. The combined solutions rapidly changed color to a deep orange-brown, and the reaction mixture was stirred for a further 3 hours. The thiol-stabilized AuNPs were then concentrated and purified by diafiltration (40.0 volume equivalents of ultrapure deionized water in a 50 kD membrane).

AuNP characterization and analysis

Synthesized functionalized AuNPs were characterized in Milli-Q water, bacteria growth medium, and *Daphnia* medium using various analytical techniques, including TEM for absolute sizes (JEOL 2100 Cryo TEM), dynamic light scattering for hydrodynamic diameter (Brookhaven ZetaPALS), zeta-potential for surface charge (Brookhaven ZetaPALS), and UV-Vis localized surface plasmon resonance (LSPR)

spectroscopy for particle concentration and aggregation (Mikropack DH-2000 UV-vis-NIR Spectrometer).

Free ligand suspensions

Free ligands, MPA and PAH (M_w 15, 000 g/mol), were obtained from Sigma Aldrich. MPA and PAH ligands are readily soluble in water and do not require a co-solvent for dispersion. The ligands were dissolved into Milli-Q water at a maximum concentration of 50 mg/L and diluted accordingly for free ligand toxicity control experiments.

***Shewanella oneidensis* MR-1 cultivation and cell respiration assay**

***S. oneidensis* MR-1 cultivation.** *S. oneidensis* MR-1 was obtained from Professor Jeffery Gralnick, University of Minnesota Department of Microbiology and was stored at -80°C before use. Bacteria were inoculated onto a LB broth agar plate and incubated at 30°C for 24 hours or until visible colonies formed. A minimal medium consisting of salts and buffering agent was used in this study. 0.68 g NaCl, 0.3 g KCl, 0.285 g $\text{MgCl}_2 \cdot 6\text{H}_2\text{O}$, 0.3975 g Na_2SO_4 , 0.15 g NH_4Cl , and 2.383 g HEPES (4-(2-hydroxyethyl) piperazine-1-ethanesulfonic acid) were dissolved in 1 liter of Milli-Q water. After autoclaving and cooling down, 0.0125 g Na_2HPO_4 and 0.0056 g CaCl_2 were added per liter. Right before use, 1.86 mL sodium DL-lactate syrup (60% w/w, Sigma-Aldrich) was mixed with the minimal medium to make 100 mL of the final growth medium containing 129 mM sodium DL-lactate. Lactate was used as an additional carbon source to promote bacterial growth. Colonies formed on agar plates

were inoculated into the minimal medium with lactate in sterile culture tubes and grown in a 32 °C orbital shaker at 300 rpm until OD₆₀₀ ~0.25, the maximal optical density that *Shewanella oneidensis* MR-1 can reach in the minimal medium with lactate.

Monitoring *S. oneidensis* oxygen uptake. The oxygen uptake of the bacteria population over time was monitored using a PF-8000 aerobic/anaerobic respirometer system (Respirometer Systems and Applications, LLC). Bacteria were grown in minimal medium with lactate until it reached OD₆₀₀ ~0.25 and diluted 1:10 into that growth medium supplied with NP/ligands in reaction vessels that were kept in a 32 °C water bath. Exposures of PAH-NPs were conducted at 30, 100, and 5000 µg/L, and exposures of PAH ligand were 30, 100, 300, 600, 1000, 2000 and 5000 µg/L. In all subsequent experiments and comparisons, a ten-fold mass concentration of PAH free ligand and an equivalent mass concentration of MPA free ligand were used as ligand controls, which was calculated to be an overestimate of possible total free ligand present in the suspension (See SI)⁵³. A tube filled with 1 mL 30% (w/w) KOH solution was inserted into each reaction vessel to absorb carbon dioxide generated from cell respiration. The consumption of oxygen was compensated by continuous oxygen injection to keep the pressure constant in the headspace of the reaction vessels. Oxygen uptake was recorded every 10 minutes automatically for 24-48 hours by the instrument. The first derivative of oxygen uptake was plotted to identify the maximal oxygen uptake rate and the time of that maximum. To represent each cell oxygen uptake trace with a single value, the ratio of maximal oxygen uptake rate to the time when it reached maximal rate was calculated following the equation below:

$$\text{Ratio} = \frac{\text{Maximal rate } (\frac{mg}{h})}{\text{Time to reach maximal rate (h)}}$$

The ratio was then normalized to the average of control groups and represented as a percentage, where 100% indicates no inhibition of cell oxygen uptake.

***Daphnia magna* cultivation and biological assays**

***D. magna* cultivation.** Populations used in this experiment were cultivated at the UW-Milwaukee School of Freshwater Sciences in the R. Klaper laboratory. *Daphnia* neonates used for the gene expression assays were collected from populations maintained in moderately hard reconstituted water (MHRW) incubated at 20°C on a 16:8 light/dark cycle as designated by EPA protocols⁵⁴. *Daphnia* breeding populations were held at a concentration of 14 adult *Daphnia* per 1 L of media in glass beakers and were discarded once adults reached 28 days old. *Daphnia* were fed 50 mL freshwater algae (*Pseudokirchneriella subcapitata*) at an algal density of 400,000 algal cells/mL and 15 mL of dissolved alfalfa (*Medicago sativa*). Alfalfa stock was prepared by suspending 405 mg of Alfalfa in 50 mL milli-Q water after 15 minutes of stirring and 5 minutes of centrifugation at 3,829 RCF.

***D. magna* acute assay.** Acute survival assays were carried out in a 48 hr static exposure. All exposures used 5 *Daphnia* neonates (24 - 48 hours old) per 100 mL of MHRW (control), NPs, or free ligands suspended in MHRW, bringing the total volume to 100 mL. A minimum of three replicates was carried out for each treatment, and survival was determined as percentage alive at 48 hrs. Exposures were carried out to determine sublethal concentrations of NPs and free ligands. Concentrations tested for

NPs and free ligands are: 1, 5, 10, 50, 100 µg/L for PAH-AuNPs and PAH free ligand and 1, 5, 10 and 25 mg/L for MPA-AuNPs and MPA free ligand.

***D. magna* chronic assay.** *Daphnia* chronic exposures used 5 *Daphnia* neonates (24 - 48 hours old) exposed to NPs or ligands for 21 days in a static renewal exposure, and triplicate assays were performed for each condition. A total of 5 neonates were placed in 94 mL of MHRW (control) or NPs/ligands where full media change out occurred three times per week. In chronic exposures, daphnids are supplemented with 4 mL of algae (*Selenastrum capricornitum*) and 2 mL of alfalfa (*Medicago sativa*) at each media exchange to bring the total volume to 100 mL. Concentrations tested in the chronic assay were: 1 and 5 µg/L for PAH-AuNPs and PAH free ligand and 5 and 25 mg/L for MPA-AuNPs and MPA free ligand. Reproduction and mortality were measured at each media exchange, and body size was recorded at the end of the exposure.

Reproductive exposures adhered to the mortality and reproduction guidelines designated by the OECD (OECD guidelines 1998). Daphnids were kept at a concentration of 5 daphnids per 100 mL, and results were normalized to controls (i.e. daphnia exposed to only MHRW) to account for changes in reproduction and body size as these replicate exposures took place over a period of several months.

Gene expression exposures and RNA preservation

Gene expression exposures were performed in parallel with bacterial oxygen uptake and *D. magna* survival and reproduction assays.

S. oneidensis. Colonies from agar plates were inoculated in minimal medium supplied with 129 mM lactate until the bacterial suspension reached $OD_{600} \sim 0.25$. The bacterial suspension was adjusted to $OD_{600} = 0.2$ before AuNPs were added. The sublethal dosages, 30 $\mu\text{g/L}$ of PAH-AuNPs and 300 $\mu\text{g/L}$ of PAH ligand, and 5 mg/L of MPA-AuNPs/ligands, were primarily used for gene expression studies; in addition, a 100 $\mu\text{g/L}$ dose of PAH-AuNPs was used to investigate two biomarker candidates, in order to provide further evidence to link molecular pathways to inhibition of bacterial oxygen uptake. After exposure, the bacterial suspension was incubated on a 32°C orbital shaker at 300 rpm for 1 hour or 6 hours. Cells were harvested by centrifuging at 1,500 g for 10 minutes, and then the pellets were sufficiently re-suspended into either 200 μL (PAH-AuNP/ligand) or 1 mL (MPA-AuNP/ligand) of RNAzol®RT (Molecular Research Center, Inc.) for cell lysis and RNA preservation.

D. magna. *Daphnia* neonates (24 - 48 hours old) were exposed to NPs and free ligands in an acute exposure lasting 24 hours. All exposures used 10 neonates per 100 mL of MHRW (control) or NPs or free ligands suspended in MHRW (treatment) bringing the total volume to 100 mL. Exposures were carried out at sublethal concentrations of NPs/free ligands between 5-1000 mg/L depending on the NP/free ligand being considered. Sublethal concentrations for acute exposures were chosen based on previous study (Bozich et al. 2014). Greater than three replicates within an experiment were carried out for each treatment and concentration tested. At the end of the exposure duration, daphnids were collected and put in a 1.5 mL RNase-free

ependorf tube corresponding to their replicate number. Excess liquid was removed and daphnids were immediately flash frozen in liquid nitrogen and stored at -80°C to await further processing. For *D. magna* chronic exposures, exposures were carried out at sublethal concentrations of NPs/free ligands between 5-5000 mg/L, and daphnids were collected at the end of the 21-day exposure period and preserved using the same method as the acute exposure samples. All samples RNA were extracted using TRIzol® for cell lysis and RNA preservation.

RNA extraction, reverse transcription and real-time quantitative PCR

A Direct-zol™ RNA MiniPrep kit (Zymo Research) was used for total RNA isolation and purification by spin columns. The manufacturer's recommended protocol was followed using a centrifugation speed of 12,000 ×g with an on-column DNase I treatment at 30°C for 15 minutes. RNA was finally eluted from the column at 16,000 ×g for 1 minute. Total RNA was characterized using a Thermo Scientific NanoDrop 8000 and an Agilent 2100 Bioanalyzer for quality control.

Total RNA was reverse transcribed into cDNA following the manufacturer's protocols. Briefly, 100 ng of total RNA were incubated in the presence of either random primers (Promega) for *S. oneidensis* or oligo(dT)₁₅ primer (Promega) for *D. magna* at 65°C for 5 minutes. After cooling on ice for 1 minute, the SuperScript III reverse transcriptase, DTT, and RNaseOUT™ recombinant ribonuclease inhibitor (Life Technologies) were added into the mixture followed by incubation at 25°C for 5 minutes (this step was only for random primers), 50°C for 60 minutes, and 70°C for 15 minutes for primer extension. Once synthesized, cDNA were stored at -20°C.

Target genes were chosen for both *S. oneidensis* and *D. magna*. Four pairs of genes in similar pathways related to stress response in the two organisms were selected, including *gst* (*S. oneidensis*)/*gst* (*D. magna*, same order for the following pairs) in xenobiotic detoxification, *nqrF/nadh* for electron transport, *katB* and *sodB/cat* for oxidative stress attenuation, and *ibpA/hsp70* for heat shock response. To link to apical endpoints, the *vtg* gene for *D. magna* reproduction and *ftsK* for bacterial cell division were also examined. Genes for actin (*act*) in *D. magna* and for 16S ribosomal RNA (16S) and RNA polymerase (*rpoA*) in *S. oneidensis* were monitored to consider NP/ligand impacts on basic organism machinery. In addition, stress response genes including *pspB* for extracytoplasmic stress, *sodB* for oxidative stress, and *radA* for DNA repair were also examined in *S. oneidensis*. Table 1 shows a full list of genes along with their corresponding functions.

Primers for real-time quantitative PCR were designed by the PrimerQuest Tool (Integrated DNA Technologies). Two sets of primers were designed for each gene, and the one with efficiency closest to 1 was chosen to be the primer for subsequent real-time PCR. Table 1 includes a full list of primers used in this study.

Real-time quantitative PCR (qPCR) was performed on a StepOnePlus™ Real-Time PCR System (Life Technologies) using SYBR Green as the fluorescent intercalating dye (iTaq™ Universal SYBR® Green Supermix, Bio-Rad). For each qPCR reaction, cDNA and primers were mixed with the fluorescence dye following the manufacturer's protocol. Starting with an initial 10 min denaturation at 95°C, real-time PCR repeated 40 cycles of amplification, each of which was 15 s at 95°C followed by 30 s at 60°C.

Fluorescence of SYBR Green was detected at the end of each cycle. All qPCR experiments were done in technical duplicates.

NORMA-Gene analysis of qPCR data

Real-time quantitative PCR data were processed by the Miner⁵⁵ program and NORMA-Gene algorithm⁵⁶. Miner applies an objective analysis scheme to obtain the dynamic fluorescence threshold (R), threshold cycle number (C_t), and efficiency (E) for each qPCR reaction, instead of using the same threshold for all reactions. Data of normalized reporter signal (R_n) versus cycle number were extracted from amplification data exported from the StepOnePlus™ software as the input to the Miner program to obtain R, C_t, and E values for each reaction. R₀, the initial fluorescent reporter signal, was calculated based on the equation below:

$$R_0 = R \times (1 + E)^{-C_t}$$

Due to the change in housekeeping genes throughout experiments, NORMA-Gene, a qPCR normalization method based on target gene data, was applied to normalize the gene expression data and reduce the variation among replicates rather than using a single housekeeping gene. Using this technique the geometric means of R₀ values of technical duplicates were calculated as the average and were put into the NORMA-Gene workbook generously provided by Dr. Yuya Hayashi. Normalized R₀ values, which were the output of NORMA-Gene algorithm, were then further normalized to control groups by dividing the normalized R₀ of treated groups by the geometric mean of normalized R₀ values of control groups to obtain the relative fold change.

Statistical analysis

The normalized ratios from oxygen uptake traces were further subjected to statistical analysis. No normality and outliers were considered within this data set due to the limited sample size ($N < 5$). The two-tailed Student's t-test was performed on treated samples versus their respective control group with $\alpha = 0.05$. GraphPad Prism (GraphPad Software, Inc.) was used for statistical analysis.

Data from *Daphnia* acute studies failed to meet the assumptions of normality. Therefore, the effects of NP and free ligand exposures on *Daphnia* survival, were compared to controls using the Student's t-test for two-independent samples ($N < 3$). Impacts on daphnid reproduction and body size were assessed using one-way ANOVA with Tukey's multiple comparison tests after normality and variance homogeneity were determined ($N > 3$). One round of statistically determined outliers was removed, and treatments were deemed significantly different than controls at probability value < 0.05 . SPSS (IBM 2013).

The relative fold change values of *S. oneidensis* gene expression were \log_2 -transformed followed by the combination of control groups. Outliers were identified and excluded from the data set (ROUT algorithm, $Q = 1.0\%$, Prism GraphPad), and post-hoc Tukey's tests after ANOVA were performed to determine statistical significance among different treatments at one time point and one gene of interest. For the 16S and *sodB* genes upon 100 $\mu\text{g/L}$ PAH-AuNP exposure, as there was only one treatment, an unpaired t-test was used instead of ANOVA. Again, normality was not

tested due to the limited sample size ($N < 6$). GraphPad Prism was used to perform statistical analysis.

The relative gene expression data from *Daphnia* short-term and long-term gene exposures were normalized to controls and \log_2 transformed to fit a normal distribution. Outliers were removed prior to statistical analysis. Significant differences in relative expression were determined using one-way ANOVA with Tukey's multiple comparison tests after normality and variance homogeneity were determined ($p < 0.05$) ($N > 3$). SPSS (IBM 2013) was used to interpret data.

Results

Nanoparticle characterization

TEM analysis of absolute size showed that the two AuNPs had very similar core size, while the hydrodynamic diameter of PAH-AuNPs in water was larger than MPA-AuNPs, possibly due to the polyelectrolyte wrapping (Table 2). It was notable that MPA-AuNPs showed increased hydrodynamic diameter and a peak shift in UV-vis extinction upon resuspension in growth medium, indicating the aggregation of MPA-AuNPs, though the MPA-AuNPs still retained a negative surface charge in the growth medium (Table 2). The aggregation may result from elevated ionic strength in the growth medium or the pH change from slightly acidic Milli-Q water (pH ~ 6.3) to neutral growth medium (pH ~ 7.2). This aggregation might lead to altered NP toxicity, as previous studies have revealed^{19, 57}. Similar behavior was not observed on PAH-AuNPs, indicating more stability of PAH-AuNPs in growth medium than MPA-AuNPs (Table 2).

***Shewanella oneidensis* oxygen uptake**

PAH-AuNPs significantly affected bacterial oxygen uptake at 100 µg/L (unpaired t-test, $t=9.895$, $df=5$, $p < 0.05$) while its corresponding free ligand control, 1 mg/L of PAH free ligand elicited similar inhibition compared to control groups (unpaired t-test, $t=4.222$, $df=6$, $p < 0.05$) (Figure 1(c)). A concentration of 30 µg/L of PAH-AuNPs was chosen as the sublethal dose as this concentration produced no inhibition; this NP dose was paired with the 10-fold dose, 300 µg/L, as the corresponding PAH free ligand control. MPA-AuNPs did not inhibit bacterial oxygen uptake at the highest dose tested (5 mg/L), while the respective 5 mg/L of MPA free ligand demonstrated oxygen uptake inhibition ($t=9.713$, $df=2$, $p < 0.05$) (Figure S2).

As the oxygen uptake reflects bacterial population growth, the doubling time of bacterial growth at the exponential phase was calculated based on oxygen uptake traces (See SI). Results showed that *S. oneidensis* had an average doubling time between 2 and 3 hours in the growth medium used in this study; thus, 1 hour was chosen as a time point for short-term exposure and 6 hour for long-term exposure in the subsequent gene expression studies.

***S. oneidensis* gene expression response**

At the sublethal exposure dosages, differential expression levels of ten genes in *S. oneidensis* were observed at both 1-hour and 6-hour time points when comparing treatment and control. The general pattern of gene expression is summarized in the heat map (Figure 2(a)).

In all cases, the differences in gene expression appear to be dominated by ligand rather than NP exposure. All changes in gene expression induced by ligand-NP combination were accompanied by the changes in their respective free ligand control, including 16S (PAH, $F = 18.33$, $df = 22$, $p < 0.0001$), *rpoA* (PAH, $F = 8.177$, $df = 31$, $p = 0.0001$), *pspB* (PAH, $F = 8.198$, $df = 22$, $p < 0.0003$), and *ibpA* (MPA, $F = 36.92$, $df = 22$, $p < 0.0001$) at 1-hour exposure (Figure 3(a)), and *sodB* (PAH and MPA, $F = 10.06$, $df = 22$, $p < 0.0001$) at 6-hour exposure (Figure 3(b)). Exceptions are two NP-specific effects that were observed in *sodB* (PAH, $F = 7.543$, $df = 22$, $p < 0.05$) at 1-hour exposure and 16S (PAH, $F = 3.238$, $df = 22$, $p < 0.05$) at 6-hour exposure, where the free ligand control did not elicit similar effects as NPs when compared to control. For these two genes, *S. oneidensis* was exposed to a higher dosage (100 $\mu\text{g/L}$) of PAH-AuNPs to explore the link to inhibition of oxygen uptake (Figure 4). The 16S gene expression decreased upon 100 $\mu\text{g/L}$ PAH-AuNP exposure at 6-hour exposure (unpaired t-test, $t=38.67$, $df=7$, $p<0.0001$), while *sodB* gene expression did not show a significant difference compared to the control group at 1-hour exposure.

The difference in ligand-NP combination appears to be important in determining the differential gene expression pattern at 1-hour exposure, as only down-regulation was observed in PAH-AuNP exposure but only up-regulation was observed in MPA-AuNP exposure (Figure 2(a)). However, upon 6-hour exposure, the ligand-NP combination did not determine the gene expression pattern, as only down-regulation was observed for all treatments, regardless of the type of ligand (Figure 2(a)).

Time frame is also an important factor in terms of gene expression response, as differential gene expression responses were observed at different time points. In the response to PAH-AuNP/ligand exposure, effects that were observed in the *rpoA* and *pspB* genes at 1-hour exposure diminished by the 6-hour exposure timepoint. More interestingly, for MPA-AuNP/ligand exposure, the expression level compared to control at 6-hour exposure appeared to be opposite of the responses in 1-hour exposure, especially for MPA ligand exposure.

***Daphnia magna* acute toxicity**

NP surface functionalization played an important role in acute toxicity in the form of daphnid survival, with positively charged PAH-AuNPs being orders of magnitude more toxic than the negatively charged MPA-AuNPs (Figure 2(a)). PAH-AuNPs significantly affected daphnid mortality, eliciting 40% mortality at 10 µg/L ($U = 0, p < 0.05$)¹³. MPA-AuNPs did not significantly affect daphnid survival at the highest concentration tested, 25 mg/L (data not shown) ($p > 0.05$)¹³. The free ligands used in NP functionalization had no impact on daphnid survival at any concentration tested.

***Daphnia magna* chronic toxicity**

Ligand-NP combination is also important in governing the chronic impacts on daphnid reproduction. Of the two NPs tested, PAH-AuNPs significantly decreased daphnid reproduction over the 21-day chronic exposure (Figure 2(b)) while MPA-AuNPs did not (data not shown). PAH-AuNPs significantly decreased daphnid reproduction by 15% at the highest concentration tested, 5 µg/L ($F = 14.751, df = 23, p$

< 0.05). In comparison, PAH free ligand caused a statistically insignificant increase in daphnid reproduction at 50 µg/L. As previously reported, 5 mg/L MPA free ligand increased daphnid reproduction by 14% (U = 4, p < 0.05, data not shown)¹³.

***Daphnia magna* acute gene expression response**

After a 24 h acute exposure, NP functionalization is also an important factor in determining *Daphnia* response at the gene level when exposed to PAH and MPA-AuNPs, resulting in different gene expression patterns for *cat*, *nadh*, *vtg*, *gst* and *hsp70* (Figure 2). For *Daphnia* exposed to PAH-AuNPs, there was a significant 0.74 fold decrease in the relative expression of *hsp70* (F= 31.799, df= 49, P<0.05) compared to controls. *Daphnia* exposed to MPA-AuNPs caused a significant 1.36 fold increase for *hsp70* (F= 31.799, df= 49, P<0.05), 1.49 fold increase for *nadh* (F=29.066, df=55, p<0.05), 1.67 fold increase for *gst* (F=23.116, df=53, p<0.05) and 3.12 fold increase for *vtg* (F=11.556, df=47, p<0.05) over controls. MPA-AuNP-exposed *Daphnia* had significantly different gene expression patterns than *Daphnia* exposed to PAH-AuNPs for *nadh*, *vtg*, *gst* and *hsp70* (Figure 2 and 5). Notably, PAH-AuNPs caused a 0.33 fold increase in relative expression of *vtg* while MPA-AuNPs elicited a 3.12 fold increase in relative expression of *vtg* (F=11.556, df=47, p<0.05).

The impacts of free ligands used in particle functionalization closely follow the gene expression patterns observed for their respective functionalized NPs at 24 hrs (Figure 2). *Daphnia* exposed to the PAH ligand showed no statistical difference compared to *Daphnia* exposed to PAH-AuNPs for all genes tested except *cat* (F= 8.640, df=55, p<0.05) and *vtg* (F=11.556, df=47, p<0.05). Each gene that showed a

significant positive fold change in relative expression for *Daphnia* exposed to MPA-AuNPs also showed a significant fold change in relative expression for the MPA free ligand treatment and did not significantly differ between the two.

***Daphnia magna* chronic gene expression response**

Similar to the 24 hr acute exposure, AuNP surface functionalization played an important role in determining gene expression levels in *Daphnia* chronically exposed to AuNPs (Figure 2 and 5). For *Daphnia* exposed to PAH-AuNPs, there was a significant 1.33 fold decrease in the relative expression of *vtg* ($F=16.592$, $df=42$, $p<0.05$) and a significant 0.87 fold increase in the relative expression of *act* ($F=9.68$, $df=42$, $p<0.05$) over controls (Figure 5). MPA-AuNPs elicited a significant 1.24, 0.82 and 0.93 fold decreases in the relative expression of *hsp70* ($F=9.294$, $df=42$, $p<0.05$), *cat* ($F=18.128$, $df=44$, $p<0.05$) and *nadh* ($F=14.9$, $df=44$, $p<0.05$), respectively, compared to controls (Figure 2 and 5). Notably, for this treatment, there was a significant 2.2 fold increase in the relative expression of *vtg* ($F=16.592$, $df=42$, $p<0.05$) over controls (Figure 2). A significantly different gene expression response was observed for several genes when AuNP treatments were compared. PAH-AuNP treatment elicited a positive fold change in the relative expression of *cat*, *nadh* and *act* while MPA-AuNP elicited a negative fold for these same genes. The greatest difference between these two treatments was observed for *vtg*.

NP-specific impacts were observed in *Daphnia* chronically exposed functionalized AuNPs versus their respective PAH and MPA ligands as reflected in the gene expression patterns (Figure 2 and 5). PAH-AuNP and PAH ligand caused a

similar relative expression pattern in *Daphnia* for genes *gst*, *hsp70*, *vtg* and *nadh*, as no significant difference was observed among these conditions (Figure 2). However, PAH ligand caused 0.6 fold decrease in relative expression for *act* compared with the PAH-AuNP treatment that elicited a 0.98 fold increase in relative expression for *act* (F=9.68, df=42, p<0.05) (Figure 5). There were no significant differences between MPA ligand and MPA-AuNP treatments on *Daphnia* relative expression for all genes tested.

Discussion

The ligand-NP combinations used in this study determined the extent of organismal apical endpoint impacts. Both model organisms were impacted to a greater extent by positively charged ligand-NP combinations with differential sensitivities. PAH-AuNPs were determined to be 2-3 orders of magnitude more toxic than the MPA-AuNPs for both *S. oneidensis* and *D. magna*. MPA-AuNPs caused no acute mortality in *D. magna* or inhibition on *S. oneidensis* oxygen uptake at the highest concentration tested (25 mg/L for daphnids and 5 mg/L for bacteria (Figure S2))¹³. PAH-AuNPs elicited mortality in *D. magna* at concentrations as low as 10 µg/L and decreases in reproduction at 5 µg/L (Figure 1(a))¹³, while *S. oneidensis* started to show respiratory inhibition at 100 µg/L (Figure 1(c)). Electrostatic interactions could largely drive the differences in sensitivity to the differently charged particles, as both eukaryotes and prokaryotes have cell surfaces that are negatively charged^{58, 59}. It is thought that, due to electrostatic interactions, positively charged NPs are more likely to interact with cell surfaces than negatively charged NPs. Goodman et al. (2004)⁶⁰

observed similar differences in the toxicity of AuNPs functionalized with cationic and anionic side chains when exposed to mammalian cell lines and bacterial cells, and Feng et al.⁶¹ demonstrated a similar correlation between toxicity and NP-cell association where increased NP-cell association was found for positively charged NPs compared to negatively charged NPs in bacteria. In addition to electrostatic interactions, the low toxicity of MPA-AuNPs may be potentially explained by the high degree of aggregation of MPA-AuNPs experienced in both organisms' exposure media, thus reducing bioavailability (Table 2). Overall, similar differential toxicity of the two functionalized NPs were observed in our study in both model organisms, indicating these organisms may follow the same electrostatic mechanism for interacting with NPs despite having distinct membrane surface chemistry, and that the general response of whole organism may be extrapolated from the response of cell lines, although they differ in sensitivity.

The toxicity of select NPs may not be determined by their respective ligand control, which demonstrates NP-specific organismal impacts. The two model organisms showed differential sensitivities to positively-charged PAH-AuNPs; a NP-specific effect, that was unable to be replicated by the free ligand control, was observed in the impact of PAH-AuNPs to *D. magna*, but not to *S. oneidensis*. Based on bacterial oxygen uptake and *Daphnia* acute mortality results, the sublethal doses of PAH-AuNPs on *Daphnia* and *S. oneidensis* were chosen to be 5 µg/L and 30 µg/L, respectively. The differences in sensitivity observed for these two model organisms exposed to PAH-AuNPs could be attributed to the distinct differences in the cell surface chemistry of gram-negative bacteria and the aquatic eukaryotes. Besides the

cytoplasmic membrane, which are found in both bacterial and *Daphnia* cells, the gram-negative *S. oneidensis* bacterial cell also has an envelope that consists of a peptidoglycan-lipoprotein complex, periplasmic zone, and an outer membrane layer⁵⁸. The outer membrane layer is the first barrier that NPs would encounter, and this lipid bilayer retains various amounts of embedded lipopolysaccharides (LPS)⁵⁸. LPS are high molecular weight molecules with a basal lipid anchored in the lipid bilayer and a long negatively charged chain of polysaccharide. Recent work using *S. oneidensis* demonstrated that LPS is an important binding site for AuNPs (Jacobson and Gunsolus, et al. submitted⁶²). Compared to the animal cell membrane, the complex structure of the cell envelope in *S. oneidensis* may provide extra protection when NPs are in proximity to the cells, thus desensitizing bacterial cells to NP exposures. In addition, studies demonstrate that eukaryote cells have many more mechanisms for supramolecular and colloidal particle internalization (e.g. receptor mediated endocytosis, pinocytosis and phagocytosis) for both nano- and macro-sized particles, while very few studies show plausible evidence of internalization of nanomaterials into bacterial cells⁶³⁻⁶⁵. Furthermore, the manner by which multi and single-cellular organisms interact with NPs may also contribute to the difference in sensitivity. *Daphnia* actively filter their growth medium that leads to the accumulation of NPs both on and within their bodies while bacteria only passively interact with NPs through random encounters. The difference in how NP interact and accumulate in two organisms may also result in the NP-specific effect observed in *D. magna* but not in *S. oneidensis*. PAH-AuNPs resulted in a decrease in *Daphnia* survival (10 µg/L) while the respective PAH free ligand control (100 µg/L) did not show any mortality (Figure 1(a)).

However, when PAH-AuNPs elicited inhibition to bacterial oxygen uptake at 100 µg/L, the respective ligand control (1 mg/L) displayed a similar inhibition (Figure 1(c)). As *Daphnia* actively accumulate NPs in their bodies and may internalize NPs in cells, the body burden of AuNPs to *Daphnia* is expected to differ greatly with *S. oneidensis*, thus leading to the higher sensitivity and NP-specific effect in *Daphnia*. These biological differences and impacts of NP surface functionalization and free ligand type are further addressed by the presented gene expression study.

For *Daphnia*, gene expression revealed insight into potentially unique molecular pathways that may be impacted upon exposure to NPs and may explain the differences in toxicity across different ligand-NP combinations. In the responses induced by NPs on *Daphnia* gene expression, ligand-NP combination proved to be pivotal. In both acute and chronic assays, *Daphnia* exposed to PAH-AuNPs elicited a significantly different gene expression pattern compared with *Daphnia* exposed to MPA-AuNPs, despite the two NPs having the same gold core. These differences were notable in the 24 hr acute exposure for *hsp70*, *gst*, *vtg* and *nadh* and in the 21 day chronic assay for *hsp70*, *vtg*, *nadh*, *cat* and *act*. Amongst the genes that responded, a positive relative fold change for *act* was unique to the PAH-AuNP treatment and were expressed only after *Daphnia* were exposed for 21 days to this treatment. Actin (*act*) encodes for a protein important to cytoskeleton and muscle fibril production as well as other cell functions. Studies have linked an increase in protein concentration of actin as a compensatory mechanism to maintain muscular and cellular performance in times of environmental stress⁶⁶. In addition, studies have indicated a high binding affinity of microparticles for actin⁶⁷ and have shown that multiple NP types damage actin

filaments *in vitro*⁶⁸⁻⁷⁰. PAH-AuNPs could be potentially damaging muscle fibrils and cellular structure over long-term exposures in *Daphnia* and may be used as an indicator for stress to positively charged NPs, however, the relationship of this gene with apical endpoints impacted in *Daphnia* within this study remains unclear. *Daphnia* exposed to MPA-AuNPs only uniquely responded to the treatment with an increase in the relative fold change of *gst* at 24 hrs. This gene encodes for an enzyme glutathione S-transferase and is an important enzyme in xenobiotic detoxification as it conjugates compounds with glutathione and may be elevated in times of oxidative stress. Our previous studies observed *gst* induction in *Daphnia* dependent upon NP functionalization for fullerenes but only at concentrations that elicited significant mortality (> 5 mg/L)⁹. Like MPA-AuNPs, these NPs exhibited a high degree of aggregation and exhibited low toxicity in *Daphnia*. This may demonstrate an acute whole organismal response to a high amount of negatively charged NPs. Our more recent previous study examined adult daphnid guts exposed to 4 nm PAH and MPA-AuNPs and their ligands at low concentrations (< 0.05 mg/L)¹⁸. Here, we showed that significant amounts of ROS were produced for both MPA and PAH AuNPs and their respective ligands at the same concentrations. This leads us to believe that ROS production does not fully explain the adverse outcomes observed in our acute and chronic studies. Therefore, other mechanisms may be responsible for the observed impacts as *Daphnia* responded differently to MPA and PAH AuNPs but had similar amounts of ROS detected upon exposure to these treatments at the same concentrations. However, in our current study and the previous, gene expression

patterns were different for the two ligand-NP combinations. These results suggest that pathways affected by NPs are strongly dependent upon NP surface properties.

For *S. oneidensis* and the pathways investigated, gene expression assays were not as sensitive to the ligand-NP combination as *Daphnia* but were indicative of the observed apical endpoint impacts. Most of the gene expression responses for *S. oneidensis* were provoked by the free ligand exposure instead of the ligand-NP combination at both time points, as was observed in the apical endpoint study. While MPA-AuNPs did not show any impact that was specific to NPs, the decrease in expression of 16S at 6-hour exposure and *sodB* gene at 1-hour exposure were unique to the PAH-AuNP but not to PAH free ligand. The *sodB* gene encodes for one of the superoxide dismutase (SODs) that protect cells from deleterious reactions of reactive oxygen species⁷¹; it has been previously reported that the *sodB* gene was up-regulated upon *S. oneidensis* exposure to chromium (VI)⁷². More related, a previous study using 60-nm amino-functionalized polystyrene nanomaterial (PS-NH₂-NPs) on *E. coli* single-gene deletion mutants showed that the Δ *sodB* mutant was more sensitive to the exposure of PS-NH₂-NPs compared to the parent strain⁷³. As PAH-AuNPs has a similar surface-functionalization of amine groups with PS-NH₂-NPs, these results suggests that the *sodB* gene plays an essential role in bacterial cell response to amine-functionalized nanomaterials, making it possible to use *sodB* as a biomarker for this specific NP surface functionalization. 16S ribosomal RNA (rRNA) is one of the three rRNAs, which are components of prokaryotic ribosomes. The rRNA transcription is the rate-limiting step in ribosome synthesis, and thus, directly correlates to protein synthesis and cell growth⁷⁴. Previous research has reported that rRNA degradation

occurs during environmental stress, including oxidative stress and starvation⁷⁵⁻⁷⁷. Notably, it was also reported that rRNA is degraded due to a change in cell membrane permeability, potentially leading to the entry of RNase I, an endoribonuclease, from the periplasmic space into the cytoplasm^{78, 79}. Extensive cell membrane damage can also result in the efflux of RNA due to the loss of plasma membrane integrity⁸⁰. Previous research has shown the disruption of membrane integrity in *S. oneidensis* cells upon PAH-AuNP exposure⁶¹, correlating with the decrease in the expression of 16S. It should be noted that at 1-hour exposure, the respective PAH ligand control also elicited decrease in 16S expression, while at 6-hour exposure only PAH-AuNPs showed the effect; thus, the potential of 16S to be used as a biomarker that is specific for PAH-AuNPs is limited to long-term exposures. In effort to link 16S and *sodB* gene response to the apical biological endpoints, the gene expression level of these two genes was examined at a higher dosage (100 µg/L) that also caused inhibition in bacterial oxygen uptake (Figure 1(c)). While the *sodB* gene at 1-hour exposure did not elicit change in gene expression, 16S at 6-hour exposure showed a similar decrease upon 100 µg/L PAH-AuNP exposure (Figure 4), proving that 16S can be potentially used as a biomarker for the impact of PAH-AuNPs on bacterial oxygen uptake; future work will explore the adverse outcome pathway from the decrease in 16S rRNA expression to the inhibition of bacterial oxygen uptake, and we postulated the inhibition is mediated via reduced activity in protein synthesis. MPA-AuNPs did not induce a similar response of 16S rRNA expression, or any other NP-specific response, indicating a distinction between the same AuNP cores functionalized with different surface ligands.

Short-term exposures for both *D. magna* and *S. oneidensis* revealed that functionalized NP impacts on certain molecular pathways might be predicted by their respective ligand alone. Out of all *S. oneidensis* regulated genes, three genes stand out as potential predictors of NP impacts based on the ligand alone. These genes are *pspB* and *rpoA* for PAH-AuNP/ligand and *ibpA* for MPA-AuNP/ligand at 1-hour exposure, as they were influenced similarly upon exposure to both the ligand-bound AuNPs and the respective free ligand. For *D. magna*, three genes were most notable; these genes were *hsp70* and *vtg* for PAH-AuNP/ligand and *hsp70*, *vtg* and *nadh* for MPA-AuNP/ligand. These results suggest that NP impacts on specific molecular pathways may be predicted based on response to the ligand alone. This finding is especially important for ligands or functional groups that are commonly used to achieve desired physiochemical properties for NPs. However, as demonstrated with our study, ligand-NP combinations did alter several genes that the ligand alone did not, and the concentrations of NPs that impacted apical endpoints, in particular PAH-AuNPs, differed from that of the ligand. This diminishes the potential ability to use ligand information alone as a predictor for NP toxicity; rather, the overall NP characteristics, including charge or size, may be more informative.

Our study revealed that, overall, long-term exposure to NPs resulted in gene expression patterns that could not be predicted based on gene expression patterns from short-term exposures. Upon exposure to MPA-AuNP/ligand, both *S. oneidensis* and *D. magna* showed decreases in gene expression during short-term exposure and that this response flipped to mostly an increase in gene expression upon long-term exposure. Exceptions to this finding are observed in the decrease of 16S and *sodB*

expression upon PAH-AuNP exposure in *S. oneidensis* and the increase of *vgt* gene expression upon MPA-AuNP exposure in *D. magna*, which show similar response in gene expression levels at both time points. Our results indicate that, although it is possible to predict long-term gene expression impacts based on short-term impacts, it is limited to select genes, which may downplay the significance of this finding.

Gene expression responses across organisms provide an indication of how organisms are similar or different in their response to NP exposures. A notable signature shared across two organisms was the up-regulation of *ibpA/hsp70* induced by MPA-AuNP and ligand for short-term exposures. Both *ibpA* and *hsp70* encode for heat shock protein in *S. oneidensis* and *D. magna*, respectively. Heat shock proteins (Hsp) are a large family of proteins that help unfolded or misfolded proteins to fold correctly in vivo and are widely considered to be good indicators of proteotoxic stress^{81, 82}. The up-regulation of heat shock protein induced by MPA-AuNPs and ligands potentially indicate the disruption of membrane proteins, provoking pathways that help adapt to change in chemical environment caused by introduction of NPs or ligands. This feature, shared by both organisms, potentially indicates a universal stress-response to negatively charged NPs, making the genes encoding for heat shock protein a good candidate for predicting the effect of NPs based on the response to their respective ligands. However, MPA-AuNPs did not lead to any adverse outcomes at the concentrations we tested, which makes understanding the importance of this pathway within the context of our study difficult.

Conclusion

Molecular studies have the ability to tease out distinct modes of action for NP toxicity and help to develop biomarkers for assessing NP impacts on environmentally relevant endpoints. Using standard toxicological and gene expression assays, we revealed that: 1) the ligand-NP combinations determine the extent of impacts on organismal endpoints and the toxicity of select NPs may not be determined by their respective ligand alone; 2) depending on the organism considered, exposure to ligand-NP combinations⁸³ may impact unique molecular pathways that differ from the ligand alone; 3) short-term exposures reveal that ligand-NP impacts on certain molecular pathways might be predicted by their respective ligand alone but the ability to predict long-term impacts may be minimal; and 4) examining gene expression responses across organisms may provide an indication of how organisms are similar or different in their response to NP exposures. Lastly, this study reveals that there are mechanisms other than oxidative stress for NP toxicity and that these may be elucidated using molecular level experiments and exposures that consider sublethal concentrations.

ACKNOWLEDGEMENTS

This work was funded by the National Science Foundation Center for Chemical Innovations grant CHE-1240151: Center for Sustainable Nanotechnology and a Research Experience for Undergraduates fellowship supported by the National Science Foundation Center for Chemical Innovation Program (CHE-1240151)

awarded to K.G.C. We thank K.G.C for his help in gene expression work. Lastly, we want to thank Dr. Y Hayashi for access to the NORMA-Gene workbook.

Supporting Information

Ligand control estimation: PAH-AuNPs

PAH-AuNPs were purified by centrifugation, making it possible for PAH free ligand to be left over in the PAH-AuNP suspension. In order to estimate the present of PAH ligand, a fluorescence quantification method to determine primary amine was used, modified from previous work¹. 0.01 g fluorescamine (Sigma-Aldrich) was dissolved in 10 mL acetonitrile to reach a concentration of 0.1% (w/v). 0.05 M sodium borate buffer was prepared by dissolving 5.03 g $\text{Na}_2\text{B}_4\text{O}_7$ in 500 mL MilliQ water followed by the adjustment of pH to approximately 8 using 12 M HCl. PAH-AuNP suspension was centrifuged at 66,000 g for 45 minutes under 4 °C to pellet all AuNPs, and the clear supernatant was removed from the centrifugation tubes. 120 μL samples were mixed with 20 μL of borate buffer on a 96-well plate, and 60 μL of fluorescamine solution was lastly added to the mixture. The reaction was incubated at room temperature for 5 minutes, and the fluorescence intensity was measured by plate reader with Ex/Em = 425 nm/480 nm. A calibration curve using a series of PAH solutions of known concentrations was created every time before sample measurement, and the concentration of PAH in samples were calculated based the fitting results from linear regression.

The amount of PAH free ligand in 30 $\mu\text{g/L}$ PAH-AuNP suspension was determined to be 210 (192 to 228) $\mu\text{g/L}$. In addition, the amount of PAH ligand on NP surface was estimated to be 2.7 $\mu\text{g/L}$ (PAH charge density on AuNP surface: 12.8 charge/ nm^2), based on the same calculation as below for MPA-AuNPs. Thus, a 10-fold PAH free ligand control (300 $\mu\text{g/L}$ PAH free ligand in the case of 30 $\mu\text{g/L}$ PAH-AuNPs)

was chosen in this study to represent the effect of PAH free ligand in PAH-AuNP suspension.

Ligand control estimation: MPA-AuNPs

Excessive MPA free ligand from synthesis were expected to be eliminated by diafiltration, and the total MPA ligand present in MPA-AuNP suspension were estimated to be the amount of MPA ligand attached to NP surface. The surface charge density of MPA-AuNPs were determined to be $5.6 \text{ charge} \cdot \text{nm}^{-2}$ by XPS.

Calculating number of AuNPs per liter:

$$\text{AuNP diameter} \sim 4 \text{ nm}$$

$$\text{Volume per AuNP} = \frac{4}{3}\pi\left(\frac{\text{AuNP diameter}}{2}\right)^3 = 33.5 \text{ nm}^3 = 3.35 \times 10^{-20} \text{ cm}^3$$

$$\begin{aligned} \text{Mass per AuNP} &= \text{Density} \times \text{Volume per AuNP} = 19.3 \text{ g} \cdot \text{cm}^{-3} \times 3.35 \times 10^{-20} \text{ cm}^3 \\ &= 6.47 \times 10^{-19} \text{ g} \end{aligned}$$

$$N_{\text{MPA-AuNPs}} = \text{Number of MPA - AuNPs per liter} = \frac{5 \text{ mg} \cdot \text{L}^{-1}}{6.47 \times 10^{-19} \text{ g}} = 7.73 \times 10^{15} \text{ L}^{-1}$$

Calculating the mass of total amount of surface ligand:

$$\text{Ligand amount per AuNP} = \text{Charge density} \times \text{Surface area}$$

$$M_{\text{Ligand}} = \text{Total ligand mass on NPs}$$

$$= \frac{N_{\text{AuNPs}} \times \text{Ligand amount per AuNP}}{\text{Avogadro constant}} \times MW_{\text{Ligand Unit}}$$

$$\text{MPA ligand per AuNP} = 5.6 \text{ charge} \cdot \text{nm}^{-2} \times 4\pi \left(\frac{4 \text{ nm}}{2}\right)^2 = 2.8 \times 10^2$$

$$M_{\text{MPA ligand}} = \frac{2.8 \times 10^2 \times (7.73 \times 10^{15} \text{ L}^{-1})}{6.02 \times 10^{23} \text{ mol}^{-1}} \times 106.14 \text{ g} \cdot \text{mol}^{-1} = 0.38 \text{ mg} \cdot \text{L}^{-1} < 5 \text{ mg} \cdot \text{L}^{-1}$$

Based on the calculation above, the equivalent mass concentration of MPA ligand was an excessive estimation of the actual MPA ligand present in the suspension.

Bacterial doubling time estimation

A rough estimation of *S. oneidensis* doubling time in the growth medium used in this study was calculated as below. Assuming that cell oxygen uptake (M) is proportional to the cell number (N), at exponential growth phase:

$$M = M_0 \times 2^{kt} \quad (1)$$

$$N = N_0 \times 2^{kt} \quad (2)$$

k : growth rate at exponential phase (hour^{-1}); t : time (hour); $T=1/k$: doubling time (hour); N : cell number; N_0 : original cell number; M : cell oxygen uptake; M_0 : original cell oxygen uptake. Take first derivative of equation (2):

$$N'_t = N_0 \times (k \ln 2) \times 2^{kt} \quad (3)$$

The first derivative was calculated in GraphPad, Prism. Two different time points from exponential phase, t_1 and t_2 , and the first derivative at these two time points were substituted into equation (3) to get the ratio:

$$\frac{N'_{t1}}{N'_{t2}} = 2^{k(t1-t2)} \quad (4)$$

The growth rate at exponential phase (k) was calculated from equation (4) followed by the calculation of doubling time (T):

$$T = \frac{1}{k}$$

Plugging values from different traces in various experimental runs yielded bacterial doubling times between 2-3 hours.

REFERENCES

1. A. S. Arico, P. Bruce, B. Scrosati, J.-M. Tarascon and W. van Schalkwijk, *Nat Mater*, 2005, **4**, 366-377.
2. J. Xie, G. Liu, H. S. Eden, H. Ai and X. Chen, *Accounts of Chemical Research*, 2011, **44**, 883-892.
3. M. M. Pendergast and E. M. V. Hoek, *Energy & Environmental Science*, 2011, **4**, 1946-1971.
4. A. Nel, T. Xia, L. Madler and N. Li, *Science*, 2006, **311**, 622-627.
5. Y. Pan, S. Neuss, A. Leifert, M. Fischler, F. Wen, U. Simon, G. Schmid, W. Brandau and W. Jahnen-Dechent, *Small*, 2007, **3**, 1941-1949.
6. A. Albanese, P. S. Tang and W. C. Chan, *Annual review of biomedical engineering*, 2012, **14**, 1-16.
7. D. A. Arndt, M. Moua, J. Chen and R. D. Klaper, *Environmental science & technology*, 2013, **47**, 9444-9452.
8. R. Klaper, D. Arndt, K. Setyowati, J. Chen and F. Goetz, *Aquatic toxicology*, 2010, **100**, 211-217.
9. R. Klaper, J. Crago, J. Barr, D. Arndt, K. Setyowati and J. Chen, *Environmental Pollution*, 2009, **157**, 1152-1156.
10. B. D. Chithrani, A. A. Ghazani and W. C. Chan, *Nano letters*, 2006, **6**, 662-668.
11. H. Yang, C. Liu, D. Yang, H. Zhang and Z. Xi, *Journal of applied Toxicology*, 2009, **29**, 69-78.
12. K. L. Aillon, Y. Xie, N. El-Gendy, C. J. Berkland and M. L. Forrest, *Advanced drug delivery reviews*, 2009, **61**, 457-466.
13. J. S. Bozich, S. E. Lohse, M. D. Torelli, C. J. Murphy, R. J. Hamers and R. D. Klaper, *Environmental Science: Nano*, 2014, **1**, 260-270.
14. A. M. El Badawy, R. G. Silva, B. Morris, K. G. Scheckel, M. T. Suidan and T. M. Tolaymat, *Environmental science & technology*, 2010, **45**, 283-287.
15. C. He, Y. Hu, L. Yin, C. Tang and C. Yin, *Biomaterials*, 2010, **31**, 3657-3666.
16. N. M. Schaeublin, L. K. Braydich-Stolle, A. M. Schrand, J. M. Miller, J. Hutchison, J. J. Schlager and S. M. Hussain, *Nanoscale*, 2011, **3**, 410-420.
17. A. Verma and F. Stellacci, *Small*, 2010, **6**, 12-21.
18. G. A. Dominguez, S. E. Lohse, M. D. Torelli, C. J. Murphy, R. J. Hamers, G. Orr and R. D. Klaper, *Aquatic Toxicology*, 2015, **162**, 1-9.
19. A. Albanese and W. C. W. Chan, *Acs Nano*, 2011, **5**, 5478-5489.
20. N. Lewinski, V. Colvin and R. Drezek, *small*, 2008, **4**, 26-49.
21. N. Khlebtsov and L. Dykman, *Chemical Society Reviews*, 2011, **40**, 1647-1671.
22. C.-w. Lam, J. T. James, R. McCluskey, S. Arepalli and R. L. Hunter, *CRC Critical Reviews in Toxicology*, 2006, **36**, 189-217.
23. E. Fröhlich, *International journal of nanomedicine*, 2012, **7**, 5577.
24. S. K. Sohaebuddin, P. T. Thevenot, D. Baker, J. W. Eaton and L. Tang, *Particle and fibre toxicology*, 2010, **7**, 22.
25. M. Heinlaan, A. Ivask, I. Blinova, H.-C. Dubourguier and A. Kahru, *Chemosphere*, 2008, **71**, 1308-1316.
26. H. Sanderson and M. Thomsen, *Bulletin of environmental contamination and toxicology*, 2007, **79**, 331-335.

27. D. R. Moore, R. L. Breton and D. B. MacDonald, *Environmental Toxicology and chemistry*, 2003, **22**, 1799-1809.
28. A. A. Shvedova, A. Pietroiusti, B. Fadeel and V. E. Kagan, *Toxicology and Applied Pharmacology*, 2012, **261**, 121-133.
29. B. J. Marquis, S. A. Love, K. L. Braun and C. L. Haynes, *Analyst*, 2009, **134**, 425-439.
30. A. Manke, L. Wang and Y. Rojanasakul, *BioMed research international*, 2013, **2013**.
31. E. J. Park and K. Park, *Toxicology Letters*, 2009, **184**, 18-25.
32. R. Klaper, D. Arndt, J. Bozich and G. Dominguez, *Analyst*, 2014, **139**, 882-895.
33. F. Gottschalk, T. Sonderer, R. W. Scholz and B. Nowack, *Environmental science & technology*, 2009, **43**, 9216-9222.
34. A. Valavanidis, T. Vlahogianni, M. Dassenakis and M. Scoullou, *Ecotoxicology and Environmental Safety*, 2006, **64**, 178-189.
35. R. Franco, R. Sanchez-Olea, E. M. Reyes-Reyes and M. I. Panayiotidis, *Mutation Research-Genetic Toxicology and Environmental Mutagenesis*, 2009, **674**, 3-22.
36. T. Finkel and N. J. Holbrook, *Nature*, 2000, **408**, 239-247.
37. J. Ryan and L. Hightower, in *Stress-Inducible Cellular Responses*, Springer, Editon edn., 1996, pp. 411-424.
38. C. G. Kilty, J. Keenan and M. Shaw, 2007.
39. C. Eason and K. O'Halloran, *Toxicology*, 2002, **181**, 517-521.
40. N. J. Niemuth, R. Jordan, J. Crago, C. Blanksma, R. Johnson and R. D. Klaper, *Environmental Toxicology and Chemistry*, 2014.
41. G. T. Ankley, K. M. Jensen, M. D. Kahl, J. J. Korte and E. A. Makynen, *Environmental Toxicology and Chemistry*, 2001, **20**, 1276-1290.
42. S. M. Johns, M. D. Kane, N. D. Denslow, K. H. Watanabe, E. F. Orlando, D. L. Villeneuve, G. T. Ankley and M. S. Sepúlveda, *Environmental Toxicology and Chemistry*, 2009, **28**, 873-880.
43. J. S. Garvey, Preprints of Papers Presented at National Meeting, Division of Water, Air and Waste Chemistry, American Chemical Society;(USA), 1988.
44. M. Fischbach, E. Sabbioni and P. Bromley, *Cell biology and toxicology*, 1993, **9**, 177-188.
45. H. H. Hau and J. A. Gralnick, *Annu. Rev. Microbiol.*, 2007, **61**, 237-258.
46. R. Gulati, *Hydrobiologia*, 1978, **59**, 101-112.
47. N. R. Jana, L. Gearheart and C. J. Murphy, *Langmuir*, 2001, **17**, 6782-6786.
48. T. K. Sau and C. J. Murphy, *Journal of the American Chemical Society*, 2004, **126**, 8648-8649.
49. D. A. Giljohann, D. S. Seferos, W. L. Daniel, M. D. Massich, P. C. Patel and C. A. Mirkin, *Angewandte Chemie International Edition*, 2010, **49**, 3280-3294.
50. S. F. Sweeney, G. H. Woehrle and J. E. Hutchison, *Journal of the American Chemical Society*, 2006, **128**, 3190-3197.
51. J. A. Yang, S. E. Lohse and C. J. Murphy, *Small*, 2014, **10**, 1642-1651.
52. C. J. Ackerson, P. D. Jadzinsky and R. D. Kornberg, *Journal of the American Chemical Society*, 2005, **127**, 6550-6551.

53. M. D. Torelli, R. A. Putans, Y. Tan, S. E. Lohse, C. J. Murphy and R. J. Hamers, *Acs Appl Mater Inter*, 2015, **7**, 1720-1725.
54. EPA, *Standard operating procedure for moderately hard reconstituted water*, SoBran, Dayton, OH, USA, 2003.
55. S. Zhao and R. D. Fernald, *Journal of computational biology*, 2005, **12**, 1047-1064.
56. L.-H. Heckmann, P. Sorensen, P. Krogh and J. Sorensen, *BMC Bioinformatics*, 2011, **12**, 250.
57. S. Wang, W. Lu, O. Tovmachenko, U. S. Rai, H. Yu and P. C. Ray, *Chemical Physics Letters*, 2008, **463**, 145-149.
58. P. A. Rice and B. H. Iglewski, *Reviews of Infectious Diseases*, 1988, **10**, S277-S278.
59. A. Martínez-Palomo, in *International Review of Cytology*, eds. J. F. D. G.H. Bourne and K. W. Jeon, Academic Press, Editon edn., 1970, vol. Volume 29, pp. 29-75.
60. C. M. Goodman, C. D. McCusker, T. Yilmaz and V. M. Rotello, *Bioconjugate Chemistry*, 2004, **15**, 897-900.
61. Z. V. Feng, I. L. Gunsolus, T. A. Qiu, K. R. Hurley, L. H. Nyberg, H. Frew, K. P. Johnson, A. M. Vartanian, L. M. Jacob and S. E. Lohse, *Chemical Science*, 2015.
62. K. H. Jacobson, I. L. Gunsolus, T. R. Kuech, J. M. Troiano, E. S. Melby, S. E. Lohse, D. H. Hu, W. B. Chrisler, C. J. Murphy, G. Orr, F. M. Geiger, C. L. Haynes and J. A. Pedersen, *Submitted*, 2015.
63. Y. Y. Zhao, Y. Tian, Y. Cui, W. W. Liu, W. S. Ma and X. Y. Jiang, *Journal of the American Chemical Society*, 2010, **132**, 12349-12356.
64. S. Dalai, S. Pakrashi, R. S. Kumar, N. Chandrasekaran and A. Mukherjee, *Toxicology Research*, 2012, **1**, 116-130.
65. A. Kumar, A. K. Pandey, S. S. Singh, R. Shanker and A. Dhawan, *Chemosphere*, 2011, **83**, 1124-1132.
66. S. Schwerin, B. Zeis, T. Lamkemeyer, R. J. Paul, M. Koch, J. Madlung, C. Fladerer and R. Pirow, *BMC physiology*, 2009, **9**, 8.
67. M. Ehrenberg and J. L. McGrath, *Acta Biomaterialia*, 2005, **1**, 305-315.
68. P. Ruenraroengsak and A. T. Florence, *Journal of drug targeting*, 2010, **18**, 803-811.
69. V. G. Walker, Z. Li, T. Hulderman, D. Schwegler-Berry, M. L. Kashon and P. P. Simeonova, *Toxicology and applied pharmacology*, 2009, **236**, 319-328.
70. T. Mironava, M. Hadjiargyrou, M. Simon, V. Jurukovski and M. H. Rafailovich, *Nanotoxicology*, 2010, **4**, 120-137.
71. S. B. Farr and T. Kogoma, *Microbiological reviews*, 1991, **55**, 561-585.
72. K. Chourey, M. R. Thompson, J. Morrell-Falvey, N. C. VerBerkmoes, S. D. Brown, M. Shah, J. Zhou, M. Doktycz, R. L. Hettich and D. K. Thompson, *Applied and environmental microbiology*, 2006, **72**, 6331-6344.
73. A. Ivask, E. Suarez, T. Patel, D. Boren, Z. Ji, P. Holden, D. Telesca, R. Damoiseaux, K. A. Bradley and H. Godwin, *Environmental science & technology*, 2012, **46**, 2398-2405.

74. B. J. Paul, W. Ross, T. Gaal and R. L. Gourse, *Annual Review of Genetics*, 2004, **38**, 749-770.
75. D. R. Crawford, Y. H. Wang, G. P. Schools, J. Kochheiser and K. J. A. Davies, *Free Radical Biology and Medicine*, 1997, **22**, 551-559.
76. G. N. Basturea, M. A. Zundel and M. P. Deutscher, *RNA*, 2011, **17**, 338-345.
77. D. Hsu, L.-M. Shih and Y. C. Zee, *Journal of bacteriology*, 1994, **176**, 4761-4765.
78. M. P. Deutscher, *Nucleic Acids Research*, 2006, **34**, 659-666.
79. M. Kuwano, H. Taniguchi, M. Ono, H. Endo and Y. Ohnishi, *Biochemical and Biophysical Research Communications*, 1977, **75**, 156-162.
80. Z. Darzynkiewicz, S. Bruno, G. Delbino, W. Gorczyca, M. A. Hotz, P. Lassota and F. Traganos, *Cytometry*, 1992, **13**, 795-808.
81. S. D. Brown, M. R. Thompson, N. C. VerBerkmoes, K. Chourey, M. Shah, J. Z. Zhou, R. L. Hettich and D. K. Thompson, *Molecular & Cellular Proteomics*, 2006, **5**, 1054-1071.
82. K. Chourey, M. R. Thompson, J. Morrell-Falvey, N. C. VerBerkmoes, S. D. Brown, M. Shah, J. Z. Zhou, M. Doktycz, R. L. Hettich and D. K. Thompson, *Applied and Environmental Microbiology*, 2006, **72**, 6331-6344.
83. J. A. Bourdon, S. Halappanavar, A. T. Saber, N. R. Jacobsen, A. Williams, H. Wallin, U. Vogel and C. L. Yauk, *Toxicological sciences : an official journal of the Society of Toxicology*, 2012, **127**, 474-484.

SUPPORTING REFERENCES

1. Bantan-Polak, T., M. Kassai, and K.B. Grant, *Analytical Biochemistry*, 2001, **297**, 128-136.

CHAPTER 3 TABLES

Table 1 Target genes, corresponding functions, and their primers for qPCR.

Shewanella oneidensis MR-1			
Target Gene	Forward primer (5'-3')	Reverse primer (5'-3')	Accession Number
Glutathione S-transferase (<i>gst</i>)	GCA AAG CAT TCC AGC AAT TT	GAC CTT CTT GCG TTT TGA GC	NP_720213.1
Na-translocating NADH-quinone reductase subunit F (<i>nqrF</i>)	CGC TTA CTC GAT GGC TAA CTAC	GCA AGG CAG CGT CAA ATT AC	NP_716734.1
Double-stranded DNA translocase (<i>fsk</i>)	TAC GAG TCG TGT TGC GAT AAA	AAG GGC TGA CAC TGG AAT AAA	NP_717901.1
Catalase HPII (<i>katB</i>)	GGC ATT GAT CCT GAT TCT TCT C	TCC AAC GAG GGA AGT TAC CA	NP_716697.1
16 kDa heat shock protein A (<i>ibpA</i>)	GCA ACT CAG GTT ATC CTC CAT AC	CGC TAC TGA TCT CAA GCT CTT C	NP_717873.1
16S ribosomal RNA (16S)	TCA AGT CAT CAT GGC CCT TAC	TAC GAC GAG CTT TGT GAG ATT AG	NR_074798.1
RNA polymerase alpha subunit (<i>rpoA</i>)	TCG CAT CCT ATT GTC GTC TAT G	CTT CTT GTA CGC CTT CCT TAC T	NP_715896.1
ATP-dependent protease (<i>radA</i>)	TTC GGC AAT TTT CCT CTC C	ACA CCA CCA TGA CCA AGG AT	NP_716849.1
Phage shock protein B (<i>pspB</i>)	TTG ATT GCG AAA GCC GAT A	ATC AAG AAT CGC CTC TAA GGT TT	NP_717416.1
Fe/Mn superoxide dismutase (<i>sodB</i>)	GCA ATG TTC GCC CTG ACT AC	CCT GCG AAG TTT TGG TTC AC	NP_718453.1
Daphnia magna			
Target Gene	Forward primer (5'-3')	Reverse primer (5'-3')	Function
Glutathione S-transferase (<i>gst</i>)	CAA CGC GTA TGG CAA AGA TG	CTA GAC CGA AAC GGT GGT AAA	Xenobiotic detoxification
Dehydrogenase (<i>nadh</i>)	GCA GGA AAC AAT AAG GCA AAC C	GGT GGC ACA GAC CAT TTC TTA	Mitochondrial electron transport and energy production
Vitellogenin (<i>vtg</i>)	CTG TTC CTC GCT CTG TCT TG	CCA GAG AAG GAA GCG TTG TAG	Reproduction, sexual maturation and general stress
Catalase (<i>cat</i>)	CAG GAT CAT CGG CAG TTA GTT	CTG AAG GCA AAC CTG TCT ACT	Oxidative stress attenuation
Heat shock protein 70 (<i>hsp70</i>)	CCT TAG TCA TGG CTC GTT CTC	TCA AGC GGA ACA CCA CTA TC	Response to heat; protein folding
β-Actin (<i>act</i>)	CCA CAC TGT CCC CAT TTA TGA A	CGC GAC CAG CCA AAT CC	Cytoskeleton production and cell maintenance

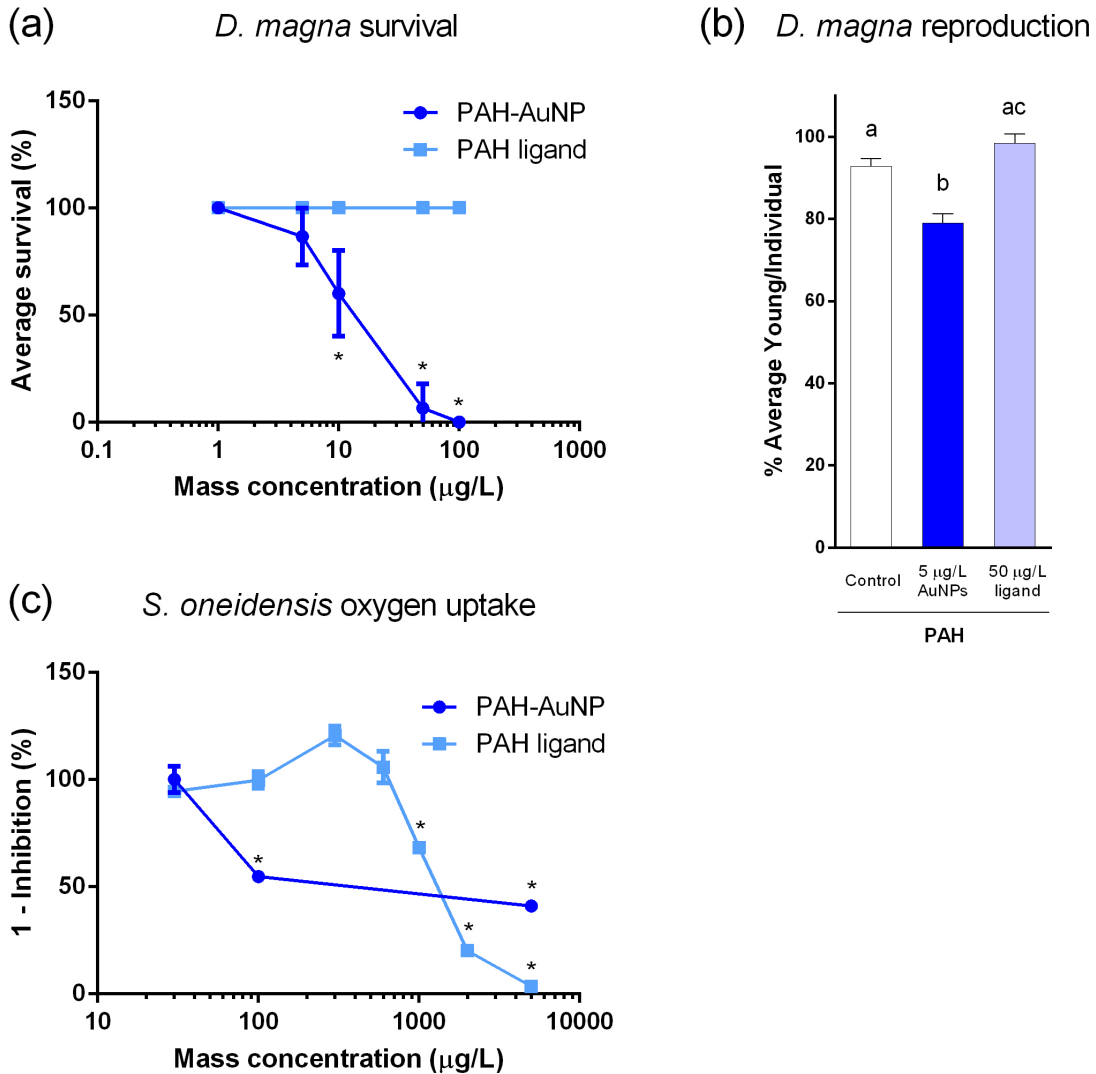
Table 2 Nanoparticle characterization based on TEM analysis.

	PAH-AuNPs		MPA-AuNPs	
	<i>S. oneidensis</i> Media	<i>D. magna</i> Media	<i>S. oneidensis</i> Media	<i>D. magna</i> Media
^b LSPR λ_{\max} (nm) (in H ₂ O)	528		515	
LSPR λ_{\max} (nm) (in medium)	530	530	555	575
d_{core} (nm) *	4.7 ± 1.5 (N ≥ 250)		4.3 ± 1.3 nm (N = 501)	
D_h (nm) (in H ₂ O)	^a 200.2 ± 3.5		126.4 ± 3.7	
D_h (nm) (in medium)	^a 159.5 ± 0.6	^a 79.43 ± 1.9	339.6 ± 21.9	364 ± 34.2
ζ -Potential (mV) (in H ₂ O)	+68.5 ± 1.6		-17.3 ± 0.6	
ζ -Potential (mV) (in medium)	+24.57 ± 5.6	+10.5 ± 4.8	-24.28 ± 3.2	-29.8 ± 1.3

See Figure S1 for TEM images. ^a For polyelectrolyte wrapped particles, hydrodynamic diameter (D_h) determined by dynamic light scattering is not accurate. ^b Localized surface plasmon resonance (LSPR) wavelength of maximum peak value (λ_{\max}).

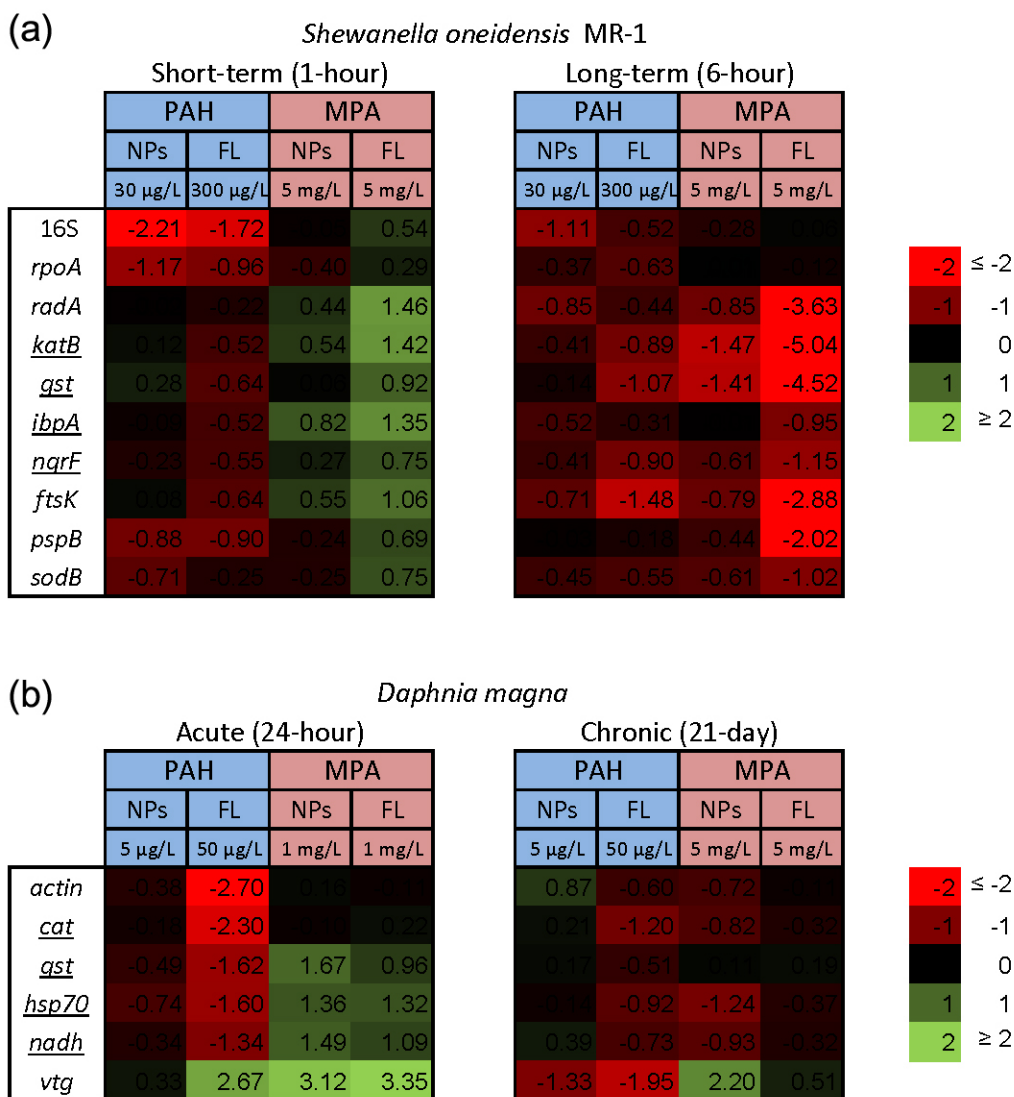
CHAPTER 3 FIGURES

Figure 1



Nanoparticle toxicity to *D. magna* and *S. oneidensis*. Impact of PAH-AuNPs and PAH ligand on (a) *D. magna* survival (%), (b) *D. magna* reproduction and (c) *S. oneidensis* oxygen uptake. Error bars represent standard error of the mean. Stars indicate significant difference compared to corresponding control groups (*S. oneidensis*, unpaired t-test, $\alpha=0.05$, $n\geq 2$; *D. magna*, unpaired t-test, $\alpha=0.05$, $n\geq 3$). Different letter designations in (b) indicate significant difference between groups (Tukey's test, $\alpha=0.05$).

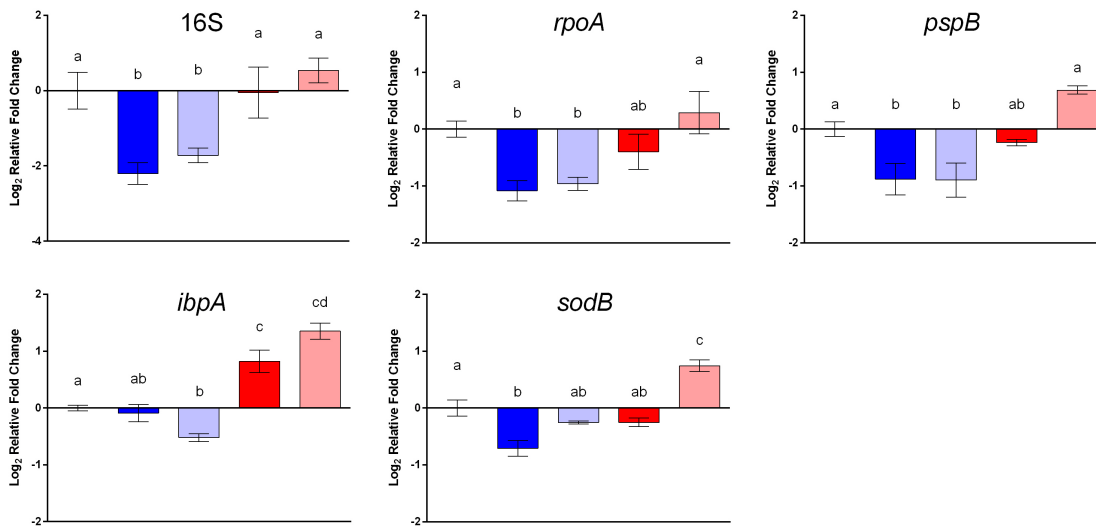
Figure 2



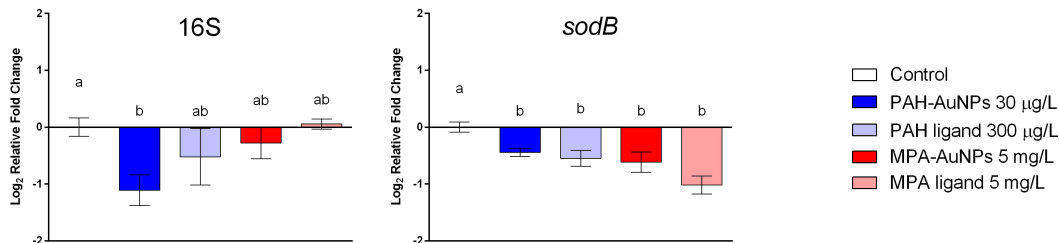
Gene expression heat map. Heat map of (a) *S. oneidensis* and (b) *D. magna* gene expression response. Sublethal dosages of AuNPs and their respective ligand control were used in the gene expression study, as shown in the figure. Genes encoding for similar cellular functions in two model organisms were underlined.

Figure 3

(a) Short-term (1-hour)

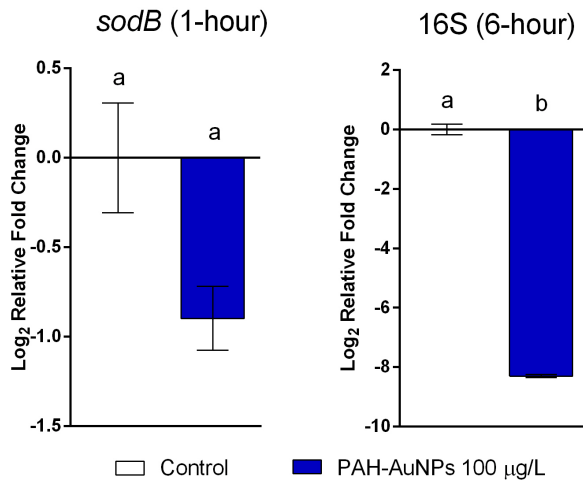


(b) Long-term (6-hour)



Selected gene responses in *S. oneidensis* upon AuNP/ligand exposure. Error bars showed standard error of the mean (PAH-AuNP, n=5; PAH ligand, n=4; MPA-AuNP/ligand, n=3). All figures follow the same legend, and the first bar in every figure indicates control group. Different letter designations between different groups indicate significant difference (Tukey's test, $\alpha=0.05$).

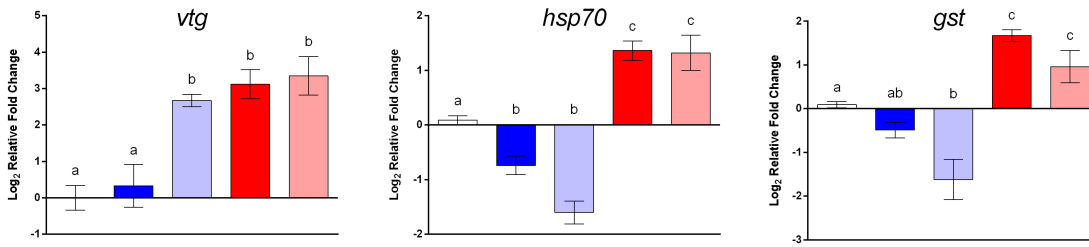
Figure 4



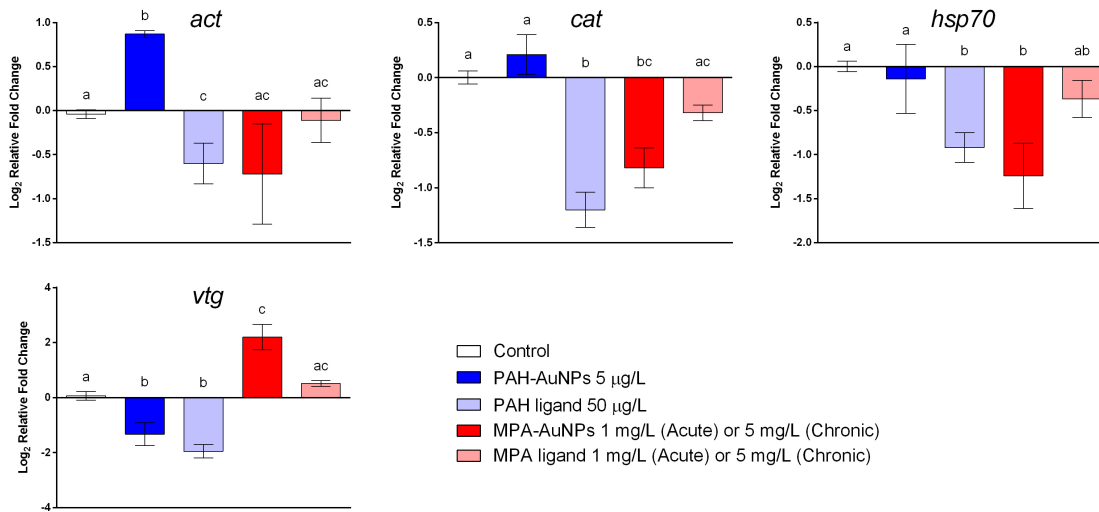
S. Oneidensis 16s and sodB gene expression. In *S. oneidensis*, 16S gene expression decreased upon 100 µg/L PAH-AuNP exposure at long-term exposure (6-hour), while *sodB* gene expression did not show significant difference compared to control group. Error bars showed standard error of the mean (n ≥ 4). Both figures follow the same legend. Different letter designations indicate significant difference between groups (unpaired t-test, α = 0.05).

Figure 5

(a) Acute (24-hour)



(b) Chronic (21-day)



Selected gene responses in *D. magna* upon AuNP/ligand exposure. Error bars showed standard error of the mean (n ≥ 6 for all exposure). All figures follow the same legend. Different letter designations between different groups indicate significant difference (Tukey's test, α = 0.05).

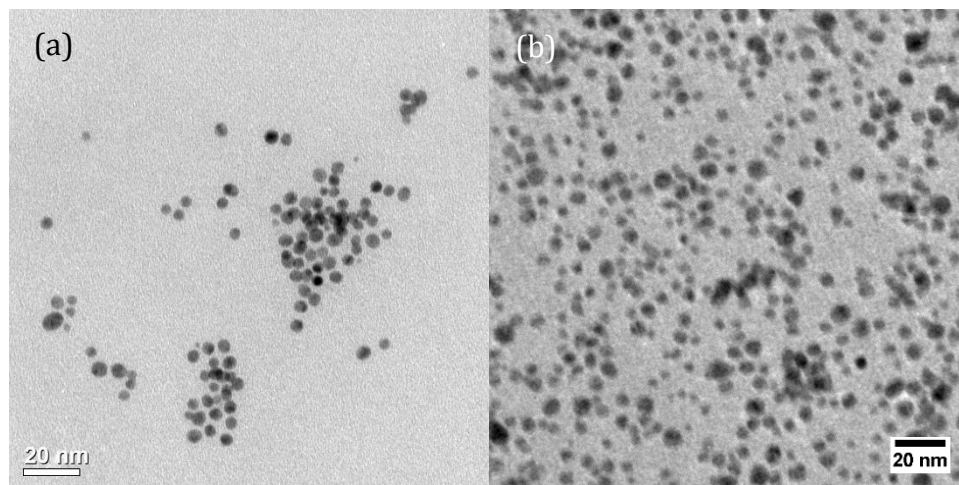
CHAPTER 3 SUPPORTING INFORMATION

Gene expression response of the Gram-negative bacterium *Shewanella oneidensis* and the water flea *Daphnia magna* exposed to functionalized gold nanoparticles

Number of supporting information pages: 6

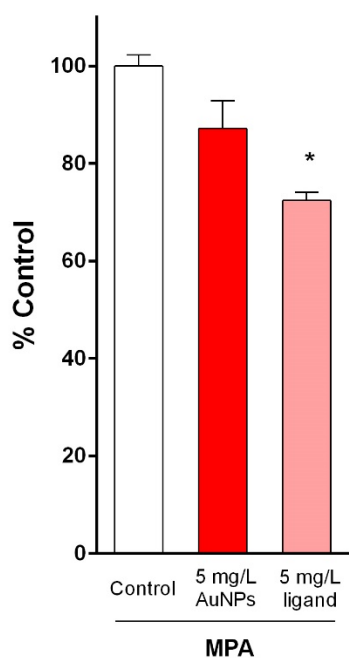
Number of Figures: 2

Figure S1



TEM image of (a) PAH-AuNPs and (b) MPA-AuNPs before exposure to either organism.

Figure S2



Inhibition on oxygen uptake of *S. oneidensis* upon MPA-AuNP and the respective ligand exposure. Error bars showed standard error of the mean (n=2). Stars indicate significant difference between treated and control groups ($p < 0.05$).

CHAPTER 4

Core chemistry influences the toxicity of multi-component metal oxide nanomaterials, lithium nickel manganese cobalt oxide and lithium cobalt oxide to *Daphnia magna*

Jared Bozich^a, Mimi Hang^b, Robert Hamers^b, and Rebecca Klaper^{a*}

^a School of Freshwater Sciences, University of Wisconsin Milwaukee, 600 E.

Greenfield Ave, Milwaukee, WI 53204

^b Department of Chemistry, University of Wisconsin-Madison, 1101 University Ave,

Madison, WI 53706

*Corresponding Author

rklaper@uwm.edu, Phone: 414-382-1713, Fax: 414-382-1705

Abstract

Lithium intercalation compounds such as lithium nickel manganese cobalt oxide (NMC) and lithium cobalt oxide (LCO) are used extensively in lithium-battery based devices. Nanoscale forms of cathode materials are increasingly explored to enhance battery performance. However, there is currently little economic incentive for recycling so chances are greater that batteries will end up in landfills or waste in the environment. In addition, the toxicity of these battery materials has not been traditionally part of the design process. Therefore, to determine the environmental impact and the possibility of alternative battery materials, representative complex battery nanomaterials LCO and NMC were synthesized and toxicity was assessed in *Daphnia magna*. Acute studies showed no effect to daphnid survival at 25 mg/L whereas chronic studies show significant impacts to daphnid reproduction and survival at concentrations of 0.25 mg/L for LCO and 1.0 mg/L for NMC. Dissolved metal exposures showed no effect at the amounts measured in suspension and supernatant controls could not reproduce the effects of the particles, indicating a nanomaterial-specific impact. Down regulation of genes important in metal detoxification, metabolism and cell maintenance was observed in a dose dependent manner. This study demonstrated that the chemical composition of battery materials could be altered to minimize environmental impacts.

Introduction

Batteries provide consumers with a portable and convenient form of stored chemical energy to fuel many everyday technologies. With increasing usage and expansion of technologies such as portable electronics and electric vehicles, complex metal oxides such as lithium intercalation materials are increasingly used as battery cathodes. Lithium intercalation materials based on layered transition metal oxides are desirable cathode materials because they have qualities such as the ability to perform high-speed reversible reactions with lithium and high voltage and energy densities¹. Lithium cobalt oxide or “LCO” (Li_xCoO_2) has been around since the 1990’s and is an example of a first generation cathode material that is in the process of being replaced by more complex materials such as lithium nickel manganese cobalt oxide or “NMC” ($\text{Li}_x\text{Ni}_y\text{Mn}_z\text{Co}_{1-y-z}\text{O}_2$, $0 < x,y,z < 1$) for higher performance, lower cost, and increased stability.^{2,3} Lithium nickel manganese cobalt oxide reduces the amount of cobalt in its layered structure by substituting cobalt with nickel and manganese.

The energy storage industry as a whole is expected to shift from bulk materials to nanomaterials (NMs) to obtain higher performing batteries⁴. Primary reasons for a switch from bulk materials to nanoscale materials are due to: 1.) Faster charge and discharge rates; 2.) Enhanced conductivity attributed to increased surface area to volume ratio⁵; and 3.) Less material fracturing from expansion and contraction during cycling⁶. Nanoscale NMC for instance, is considered to be a next generation cathode material for large-scale usage in batteries of electric vehicles. While the nanoscale form of NMC is not yet commercially available, bulk NMC has been shown to fracture into nanoscale particulates upon cycling⁷.

One of the most important aspects to consider in battery material design is its potential environmental impact, yet cost reduction is often considered over environmental compatibility. Recycling infrastructures are therefore limited due to little economic incentive^{7,8}. This leads to greater potential for batteries to end up in landfills or waste in the environment. However, it may be possible that alternative battery forms could be chosen to minimize impact but retain function. Nanoscale cathode materials should be designed to be environmentally benign to have the greatest impact as a sustainable form of energy storage¹. Few studies have determined the potential for environmental impact of next generation multicomponent metal oxides; therefore it is critical that we determine the environmental impacts now, ahead of the production cycle. Two important considerations are the impacts of using nanoscale versions of these materials as well as the consequences of replacing nickel and manganese for cobalt as we shift from LCO to NMC.

Only a few studies have highlighted the implications and mechanisms for toxicity of these nanoscale complex metal oxides. A preceding study of LCO nanosheets and supported lipid bilayers showed that this material had the ability to alter synthetic bilayer compositional symmetry⁹ and in bacteria toxicity was due to dissolution of nickel and cobalt ions¹⁰. The impact of nanoscale LCO and NMC on multicellular organisms is largely unknown. There have, however, been many studies that report the toxic effects of more simple metal oxide NMs. These studies show that, similar to the bacteria, effects are primarily due to metal dissolution or direct particle adherence¹¹⁻¹⁶. Therefore designing battery NMs where the ions released are not toxic

may reduce toxicity. In the past, the toxicity of these materials has not been part of the design process.

This study investigated the impact of NMC and LCO on survival and reproduction in the model multicellular aquatic organism, *Daphnia magna*. These materials have similar sheet-like morphology and size and only differ in chemical composition enabling us to evaluate how the metal composition of these materials impacts toxicity. *Daphnia magna* are critical components of freshwater food webs, are sensitive to a wide range of environmental contaminants and are designated environmental model organisms by the EPA and OECD.

In this study, acute and chronic assays were conducted to determine both short and long term impacts of these materials to *D. magna*. Additionally, gene expression assays were performed to determine organism molecular response upon exposure and determine whether the observed effects were from the NM exposure or the solubilized metals in solution. Metal ion control experiments accounted for metals leached from NMC and LCO particles and body burden assays were conducted to differentiate metals adsorbed to the daphnid carapace versus metals ingested and/or incorporated into tissues. This study seeks to assess the potential environmental hazard associated with these materials, provide molecular level information for mechanisms for toxicity and determine if materials could be redesigned to mitigate biological impacts.

Methods

Synthesis of NMC and LCO Nanosheets

Nanosheets of NMC and LCO were synthesized by adapting a previously reported method^{9, 10, 17}. Briefly, to make NMC, a $\text{LiNi}_{1/3}\text{Mn}_{1/3}\text{Co}_{1/3}(\text{OH})_2$ precursor was synthesized by adding an aqueous transition salt mixture containing 0.2 M cobalt(II) acetate, 0.2 M nickel(II) acetate, and 0.2 M manganese(II) acetate dropwise into 0.1 M aqueous LiOH under magnetic stirring. The resulting dark brown precursor was isolated by repeated cycles of centrifugation and resuspension in water (1X) and methanol (4X) followed by drying in a desiccator. The dried mixed metal hydroxide (0.250 g) was then added to a 10 g molten salt flux (6:4 molar ratio of LiNO_3 :LiOH) at 205 °C with magnetic stirring. After 30 min, the reaction was quenched with water and the NMC was isolated via repeated cycles of centrifugation and resuspension in water (1X) and methanol (4X) followed by drying in a desiccator. To make LCO, the same method for making NMC was used, with the exception that the precursor was made using only 0.5 M cobalt(II) nitrate for the aqueous transition salt mixture. All centrifugation was completed using the Thermo Scientific Sorvall legend X1R Centrifuge with a Thermo TX-400 rotor at 4686 g. All reagents were purchased from Sigma-Aldrich and ultrapure water (18 M Ω cm resistivity; Barnstead Nanopure) was used.

Characterization of NMC and LCO stoichiometry

A PerkinElmer Optima 2000 ICP-OES was used to determine the stoichiometry of samples. NMC and LCO were separately digested in freshly prepared *aqua regia* (3:1 v/v mixture of 37% v/v HCl and 70% v/v HNO₃) for 4 h and subsequently diluted in ultrapure water. Three replicate measurements were made of the ion concentrations.

ICP-OES measurements for digested NMC yielded metal ratios of Li/Ni = (0.812 ± 0.015) , Mn/Ni = (1.033 ± 0.011) , and Co/Ni = (1.017 ± 0.006) . These ratios indicate that the NMC material contains 1:1:1 of Ni:Mn:Co and lithiated to roughly 27% to give $\text{Li}_{0.27}\text{Ni}_{0.33}\text{Mn}_{0.33}\text{Co}_{0.33}\text{O}_2$. ICP-OES measurements for digested LCO yielded Li/Co = (1.002 ± 0.355) , indicating that the material was lithiated to 100% to give LiCoO_2 .

Characterization of NMC and LCO crystal phase

A Bruker D8 Advance powder X-ray diffractometer (PXRD) was used to obtain diffraction patterns for synthesized NMC and LCO. The dry powder samples were deposited onto a zero-diffraction plate (SiO_2 from MTI corp) for analysis using a Cu K α radiation source. The samples can be indexed to a R-3m space group previously reported for NMC and LCO.

Characterization of nanomaterial morphology

Scanning electron microscopy (SEM)

To determine average nanomaterial shape and size a Leo Supra55 VP scanning electron microscope with a 1kV incident electron energy with a standard in-lens detector was used to obtain images of NMC and LCO. Samples for SEM images were prepared by spin-coating (1000 rpm) a dilute methanolic solution of either NMC or LiCoO_2 onto a pristine boron-doped SiO_2 wafer.

Characterization of NMC and LCO sedimentation behavior in culture media

To characterize how quickly NMC and LCO nanosheets sedimented out of the aqueous phase, a Shimadzu UV-2401PC Research-Grade UV-vis spectrophotometer was used to analyze change in relative particle concentration the aqueous phase. NMC or LCO were suspended into medium at 10 mg/L and UV-vis measurements were made periodically over 24 h. UV-vis measurements of NMC or LCO in medium were referenced to a sample of medium to subtract out UV-vis signals from medium.

Characterization of metal release into culture media

To characterize metal release into the daphnid media, NMC or LiCoO_2 were suspended into the medium at concentrations of 0.5, 1, 5, and 25 mg/L for 72 h. The samples were then centrifuged at 4696 g for 10 min to remove the majority of particles in solution. The supernatant was subsequently ultracentrifuged for 2 h at 288,000g using a Beckman Coulter Optima Ultracentrifuge with a SW-41 Ti Rotor to ensure removal of remaining particles. The supernatant was analyzed for free Li, Ni, Mn, and Co content using a Thermo Scientific XSERIES 2 ICP-MS instrument with 3 sample replicates and 5 analytical replicates. Dynamic light scattering (Malvern Zetasizer Nano ZS) was used to evaluate effective removal of particles under the specified centrifugation conditions.

***D. magna* culture and exposures**

Daphnids used in this study were harvested from cultures maintained at the UW-Milwaukee School of Freshwater Sciences in the R. Klaper laboratory. Daphnid populations were maintained in moderately hard reconstituted water (MHRW: 60 mg/L

CaSO₄ and MgSO₄, 96 mg/L NaHCO₃, 4 mg/L KCl and .02 mL/L of a 330 mg/L Na₂SeO₃*5H₂O solution)¹⁸ incubated at 20 °C on a 16 : 8 light/dark cycle as described by EPA recommendations. Media was oxygenated for 48 hours with an oxygen stone prior to use. Daphnids were fed a combination of 20 mL freshwater algae (*Pseudokirchneriella subcapitata*) at an algal density of ~400,000 algal cells per mL and 10 mL of dissolved alfalfa (*Medicago sativa*) three times a week. Alfalfa stock was prepared by suspending 405 mg of alfalfa in 50 mL Milli-Q water after 20 minutes of agitation and 5 minutes of centrifugation at 5,000 RPM. Breeding populations were held at a concentration no greater than 1 adult daphnid per 50 mL of media in 1-liter glass beakers at a population density of 20 adult daphnids per liter. Neonates were only harvested from adults 14 - 28 days old, ensuring healthy daphnid neonates.

Acute exposures. Acute exposures adhered to OECD 202 guidelines for *D. magna* acute immobilization test. Briefly, five daphnid neonates ≤ 24 hours old were placed in 100 mL moderately hard reconstituted water (MHRW, control)¹⁸, NMC or LCO NMs, supernatants or metal ions. For each treatment, a minimum of three replicates was performed and the percent of animals alive at the end of 48 hours was determined. Lithium nickel manganese cobalt oxide and LCO NMs were tested in acute exposures at nominal concentrations of 1.0, 10 and 25 mg/L.

Chronic exposures. Chronic experiments were performed using five daphnid neonates < 24 hours old exposed to control water, NMs or metal ion controls for 21 days in a static renewal exposure. Media was renewed three times a week and treatments were

performed in quadruplicates. A total of five neonates were placed in 94 mL of MHRW, NMs, supernatants or metal ions. Daphnids were supplemented with 4 mL of algae (*Selenastrum capricornitum*) and 2 mL of alfalfa (*Medicago sativa*) at each media exchange to bring the total volume to 100 mL. Lithium nickel manganese cobalt oxide, LCO NMs and their respective supernatants were tested in chronic exposures at nominal concentrations of 0.25, 0.5, 1.0, 5.0 and 25 mg/L and 0.05, 0.1, 0.25, 0.5, 1, 5, and 25 mg/L, respectively. Samples from chronic exposures were then flash frozen in liquid nitrogen at day 21 to determine daphnid gene expression. Samples were selected by determining treatments that caused equal impacts to daphnid survival and reproduction (one sub lethal concentration and one concentration that caused equal impacts to daphnid survival and reproduction). These concentrations were determined to be 0.10 and 0.25 mg/L for LCO and 0.25 and 1.0 mg/L for NMC.

Solution and suspension preparation. The highest concentration of NMC and LCO NMs and their respective supernatants tested was 25 mg/L. Five metal ion concentrations were tested for each metal. These concentrations overlapped with the concentrations of metals determined to leach from the NMs in daphnid media. The highest concentrations tested were 10, 0.4, and 0.2 mg/L for lithium, nickel and cobalt, respectively, in both acute and chronic exposures. Manganese was not assessed because it was not found in solution at a relevant concentration.

NMC and LCO stock suspensions were prepared by measuring out and mixing 100 mg of material with one-liter of ultra pure water in a one-liter vessel. Stocks were then sonicated for 20 minutes followed by an additional sonication time of 10 minutes

prior to use. Suspensions were used for the entire 21-day exposure. NMC and LCO supernatants were prepared by sampling from the stocks on the day of the exposure media exchange after sonication. Samples were then placed into 50 ml conical tubes and centrifuged for 10 minutes at 10,000 rpm. Care was taken to not disturb the pellet and minimize contamination of supernatant by particulate metals.

Metal salts were weighed and similarly placed in one-liter vessels and sonicated for 10 minutes to properly dissolve salt. The salts used in this study to test free ion toxicity were cobalt chloride hexahydrate, lithium hydroxide and nickel (II) chloride. Molecular weight was accounted for to reach desired concentration of metal ion.

Body burden assay. The body burden assay was performed to determine the total amount of material adhered vs. ingested/adhered/internalized. Adult daphnids, 26 ≤ 27 days old, were exposed to either control water or NMC particles at 1 mg/L for 24 hours. Specifically, the exposure consisted of a total of five adult daphnids that were placed in 94 mL of MHRW or NMs and daphnids were supplemented with 4 mL of algae (*Selenastrum capricornitum*) and 2 mL of alfalfa (*Medicago sativa*) bringing the total volume to 100 mL. At the end of 24 hours the daphnids in the treated groups were pooled into six samples of 35 daphnids each, control groups were pooled into three samples of 15 daphnids each. For the treated samples, three of the six samples were treated with 4 mL of aqua regia for two minutes to dissolve adhered NMC particles. All six treated samples were rinsed with 30 mL of ultra pure water three times before ICP-OES analysis.

RNA extraction, reverse transcription and gene expression

RNA extraction. To determine the level of expression of genes involved with various cellular functions daphnids were harvested from chronic exposures at the end of the 21-day exposure period. At the end of 21 days, daphnids were immediately frozen with liquid nitrogen and stored at -80°C until extraction. The surviving daphnids harvested from each replicate were pooled together to have a final total of 4 replicates per treatment ($n \leq 5$ daphnids per sample) for gene expression analysis. The RNA from these samples was isolated using A Direct-zol™ RNA MiniPrep kit (Zymo Research). The isolation and purification of total RNA followed the manufacturers recommended protocol. A Thermo Scientific NanoDrop 8000 characterized total RNA immediately after elution using $1.5\ \mu\text{L}$ total RNA to ensure quality and determine concentration. During this time the samples were stored on ice. The remaining sample was stored at -80°C to wait further processing.

Reverse transcription. The manufacturers protocol was followed in order to reverse transcribe the total RNA into cDNA. $250\ \mu\text{g}$ of total RNA was incubated in the presence of oligo(dT)₁₅ primer (Promega) and dNTPs at 65°C for 5 minutes. After a 4 minute cooling period at 4°C , the samples were combined with a 5x buffer solution, SuperScript III reverse transcriptase, DTT, and RNaseOUT™ recombinant ribonuclease inhibitor (Life Technologies), mixed and incubated at 50°C for 60 minutes. Lastly, the mixture was incubated at 70°C for 15 minutes for primer extension and the final product was permanently stored at -20°C immediately following synthesis.

Gene expression. Several genes were chosen to investigate the molecular impacts of NMC and LCO NMs. These genes included actin (*act*), which encodes for a protein important in cytoskeleton production and cell motility, glutathione s transferase (*gst*) and catalase (*cat*), important to xenobiotic detoxification and oxidative stress attenuation, metallothionein (*mtl1a*) and heat shock protein 70 kDa (*hsp70*), which respond to metal stressors, vitellogenin (*vtg1*) a gene that encodes for an egg yolk precursor protein and *18s* ribosomal RNA (*18s*), a gene important to cell function. Additional information on these genes may be found in Table 1. Primers for determining changes in gene expression were created using real-time Primer Quest Tool (Integrated DNA Technologies). Table 1 depicts the list of primers and their sequences tailored for this study.

Real-time quantitative PCR (qPCR) was performed on a StepOnePlus™ Real-Time PCR System (Life Technologies) using SYBR Green as the fluorescent intercalating dye (iTaq™ Universal SYBR® Green Supermix, Bio-Rad). Per reaction, cDNA and primers were mixed with SYBR Green following the recommended protocol. Starting with an initial 10 min denaturation at 95 °C, real-time PCR repeated 40 cycles of amplification, each cycle consisting of a 15 s at 95 °C period followed by 30 s at 62 °C period. Fluorescence of SYBR Green was detected at the end of each cycle. All qPCR experiments were done in two technical replicates. Miner and NORMA-Gene algorithm were used to analyze real-time quantitative PCR data, as previously reported.¹⁹⁻²¹ All final relative fold change gene expression values obtained were log₂ transformed before reporting.

Statistics

To determine the significance of the impacts of treatments compared to the controls, two statistical analyses (Mann Whitney U-test or One-Way ANOVA) were chosen depending on the distribution of the data and homogeneity of variances. The statistical analyses were performed using SPSS (IBM 2015). Impacts to daphnid survival were assessed using the nonparametric Mann Whitney U-test for two independent samples after the data failed normality and homogeneity of variances were determined. No outliers were found, and treatments were deemed significantly different than controls at probability value < 0.05 . Impacts to daphnid reproduction were determined using One-Way ANOVA with Tukey HSD Post Hoc Test after the data was found to be normal and variances considered homogenous. No outliers were found, and treatments were deemed significantly different than controls at probability value < 0.05 .

The relative gene expression data from *Daphnia* chronic exposures were normalized to controls and \log_2 transformed to fit a normal distribution. Outliers were removed prior to statistical analysis. Significant differences in relative expression were determined using either One-Way ANOVA with Tukey HSD Post Hoc Test or One-Way ANOVA with Dunnett's T3 Post Hoc Test after normality and homogeneity of variances were determined ($p < 0.05$) ($N > 3$).

Results

Characterization of Nanoscale NMC and LCO

Upon exposure to daphnid media, the electrophoretic mobilities of the NMC and LCO nanosheets were (0.19 ± 0.03) and (0.21 ± 0.06) $\mu\text{mcm}/(\text{Vs})$, respectively (Table

2). The colloidal stability of 10 mg/L NMC and LCO in daphnid medium was also assessed using UV-vis to analyze how the relative concentrations of NMC and LCO changed in the water column over time. Figure S1a† shows that for NMC, an initial measurement at 0 h yielded a broad peak centering around 263 nm. At 3h, a sharper peak centered at 253 nm appeared with an absorbance reading of 0.127. Over 22.5 h, this peak at 253 nm decreased to an absorbance reading of 0.085, indicating an absorbance loss of 33%. Figure S1b† shows that for LCO, an initial measurement at 0 h yielded a peak at 278 nm with an absorbance reading of 0.228. Over 22.5 h, this peak shifted toward 269 nm with a final absorbance reading of 0.078; indicating a relative absorbance loss of 66%. These UV-vis measurements show that LCO nanosheets sediment out of the water column much faster than NMC over the course of 22.5 h.

Figure S2† show SEM images of synthesized nanoscale NMC and LCO, both of which show sheet-like morphology. While the SEM resolution is limited by charging effects, the edge-on features can be approximated to be <5 nm in thickness can be seen in figures S2a and b†. The nanosheets of NMC and LCO have a range of sizes in terms of their basal diameter because the sheet-like character of nanoscale NMC renders them fragile. Both synthesized NMC and LCO nanosheets were indexed to an R3m space group via powder X-ray diffraction measurements (Fig. S3a and b†).

Dissolution study

Lithium cobalt oxide and NMC leached measurable amounts of metal ions into solution when measured at 72 hours in daphnid media (Fig. 1a and 1b). Most notably,

for both materials, large quantities of lithium were released into solution in a dose dependent manner. For LCO, at 0.5, 1.0, 5.0 and 25 mg/L, lithium was found at concentrations of 0.03, 0.06, 0.28, and 1.32 mg/L in solution, respectively. For NMC, at 0.5, 1.0, 5.0 and 25 mg/L, lithium was found at concentrations of 0.04, 0.09, 0.41, and 2.04 mg/L in solution, respectively. Cobalt was found at lower concentrations, a maximum of 0.02 for LCO and 0.003 for NMC per 5 mg/L of material. Nickel was measured in solution at a maximum concentration of 0.08 mg/L for NMC at 5 mg/L. Manganese was found to be in solution below detection limits for NMC (< 0.001).

***Daphnia* body burden study**

Daphnids exposed to 1 mg/L NMC for 24 hours exhibited greater accumulation of NMC particles and or dissolved metals than daphnids with the same treatment plus an acid wash (Supporting information, Fig. S4†). Daphnids exposed to NMC particles accumulated 0.001, 0.092, 0.098 and 0.110 mg/daphnid for lithium, nickel, manganese and cobalt, respectively. Smaller amounts of particle and metal accumulation were measured for daphnids exposed to 1 mg/L NMC for 24 hours and treated with an acid wash. Daphnids with the acid wash contained amounts of lithium, nickel, manganese and cobalt equal to 0.001, 0.054, 0.062 and 0.078 mg/daphnid, respectively. Controls showed very little amounts of metal contamination. Nickel was found below the detection limit in control daphnids. The remaining three metals were measured at 0.003, 0.003, and 0.029 mg/daphnid for lithium, manganese and cobalt, respectively.

***Daphnia magna* acute and chronic toxicity**

Lithium nickel manganese cobalt oxide and LCO NMs had no impact on daphnid mortality at any of the tested concentrations ($p > 0.05$, 1-25 mg/L). However these materials were visible in the digestive tract and adhered to carapace of *D. magna*.

LCO nanoparticles and supernatant. Chronic exposures of LCO demonstrated significant negative impacts to daphnid survival, reproduction at concentrations greater than 0.25 mg/L (Fig. 2a and 3a, respectively). The lowest concentration tested, 0.05 mg/L caused no impacts to measured endpoints. A concentration of 0.1 mg/L caused a 23.2% increase in daphnid reproduction compared to control. A concentration of 0.25 mg/L, decreased daphnid reproduction by 79.8% ($F = 32.942$, $df = 15$, $p < 0.05$) and daphnid survival by 40% at day 21 compared to control ($U = 0.0$, $p > 0.05$). Concentrations of LCO at 0.5, 1 and 5 mg/L caused 100% mortality by day 21 ($U = 0.0$, $p < 0.05$) and no reproduction was observed compared to control. No impacts to daphnid body size at any concentration were observed. Exposure to the LCO supernatant caused no impacts at similar concentrations where impacts were observed from LCO NMs.

NMC nanoparticles and supernatant. Chronic exposures caused significant impacts to daphnid survival, reproduction and body size at concentrations greater than 0.25 mg/L, in a dose-dependent manner (Fig. 2b, 3b and supporting information, S5†, respectively). The lowest concentration tested, 0.25 mg/L caused a 21% increase in reproduction, though not significant, and no impacts to daphnid survival or. However,

0.5 mg/L caused a significant 44% reduction in daphnid reproduction ($F = 28.740$, $df = 19$, $p < 0.05$) compared to control. No significant differences in body size or survival were found at this concentration. Daphnids exposed to 1.0 mg/L NMC particles exhibited significant impacts to body size, mortality and reproduction compared to control. This concentration caused an 87% decrease in daphnid reproduction ($F = 28.740$, $df = 19$, $p < 0.05$), a reduced body size by 15.5% ($p < 0.05$)(Fig. S5†), and a 60% reduced survival rate at day 21 ($U = 0.0$, $p < 0.05$) when compared to control. The two highest concentrations, 5.0 and 25 mg/L, elicited significant impacts to daphnid survival with 100% reduction in survival by day 21 ($U = 0$, $p < 0.05$). Exposure to the NMC supernatant caused no impacts at similar concentrations where impacts were observed from NMC NMs.

Nickel. Measured concentrations of nickel leached in the dissolution study did not cause impacts to daphnia survival or reproduction. However, chronic exposures to nickel caused significant impacts to daphnid survival and reproduction at 0.4 mg/L (Fig. 4a and 5a, respectively). At this concentration, 100% daphnid mortality occurred at day 21 ($U = 0.0$, $p < 0.05$) and an 80.3 % reduction in daphnid reproduction was recorded ($F = 35.651$, $df = 18$, $p < 0.05$). At 0.1 and 0.2 mg/L nickel there was a 17.7 and 25.4% increase in daphnid reproduction. No impacts to daphnid body size were observed.

Cobalt. Concentrations of leached cobalt from the dissolution study did not cause significant impacts to daphnid survival or reproduction. Instead, exposure to cobalt

caused a significant reduction to daphnid survival at 0.2 and 0.1 mg/L and significant impacts to reproduction at 0.1 mg/L (Fig. 4b and 5b, respectively). At 0.1 mg/L cobalt, daphnids experienced an 89.6% reduction in reproduction ($F = 42.276$, $df = 15$, $p < 0.05$) and a 20% reduction in daphnid survival ($U = 0.0$, $p < 0.05$) when compared to controls. At 0.2 mg/L 100% reduction in daphnid survival was observed at day 21 ($U = 0.0$, $p < 0.05$). No impacts to daphnid body size were observed.

Lithium. Only the highest measured concentration of lithium leached from 25 mg/L of NMC caused significant impairments to daphnid survival and to reproduction (Fig. 4c and 5c, respectively), no other concentration of NMC or LCO measured lithium leachate caused significant impacts. At 2.5 mg/L lithium, daphnids exhibited a 97.8% reduction in reproduction ($F = 85.223$, $df = 12$, $p < 0.05$). At 2.5, 5.0 and 10 mg/L 100% reduction in daphnid survival was observed at day 21 ($U = 0.0$, $p < 0.05$). No impacts to daphnid body size were observed.

Gene expression

Daphnids exposed to LCO and NMC for 21 days exhibited dose dependent down regulation of a number of genes explored in this study (Fig. 6a and 6b, respectively and Supporting information, Table. S1†). Of the NMs we tested, NMC appeared to down regulate genes to a greater extent than LCO.

Daphnids exposed to NMC and LCO supernatant controls exhibited a different response compared to the NMs themselves. LCO supernatant caused no significant changes in gene expression but increased in the expression of *18s*, *vtg1* and *Mtla* ($p >$

0.05). However, LCO at 0.25 mg/L significantly decreased Daphnid relative expression of *18s*, *cat*, *vtg1*, *gst*, *act*, and *hsp70* ($p < 0.05$, Table S1†). LCO at 0.1 mg/L only significantly down regulated *vtg1* ($p < 0.05$, Table S1†). Gene expression for NMC supernatant showed no significant changes ($p < 0.05$). Daphnids exposed to concentrations of NMC at 1.0 mg/L showed genes *18s*, *cat*, *gst*, *act*, *Mtla* and *hsp70* significantly down regulated ($p < 0.05$, Table S1†). Daphnids exposed to a lower concentration of NMC, 0.25 mg/L, showed significant decreases in the relative expression of *cat*, *vtg1*, *gst* and *hsp70* ($p < 0.05$, Table S1†). For specific gene expression values and statistical information see table 1 in the supporting information (Table S1†).

Discussion

The results suggest that the effects elicited from both NMC and LCO particles were not due to the free ions alone rather a specific effect caused by the ingestion of the NMs themselves (Fig. 2 and 3). Lithium nickel manganese cobalt oxide and LCO NMs impacted *Daphnia magna* survival, reproduction and body size in a dose dependent manner independent of the free ions present in suspension. In our study, the NMC and LCO particles visibly adhered to the daphnid carapace and accumulated inside the digestive tract of the organism. This was further supported by the body burden assay with NMC that demonstrated a significant amount of NMs both adhered and ingested/internalized in *D. magna*. Other studies report similar effects with metallic NMs. For instance, it was found that metallic nanoparticles adhere to bacteria and algae. These studies concluded that it was nanoparticle adherence that caused toxicity due to localized delivery of toxic ionic metals^{15, 16}. While free ions in suspension do not

explain the observed effects, NMC and LCO particulates could potentially be delivering a localized high concentration of free ions on or inside daphnid cells that were not accounted for by the free ion and supernatant control treatments. Toxic metals have been shown to damage gut epithelial cells involved in nutrient uptake and sensitive organs such as the gills.

In addition, these sites in particular have been shown to be the main sites of accumulation for water borne metals such as silver²² and nickel.²³ One study found that, upon exposure to sub-lethal concentrations of nickel and cobalt, degeneration of the hepatic caeca located in the digestive tract of *Daphnia magna* occurred.²⁴ In daphnids, the hepatic caeca (diverticula) are important to acid production²⁵, food digestion²⁶ and nutrient uptake.²⁷ In the presence of nickel, *D. magna* suffer from drastically reduced whole body glycogen content.²⁸ LCO and NMC nanomaterials may undergo chemical transformations such as redox-enabled dissolution of the material upon accumulation inside the digestive tract. Therefore, upon exposure to LCO and NMC materials, potential localized high concentrations of these metals in their bodies may cause daphnids to experience an impact to their energy budgets due to impaired nutrient assimilation. This might explain the decrease in reproduction, body size and increased mortality rate at low concentrations.

Chemical composition appeared to be important for determining toxicity ((LCO (100% Co) vs. NMC (33% Ni, 33% Mn, and 33% Co)) indicating that choice of material may mitigate toxicity for these next-generation materials. Other studies have made similar conclusions but with different materials. For example, CdSe/ZnS and InP/ZnS core/shell NMs were exposed to two cell lines, SH SYSY and A549 cells. CdSe/ZnS

and InP/ZnS were well characterized with comparable physical and chemical properties only differing in chemical composition²⁹. This study concluded that, substituting Cd and Se with In and P as the core material components in the core/shell NM mitigated all impacts to cellular viability at the tested concentrations²⁹. LCO was more toxic than NMC causing similar impacts to long term survival and reproduction at concentrations four times lower indicating chemical specific impacts. Of the three individual metals assessed in this study, cobalt was the most toxic to *D. magna* (Fig. 4b and 5b), impacting reproduction and survival at concentrations as low as 0.1 mg/L. Dissolution studies revealed higher amounts of cobalt leached from LCO NMs potentially explaining why this material was more toxic to daphnids (Fig. 1). These results indicate that replacing toxic metals with less toxic metals may reduce the potential for impacts to environmental health.

Nanospecific impact may also be related to physical impact as they were found to adhere to daphnids, however, the physical adherence may have caused a localized high concentration of toxic metal ions. Previous studies have shown that metal and clay particulates may cause physical insults to invertebrates at high concentrations due to constipation and feeding inhibition (e.g. disruption of collection and ingestion of algae) and that there may be unique impacts due to the particulate chemical composition.³⁰ Because LCO and NMC have the same morphology, similar density and aggregation but differ greatly in their impacts may indicate that physical effects were not an important factor at low concentrations. Our previous studies showed that citrate coated gold nanoparticles adhered to daphnids and physically impaired daphnid reproduction and body size³¹. These effects were only observed at high

concentrations (25 mg/L) and were thought to be due to the extended fused networks the aggregated gold nanoparticles formed. Similar sized gold nanoparticles that did not form extended fused networks of particles; rather aggregated groups of individual nanoparticles and did not cause any effects at high concentrations (25 mg/L)³¹. This further supports our hypothesis that effects are chemical related rather than physical, as LCO and NMC particles caused apical endpoint impacts at low concentrations (0.25 and 1 mg/L, respectively)(Fig. 2 and 3).

Gene expression results further demonstrated that the NMs themselves caused unique impacts that could not be explained by the supernatant controls that accounted for background dissolved metals in suspension (Fig. 6). Another study exploring different metal oxides found that the metal oxide and their respective soluble metal had a distinct molecular fingerprint¹². These results are in agreement with ours, in that the solubilized metals could not replicate the molecular level response upon exposure to their respective NM. Lithium nickel manganese cobalt oxide and LCO caused a significant down regulation of genes involved in oxidative stress, heavy metal toxicity, reproduction and cell maintenance related pathways. Other studies report that upon exposure to metal oxide NMs have trigger the down regulation of a wide range of genes, more so than up regulation¹². Although we only were able to examine two concentrations (one sub lethal and one lethal concentration), the impacts to gene expression appeared to be dose dependent with the high concentrations of NMC and LCO NMs down-regulating gene expression to a greater extent than low concentrations. This was potentially because the organism was dying. Overall NMC NMs altered gene expression to a greater extent than LCO NMs, however daphnids

were exposed to NMC at higher concentrations and exhibited greater impacts to survival and reproduction.

Conclusion

With the growth in lithium ion based energy storage technologies industry seeks to develop new materials with enhanced qualities, such as increased intercalation rates, energy storage capacity and resistance to degradation. First generation materials such as LCO are being replaced by NMC and there is a switch from bulk materials to NMs as they enable industry to achieve their performance standards. NMs such as NMC will increase in production, as they will be primary components of these technologies. However, current recycling infrastructure is in its infancy, which leads to the disposal of batteries containing NMC in landfills and potential for these materials to enter aquatic environments. The most important quality of battery material design should be its environmental biocompatibility, however, the toxicity of these materials has not been part of the design process. In order to develop sustainable cathode NMs we must get ahead of the production cycle. Two important considerations are the impacts of using NM versions of these materials as well as the consequences of replacing nickel and manganese for cobalt as we shift from LCO to NMC.

In this study, we found that NMC and LCO NMs leached measurable amounts of lithium, nickel and cobalt into solution; however, controls that accounted for free ion and supernatant toxicity could not explain the observed effects when NMC and LCO NMs were present in suspension. Furthermore, particles were ingested by daphnids and found to adhere to their carapace leading us to believe that the effects we

observed are NM specific. While we cannot rule out a metal ion-induced mechanism for toxicity, we hypothesize that the observed impacts are caused by the physical adherence of the NM to biological membranes and a localized delivery of a high concentration of toxic metals. In addition, our study demonstrated that the toxicity of the materials in question is dependent upon chemical composition with the replacement of cobalt by nickel and manganese leading to increased daphnid survival and reproduction. Therefore, replacing toxic metals with more benign metals may increase the environmental compatibility and sustainability of next generation battery materials. To our knowledge this is the first study assessing the toxicity of a multicomponent complex metal oxide to *Daphnia magna*.

Acknowledgements

This work was funded by the National Science Foundation Center for Chemical Innovations grant CHE-1503408: Center for Sustainable Nanotechnology.

REFERENCES:

1. M. S. Whittingham, *Chemical reviews*, 2004, **104**, 4271-4302.
2. K. Kang, Y. S. Meng, J. Bréger, C. P. Grey and G. Ceder, *Science*, 2006, **311**, 977-980.
3. P. Poizot, S. Laruelle, S. Grugeon, L. Dupont and J. Tarascon, *Nature*, 2000, **407**, 496-499.
4. H. Flynn, *Lux research*, 2014.
5. M. Tang, H.-Y. Huang, N. Meethong, Y.-H. Kao, W. C. Carter and Y.-M. Chiang, *Chemistry of Materials*, 2009, **21**, 1557-1571.
6. A. Mukhopadhyay and B. W. Sheldon, *Progress in Materials Science*, 2014, **63**, 58-116.
7. M. N. Hang, I. L. Gunsolus, H. Wayland, E. S. Melby, A. C. Mensch, K. R. Hurley, J. A. Pedersen, C. L. Haynes and R. J. Hamers, *Chemistry of Materials*, 2016, **28**, 1092-1100.
8. J. Dunn, L. Gaines, J. Kelly, C. James and K. Gallagher, *Energy & Environmental Science*, 2015, **8**, 158-168.
9. M. Doğangün, M. N. Hang, J. M. Troiano, A. C. McGeachy, E. S. Melby, J. A. Pedersen, R. J. Hamers and F. M. Geiger, *ACS nano*, 2015, **9**, 8755-8765.
10. M. N. Hang, I. L. Gunsolus, H. Wayland, E. S. Melby, A. C. Mensch, K. R. Hurley, J. A. Pedersen, C. L. Haynes and R. J. Hamers, *Chemistry of Materials*, 2016.
11. A. Nel, T. Xia, L. Mädler and N. Li, *science*, 2006, **311**, 622-627.
12. R. J. Griffitt, K. Hyndman, N. D. Denslow and D. S. Barber, *Toxicological sciences : an official journal of the Society of Toxicology*, 2009, **107**, 404-415.
13. M. Li, D. Lin and L. Zhu, *Environmental pollution*, 2013, **173**, 97-102.
14. T. Li, B. Albee, M. Alemayehu, R. Diaz, L. Ingham, S. Kamal, M. Rodriguez and S. W. Bishnoi, *Analytical and bioanalytical chemistry*, 2010, **398**, 689-700.
15. D. Lin, J. Ji, Z. Long, K. Yang and F. Wu, *Water research*, 2012, **46**, 4477-4487.
16. J. Chen, Z. Xiu, G. V. Lowry and P. J. Alvarez, *water research*, 2011, **45**, 1995-2001.
17. D. Qian, Y. Hinuma, H. Chen, L.-S. Du, K. J. Carroll, G. Ceder, C. P. Grey and Y. S. Meng, *Journal of the American Chemical Society*, 2012, **134**, 6096-6099.
18. M. E. Smith, J. M. Lazorchak, L. E. Herrin, S. Brewer - Swartz and W. T. Thoeny, *Environmental Toxicology and Chemistry*, 1997, **16**, 1229-1233.
19. S. Zhao and R. D. Fernald, *Journal of computational biology*, 2005, **12**, 1047-1064.
20. L.-H. Heckmann, P. B. Sørensen, P. H. Krogh and J. G. Sørensen, *Bmc Bioinformatics*, 2011, **12**, 1.
21. T. Qiu, J. Bozich, S. Lohse, A. Vartanian, L. Jacob, B. Meyer, I. Gunsolus, N. Niemuth, C. Murphy and C. Haynes, *Environmental Science: Nano*, 2015, **2**, 615-629.
22. A. Bianchini, C. Rouleau and C. M. Wood, *Aquatic toxicology*, 2005, **72**, 339-349.
23. T. Hall, *Limnology and Oceanography*, 1982, **27**, 718-727.
24. V. Luzgin, *Biologiya*, 1982a, **2**, 8-13.
25. G. Rankin, *Contributions to Canadian Biology and Fisheries*, 1929, **4**, 107-113.
26. N. N. Smirnov, *Physiology of the Cladocera*, Academic Press, 2013.
27. M. Yamamura, S. Hatakeyama and K. T. Suzuki, *Bulletin of environmental contamination and toxicology*, 1983, **30**, 298-302.

28. E. F. Pane, J. C. McGeer and C. M. Wood, *Environmental toxicology and chemistry*, 2004, **23**, 1051-1056.
29. V. Brunetti, H. Chibli, R. Fiammengo, A. Galeone, M. A. Malvindi, G. Vecchio, R. Cingolani, J. L. Nadeau and P. P. Pompa, *Nanoscale*, 2013, **5**, 307-317.
30. S. Randall, D. Harper and B. Brierley, *Hydrobiologia*, 1999, **395**, 355-364.
31. J. S. Bozich, S. E. Lohse, M. D. Torelli, C. J. Murphy, R. J. Hamers and R. D. Klaper, *Environmental Science: Nano*, 2014, **1**, 260-270.

CHAPTER 4 TABLES

Table 1 Genes explored, primer sequence information, gene description and accession number.

Target Gene	Forward primer (5'-3')	Reverse primer (5'-3')	Function	Accession #
Glutathione S-transferase (<i>gst</i>)	CAA CGC GTA TGG CAA AGA TG	CTA GAC CGA AAC GGT GGT AAA	Xenobiotic detoxification	AF448500.1
Catalase (<i>cat</i>)	CAG GAT CAT CGG CAG TTA GTT	CTG AAG GCA AAC CTG TCT ACT	Oxidative stress attenuation	GQ389639.1
Metallothionein (<i>mtla</i>)	TTG CCA AAA CAA TTG CTC AT	CAC CTC CAG TGG CAC AAA	Metal detoxification	KF561474.1
Vitellogenin (<i>vtg1</i>)	CTG TTC CTC GCT CTG TCT TG	CCA GAG AAG GAA GCG TTG TAG	Reproduction, sexual maturation and general stress	AB252737.1
18s (<i>18s</i>)	CGC TCT GAA TCA AGG GTG TT	TGT CCG ACC GTG AAG AGA	Protein synthesis	AM490278.1
Heat shock protein 70 (<i>hsp70</i>)	CCT TAG TCA TGG CTC GTT CTC	TCA AGC GGA ACA CCA CTA TC	Response to heat; protein folding	EU514494.1
β -Actin (<i>act</i>)	CCA CAC TGT CCC CAT TTA TGA A	CGC GAC CAG CCA AAT CC	Cytoskeleton production, cell maintenance	AJ292554.1

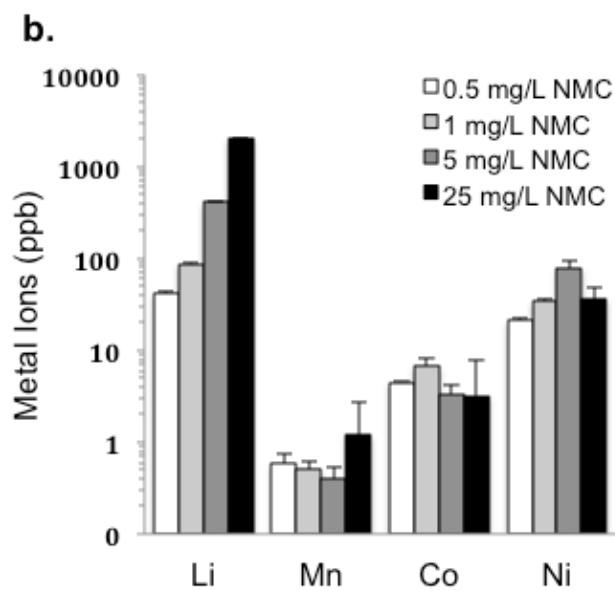
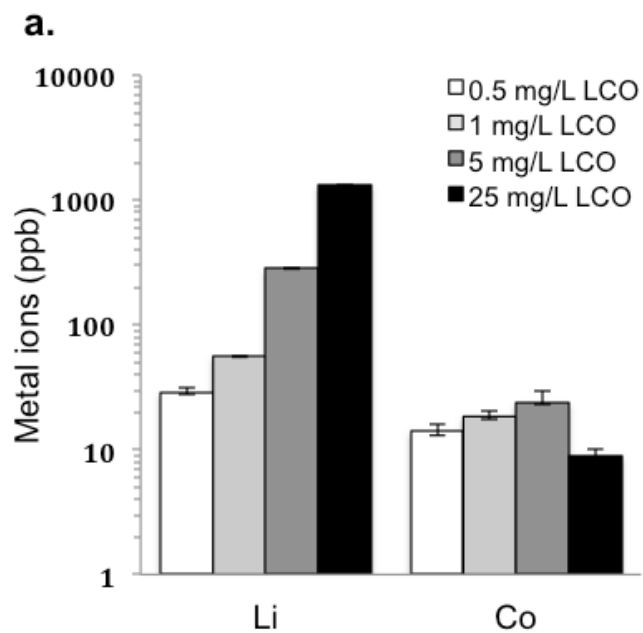
Table 2 Nanomaterial characterization

Milli-Q water	ζ -Potential (mV)	Mobility ($\mu\text{mcm/Vs}$)
LCO	-6.25 \pm 0.45	-0.49 \pm 0.03
NMC	-7.08 \pm 1.75	-0.55 \pm 0.33
Daphnia media		
LCO	2.73 \pm 0.70	0.21 \pm 0.05
NMC	2.50 \pm 0.40	0.20 \pm 0.02

Lithium cobalt oxide (LCO) and lithium nickel manganese cobalt oxide (NMC) nanoparticle zeta potential and electrophoretic mobility in ultra pure water (milli-Q) and *Daphnia* medium.

CHAPTER 4 FIGURES

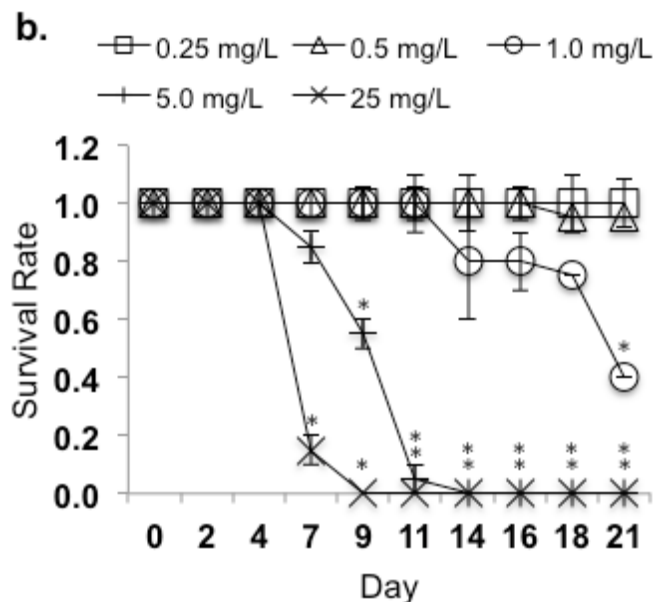
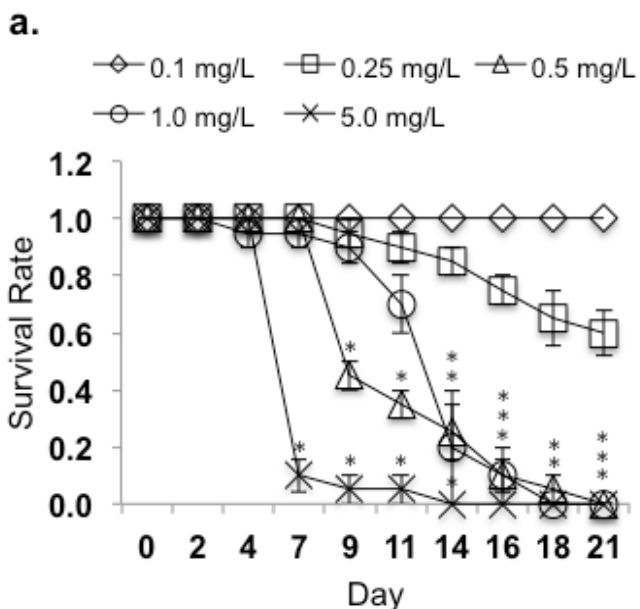
Figure 1



ICPMS results for metal dissolution in daphnid media at 72 hours. Particle dissolution for (a) lithium cobalt oxide (LCO) nanoparticles and supernatant and (b)

lithium nickel manganese cobalt oxide (NMC) nanoparticles and supernatant. Error bars represent standard deviation, $n = 3$.

Figure 2

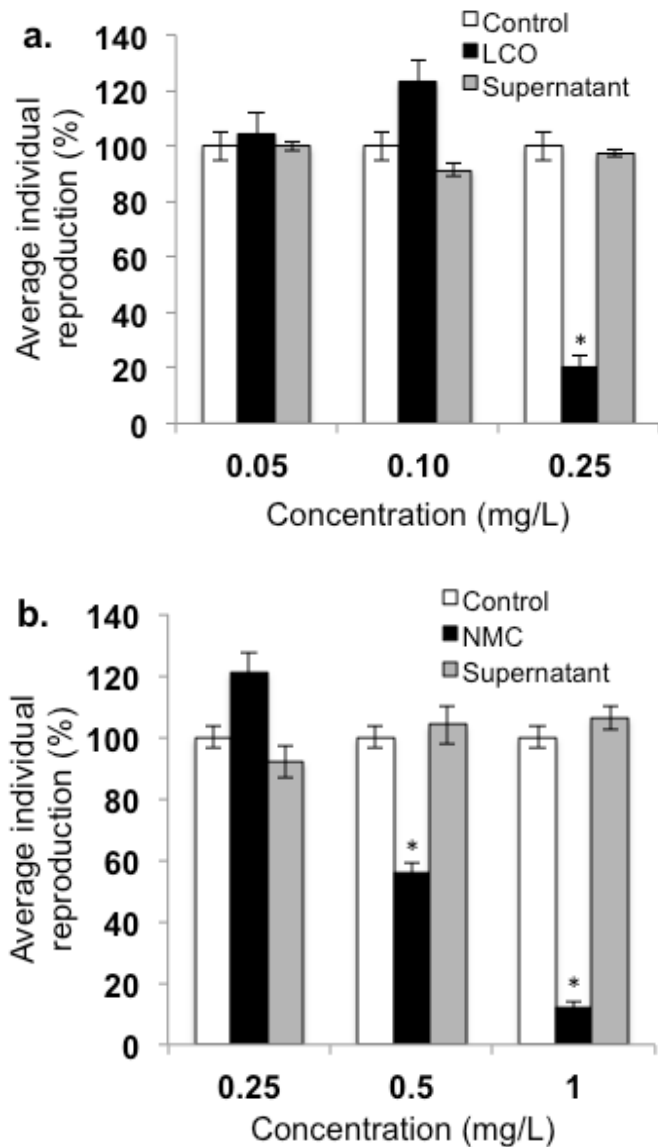


Average chronic daphnid survival rate over 21 days compared to controls.

Survival rate for (a) lithium cobalt oxide (LCO) nanoparticles and supernatant and (b) lithium nickel manganese cobalt oxide (NMC) nanoparticles and supernatant. Error

bars represent standard error of the mean, $n \geq 4$. Asterisks indicate significance compared to control ($p < 0.05$).

Figure 3



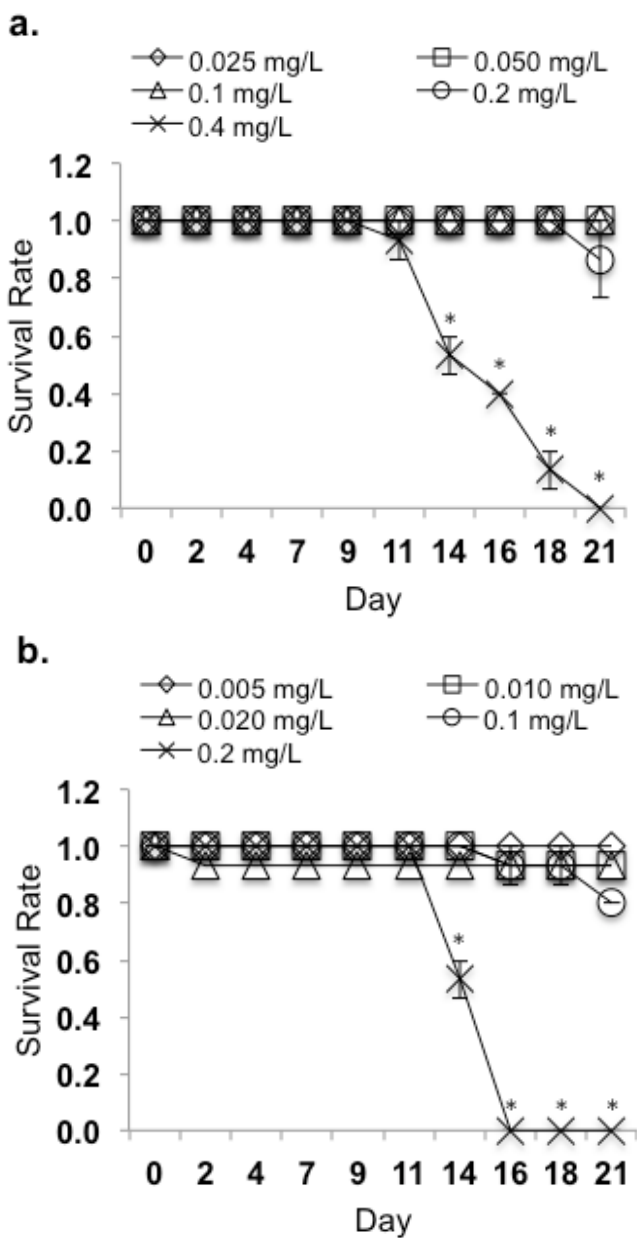
Average chronic daphnid reproduction over 21 days compared to controls.

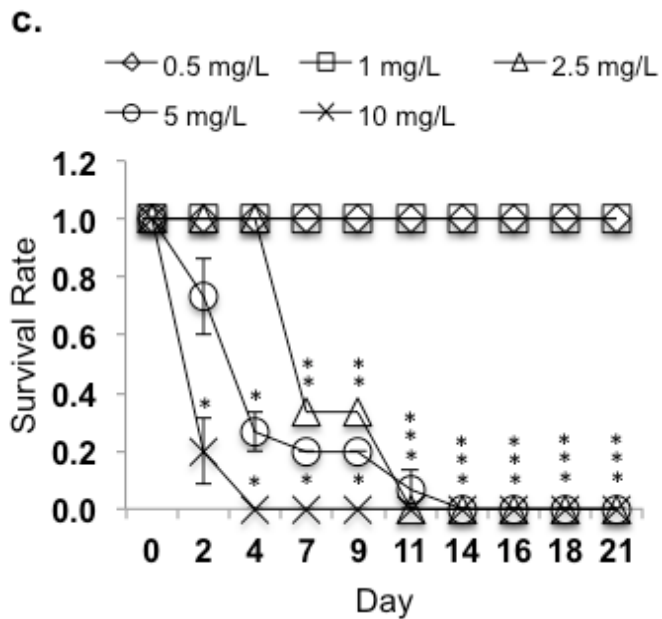
Percent control reproduction per individual (a) for lithium cobalt oxide (LCO)

nanoparticles and (b) for lithium nickel manganese cobalt oxide (NMC) nanoparticles.

Error bars represent standard error of the mean, $n \geq 4$. Asterisks indicate significance compared to control ($p < 0.05$).

Figure 4

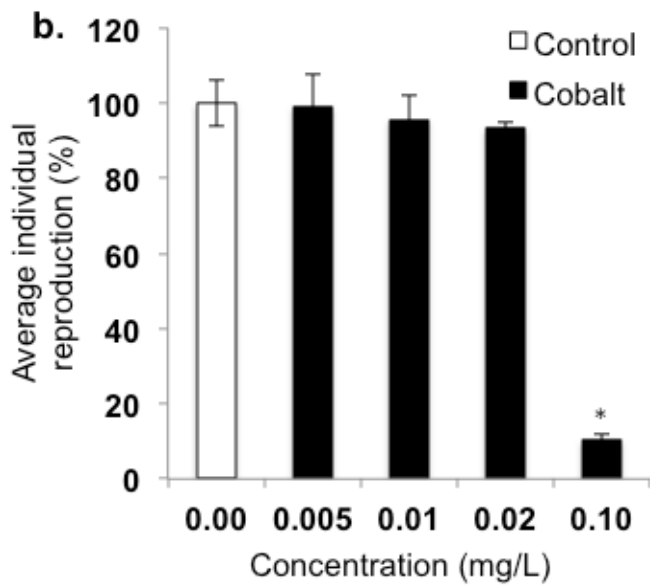
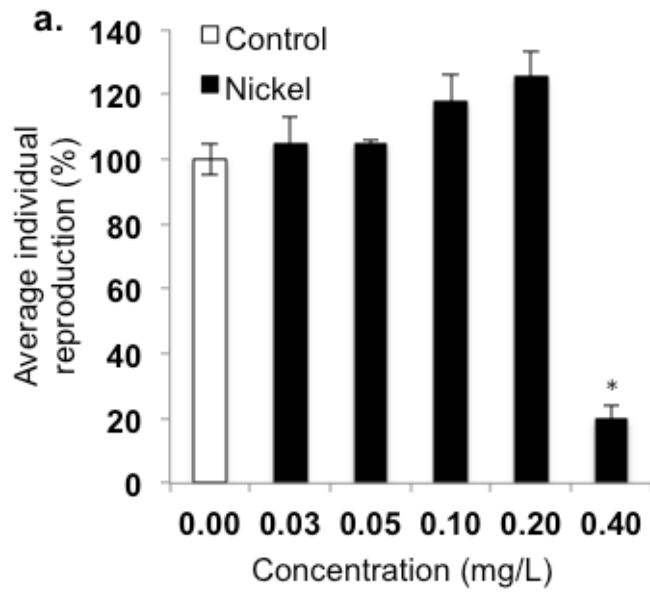


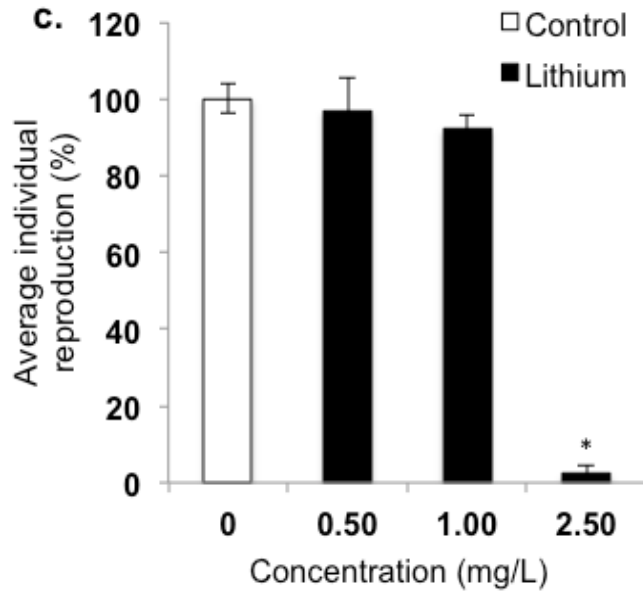


Average chronic daphnid survival rate over 21 days compared to controls.

Average survival rate for (a) nickel, (b) cobalt and (c) lithium. Error bars represent standard error of the mean, $n = 3$. Asterisks indicate significance compared to control ($p < 0.05$).

Figure 5





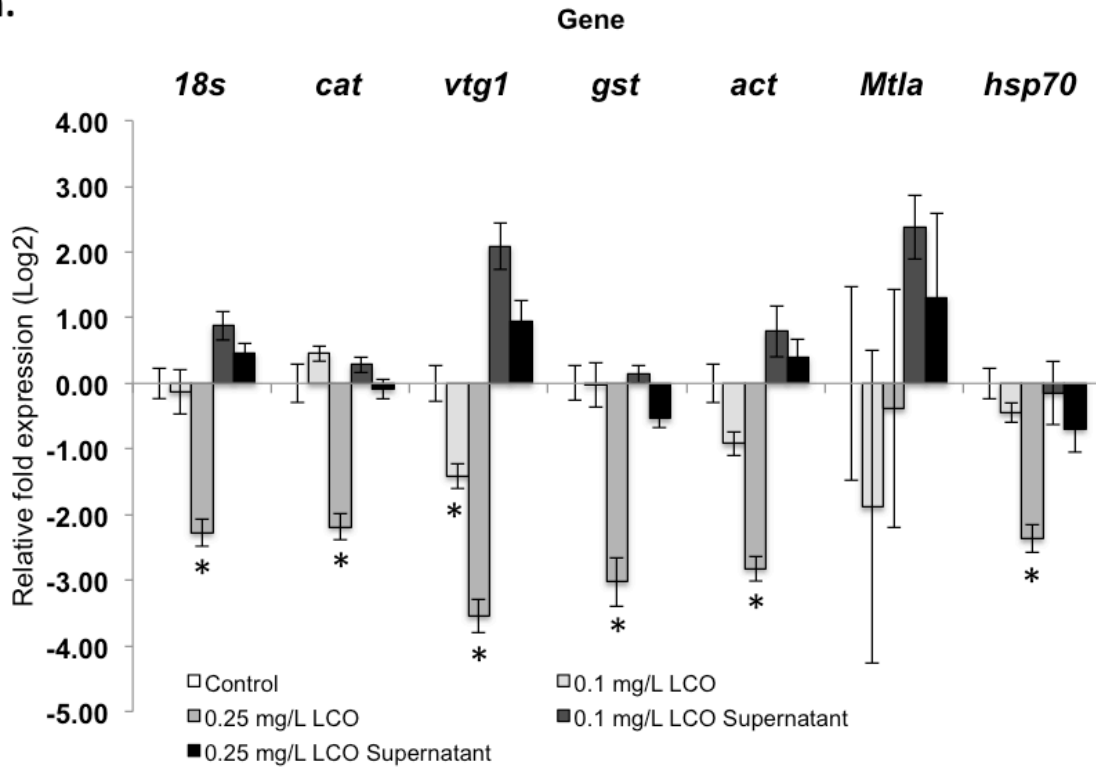
Average chronic daphnid reproduction over 21 days compared to controls.

Percent control reproduction per individual for (a) nickel, (b) for cobalt and (c) lithium.

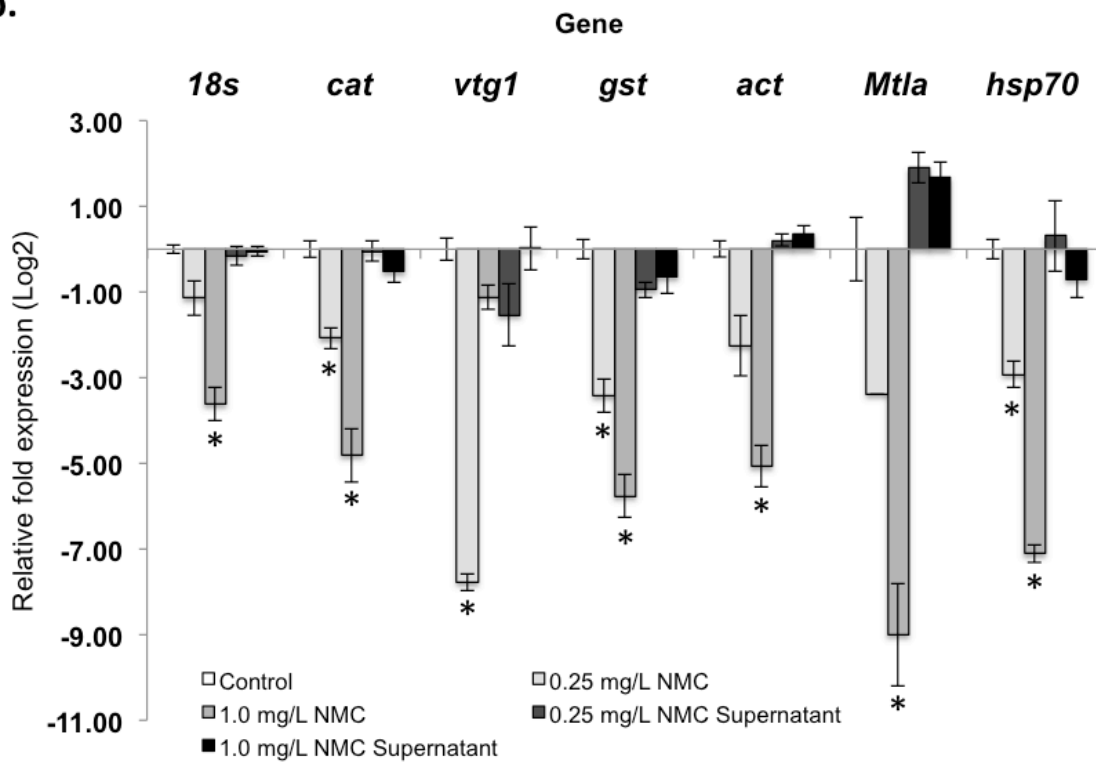
Error bars represent standard error of the mean, $n = 3$. Asterisks indicate significance compared to control ($p < 0.05$).

Figure 6

a.



b.



Fold change gene expression. Average daphnid relative fold change gene expression (Log_2) at day 21 compared to controls. Average Gene expression for (a) lithium cobalt oxide (LCO) nanoparticles and supernatant and (b) lithium nickel manganese cobalt oxide (NMC) nanoparticles and supernatant. Error bars represent standard error of the mean, $n \geq 4$. Asterisks indicate significance compared to control ($p < 0.05$).

CHAPTER 4 SUPPORTING INFORMATION

Core chemistry influences the toxicity of multi-component metal oxide nanomaterials, lithium nickel manganese cobalt oxide and lithium cobalt oxide to *Daphnia magna*

Number of supporting information pages: 6

Number of Figures: 5

Number of Tables: 1

Table S1

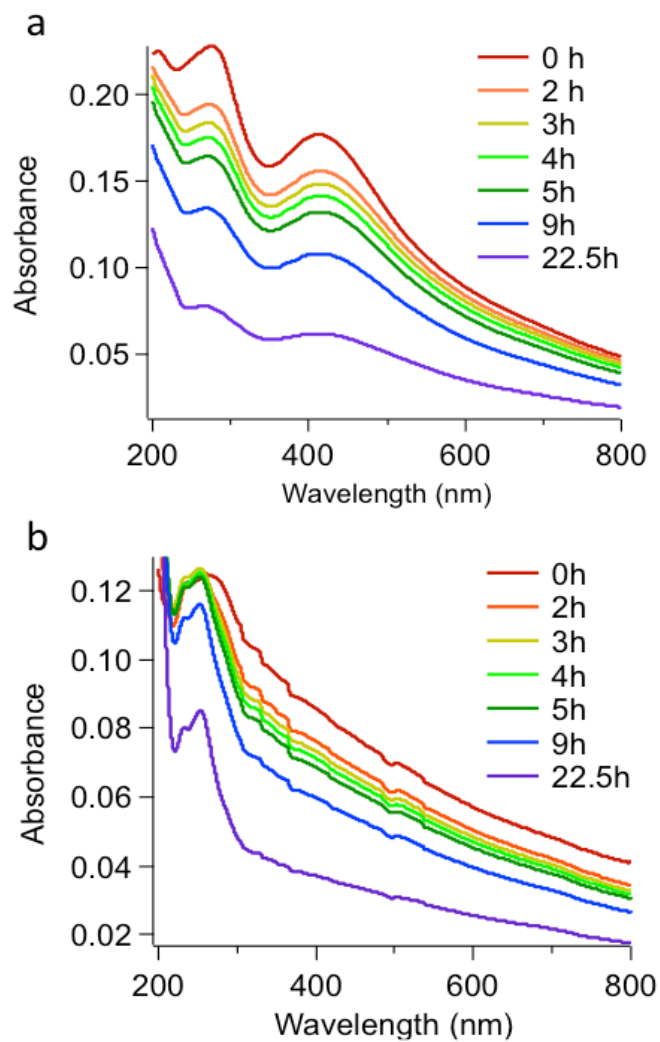
Treatment	Gene	Average Fold Change	SE	F Score	df	P value
LCO 0.1 mg/L						
	<i>18s</i>	-0.13	0.34	19.77	23	p > 0.05
	<i>cat</i>	0.45	0.11	15.37	23	p > 0.05
	<i>vtg1</i>	-1.41	0.19	44.62	23	p < 0.05
	<i>gst</i>	-0.02	0.34	19.05	23	p > 0.05
	<i>act</i>	-0.92	0.18	19.64	23	p > 0.05
	<i>mtla</i>	-1.89	2.38	0.81	23	p > 0.05
	<i>hsp70</i>	-0.44	0.46	12.32	23	p > 0.05
LCO Supernatant 0.1 mg/L						
	<i>18s</i>	0.88	0.22	19.77	23	p > 0.05
	<i>cat</i>	0.28	0.12	15.37	23	p > 0.05
	<i>vtg1</i>	2.09	0.35	44.62	23	p < 0.05
	<i>gst</i>	0.14	0.14	19.05	23	p > 0.05
	<i>act</i>	0.80	0.39	19.64	23	p > 0.05
	<i>mtla</i>	2.38	0.49	0.81	23	p > 0.05
	<i>hsp70</i>	-0.15	0.11	12.32	23	p > 0.05
LCO 0.25 mg/L						
	<i>18s</i>	-2.28	0.20	19.77	23	p < 0.05
	<i>cat</i>	-2.18	0.20	15.37	23	p < 0.05
	<i>vtg1</i>	-3.54	0.26	44.62	23	p < 0.05
	<i>gst</i>	-3.03	0.38	19.05	23	p < 0.05
	<i>act</i>	-2.82	0.19	19.64	23	p < 0.05
	<i>mtla</i>	-0.39	1.81	0.81	23	p > 0.05
	<i>hsp70</i>	-2.37	0.21	12.32	23	p < 0.05
LCO Supernatant 0.25 mg/L						
	<i>18s</i>	0.46	0.15	19.77	23	p > 0.05
	<i>cat</i>	-0.09	0.14	15.37	23	p > 0.05
	<i>vtg1</i>	0.94	0.33	44.62	23	p > 0.05
	<i>gst</i>	-0.54	0.14	19.05	23	p > 0.05
	<i>act</i>	0.40	0.27	19.64	23	p > 0.05
	<i>mtla</i>	1.31	1.28	0.81	23	p > 0.05
	<i>hsp70</i>	-0.70	0.07	12.32	23	p > 0.05

NMC 0.25 mg/L						
<i>18s</i>	-1.14	0.41	40.61	27	p < 0.05	
<i>cat</i>	-2.08	0.26	38.97	27	p < 0.05	
<i>vtg1</i>	-7.78	0.20	54.14	27	p < 0.05	
<i>gst</i>	-3.43	0.39	47.22	27	p < 0.05	
<i>act</i>	-2.26	0.70	40.94	27	p > 0.05	
<i>mtla</i>	-3.39	N/A	23.71	23	p > 0.05	
<i>hsp70</i>	-2.92	0.39	105.43	27	p < 0.05	
NMC Supernatant 0.25 mg/L						
<i>18s</i>	-0.16	0.22	40.61	27	p > 0.05	
<i>cat</i>	-0.05	0.23	38.97	27	p > 0.05	
<i>vtg1</i>	-1.54	0.73	54.14	27	p > 0.05	
<i>gst</i>	-0.95	0.18	47.22	27	p > 0.05	
<i>act</i>	0.21	0.13	40.94	27	p > 0.05	
<i>mtla</i>	1.90	0.36	23.71	23	p > 0.05	
<i>hsp70</i>	0.31	0.38	105.43	27	p > 0.05	
NMC 1.0 mg/L						
<i>18s</i>	-3.62	0.40	40.61	27	p < 0.05	
<i>cat</i>	-4.81	0.63	38.97	27	p < 0.05	
<i>vtg1</i>	-1.12	0.28	54.14	27	p > 0.05	
<i>gst</i>	-5.77	0.50	47.22	27	p < 0.05	
<i>act</i>	-5.07	0.49	40.94	27	p < 0.05	
<i>mtla</i>	-9.00	1.21	23.71	23	p < 0.05	
<i>hsp70</i>	-7.11	0.37	105.43	27	p < 0.05	
NMC Supernatant 1.0 mg/L						
<i>18s</i>	-0.06	0.12	40.61	27	p > 0.05	
<i>cat</i>	-0.52	0.25	38.97	27	p > 0.05	
<i>vtg1</i>	0.02	0.50	54.14	27	p > 0.05	
<i>gst</i>	-0.65	0.38	47.22	27	p > 0.05	
<i>act</i>	0.36	0.19	40.94	27	p > 0.05	
<i>mtla</i>	1.67	0.36	23.71	23	p > 0.05	
<i>hsp70</i>	-0.71	0.17	105.43	27	p > 0.05	

Table S1†. Chronic daphnid body size over 21 days compared to controls. Percent control body size per average individual exposed to lithium nickel manganese cobalt

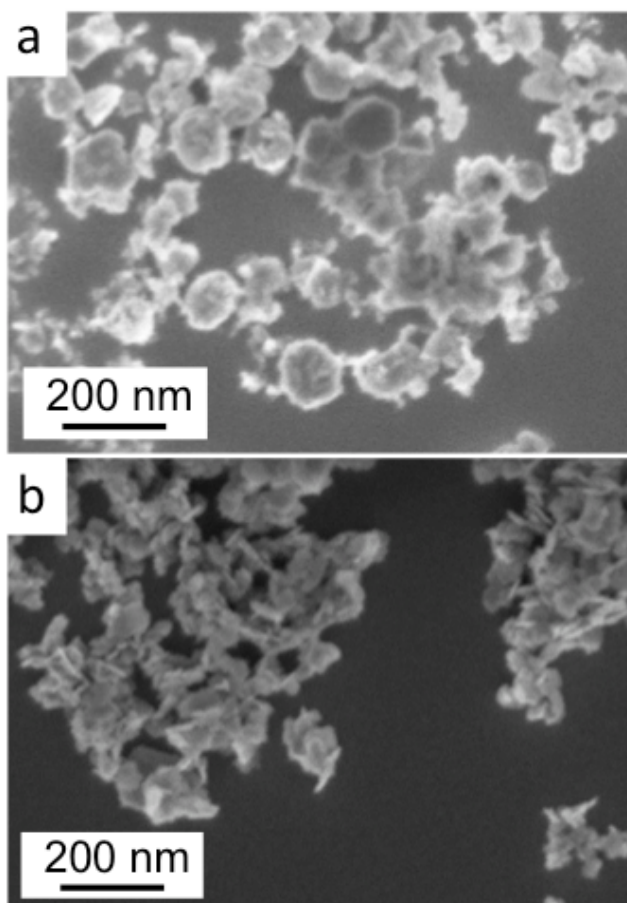
oxide (NMC) nanoparticles. Error bars represent standard error of the mean, $n \geq 4$. Asterisks indicated significance ($p < 0.05$).

Figure S1



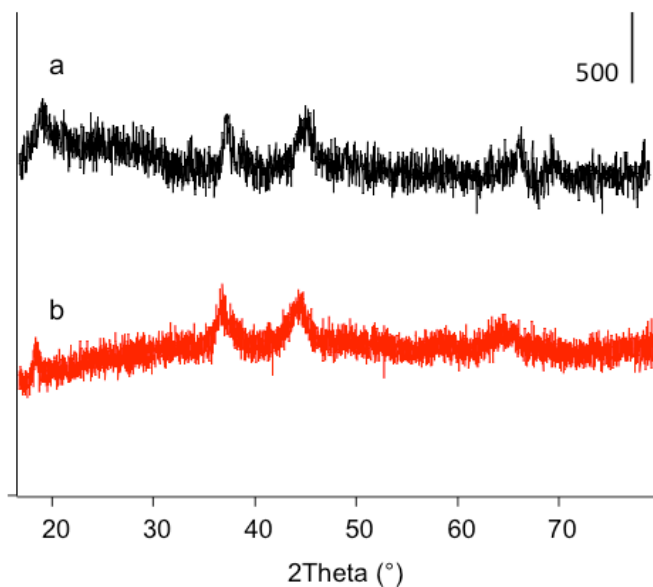
Analysis of colloidal stability of 10 mg/L a.) LCO and b.) NMC nanomaterials in daphnid growth medium over time using UV-vis spectroscopy of the water column.

Figure S2



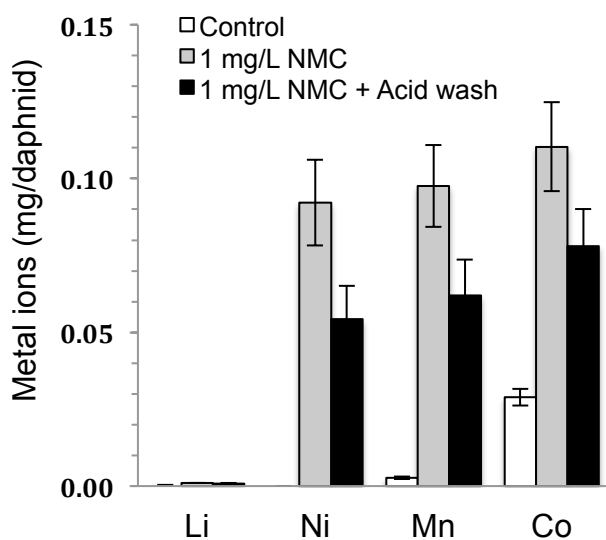
Scanning electron micrographs of a.) LCO and b.) NMC nanomaterials dropcasted onto silicon wafers.

Figure S3



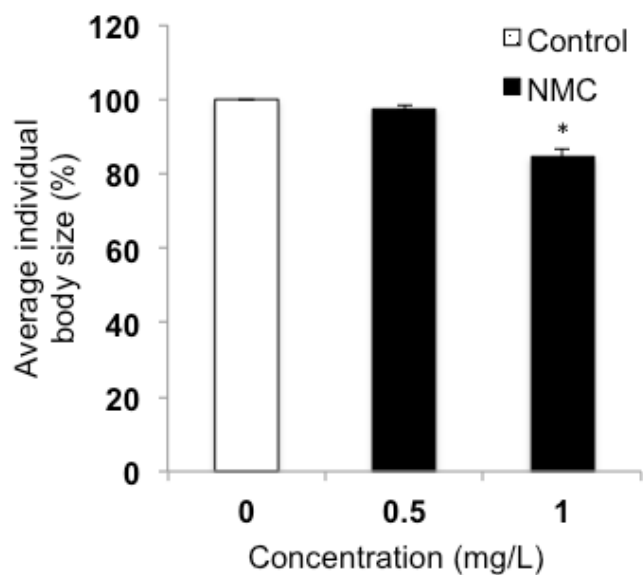
Powder X-ray diffraction patterns of a.) LCO and b.) NMC nanomaterials.

Figure S4



Daphnid body burden assay. ICP results from daphnids exposed to lithium nickel manganese cobalt oxide (NMC) nanomaterials or NMC and an acid wash.

Figure S5



Chronic daphnid body size over 21 days compared to controls. Percent control body size per average individual exposed to lithium nickel manganese cobalt oxide (NMC) nanoparticles. Error bars represent standard error of the mean, $n \geq 4$. Asterisks indicated significance ($p < 0.05$).

Chapter 5 DISCUSSION AND CONCLUSIONS

The goal of this work was to add to our baseline understanding for NM toxicity by addressing the needs of key areas in nanotoxicology. In order to achieve this goal I asked three main questions based on the knowledge gaps I identified in the literature: 1) How do variations in NM surface charge and ligand chemistry alter NM toxicity to *Daphnia*? 2) How does the molecular response differ when an organism is exposed to NMs with different surface properties? and 3) Can altering the core chemical composition of a NM alleviate impacts to molecular and apical endpoints in *Daphnia*? In addressing these three main questions I was able to provide data, which indicate that not only the charge of the NM but the component that imparts the charge is important for determining toxicity. My studies show that NMs can have nanospecific impacts resulting in cellular changes and acute and chronic impacts. In addition, I demonstrated that NMs could be altered to have reduced toxicity. This research also highlighted the importance of controlling for experimental artifacts and confounding factors in nanotoxicology assays that impede our ability to identify nanospecific impacts.

How do variations in nanomaterial surface charge and ligand chemistry alter nanomaterial toxicity?

The results from chapter two of this dissertation indicated that charge and the ligand type used in NM functionalization both impact NM toxicity and should be taken into consideration when developing predictive models. My study showed that positively charged NMs are more toxic than negatively charged particles¹⁻⁵. In my study,

positively charged PAH-AuNPs were found to cause impacts to daphnid reproduction and survival at low part per billion concentrations, compared to the negatively charged particles which showed no impacts at concentrations orders of magnitude higher.

My results indicate that the ligand used in NM functionalization itself might be toxic and that this may explain some of the observed effects in NM toxicity assays. For CTAB-AuNPs, CTAB the ligand itself was shown to be just as detrimental to daphnid survival as the ligand-NM combination. My study was contradictory to others in that I was unable to observe greater NM ingestion/accumulation of positively charged NMs than negatively charged NMs^{1, 6, 7}. However, I did not specifically investigate cellular uptake, which is what most studies report. Based on this finding I concluded that total particle accumulation does not explain the greater toxicity of the positively charged AuNPs. The differences in density of charge in the various NM-ligand combinations may also play a role in toxicity. After measuring charge density it was determined not to be a significant effect. This leads us to believe that the positively charged AuNPs as a whole are inherently more toxic.

Historically, positively charged chemicals have shown greater potential for biological impact as they have an increased affinity towards negatively charged biological surfaces⁸. Others have shown specifically that positively charged particles to be toxic to cells, invertebrates and fish^{1, 9, 10}. Studies also have shown different mechanisms for positively charged particles to induce toxicity than negatively charged particles¹¹. For example, cellular exposure to positively charged particles indicated membrane disruption while exposure to anionic charged particle induced intracellular damage and apoptosis¹¹. The increased affinity of positively charged particles may

lead to a greater interaction with the negatively charged membranes of cells and therefore may explain the greater impact of positively charged AuNPs. However, these studies did not incorporate the necessary controls making it difficult to understand if the observed effects were nanospecific or just due to the ligand alone.

Aggregation may also have played a role in toxicity. When NMs aggregate their size may dramatically increase therefore reducing the number of potential mechanisms for cellular uptake and toxicity¹². Smaller sized NMs have greater surface area and may also have a greater ability to pass through the peritrophic membrane of *Daphnia*. The peritrophic membrane separates food particles from the gut mucosa and acts as a kind of dialyzer¹³. This membrane has been shown to be impermeable to latex beads with a diameter greater than 139 nm therefore preventing larger objects from interacting with daphnid gut epithelial cells¹³. While positively charged AuNPs were stable in daphnid media, negatively charged AuNPs, MPA and Cit-AuNPs, were not and aggregated rapidly, potentially reducing their bioavailability to *D. magna* and decreasing their toxicity.

My study demonstrated that the type of aggregation also might determine whether negatively charged particles impact daphnids or not. For example, Cit-AuNPs irreversibly formed extended fused networks of aggregates and shut down daphnid reproduction at 25 mg/L whereas MPA-AuNPs reversibly aggregated and did not impact daphnid reproduction at 25 mg/L. I also observed Cit-AuNPs forming algal/nano agglomerates in chronic exposures, adhering to daphnid carapaces. I hypothesize that this led to physical impairments of daphnids potentially increasing energy expenditure and blocking nutrient absorption in their digestive tract. For certain

NM types and NM-ligand combinations and depending on how they aggregate, physical effects could therefore play a major role in the observed impacts to organism apical endpoints.

Further validation of the trends I observed are required in order to make definitive decisions as to which surface properties are most important for NM toxicity. Understanding specific surface properties that dictate NM toxicity requires model NMs that span many different core types and have subtle alterations in their properties that enable the testing of specific hypotheses. While many *in vitro* studies show the effects of charge and altered surface properties to NM toxicity, few *in vivo* studies have done similar. In my study I showed the impacts of charge and ligand chemistry on toxicity to an environmentally relevant whole organism. The next step would be to test the impacts of altered charge density to toxicity by using ligands bound to chemically inert cores, such as gold or diamond, with differing functional groups. This would increase our ability to predict toxicity based on charge alone. Systematically testing how altered charge density impacts toxicity has been used to develop models to predict the aquatic toxicity of cationic polymers¹⁴. This has led to an increase in the efficiency of assessing the toxicity of this technologically important class of chemicals.

This study demonstrates the difficulties of testing even model systems as factors such as aggregation are dependent on the surface chemistry of the NM in question and may lead to physical effects which are not considered to be part of the intrinsic toxicity of a chemical. In addition, increased aggregation may reduce organism exposure making it difficult to make direct comparisons. Taking these factors into consideration as conclusions are drawn will increase our ability to predict NM

toxicity solely on their physiochemical properties. This study and studies alike are crucial for closing the knowledge gap that exists in nanotoxicology and informing the NM design process for the development of sustainable nanotechnologies.

How do the molecular responses differ when an organism is exposed to NMs with different surface properties?

Chapter three of this dissertation revealed the distinct gene expression response when *D. magna* is exposed to different charged AuNPs and their respective free ligands over acute and chronic time points. Very little information exists in regards to the short term and long term *in vivo* impacts of functionalized NMs and whole organism response at the gene expression level¹⁵. When I compared the organism gene expression response when exposed to one MPA-AuNPs vs. PAH-AuNPs, the gene expression response for the majority of the genes I investigated was opposite (i.e. when one particle up regulated gene expression the other down regulated gene expression and were found to be significantly different from one another). Gene expression has been shown to reveal unique molecular fingerprints for NMs with different surface properties but similar core materials^{16, 17}. In my study, it took much larger concentrations to get any result of negatively charged particles, which is notable. In addition, as previously mentioned, MPA-AuNPs aggregated whereas PAH-AuNPs did not. Therefore the different expression patterns may be due to the difference in concentration, surface charge, their aggregation or the actual chemistry of the ligand-NM combination. Studies such as the one presented in this dissertation

are few and further information is needed to determine if the trends in the molecular response NMs provoke can be validated across many different NM types.

Nanospecific impacts to *Daphnia* gene expression were observed in this study. However, for the most part for the genes I studied, the ligand used in NM functionalization and the ligand-NM combination had a similar pattern of gene expression. The relative expression of *actin*, a gene encoding for protein filaments important to cytoskeleton production and cellular organelle motility, was significantly up regulated when daphnids were exposed to PAH-AuNPs but not the PAH ligand alone. Others have described a high ability for microparticles to bind actin filaments and demonstrate the damages NMs can elicit on actin filaments *in vitro*¹⁸. Others have reported NM induced damage to actin filaments^{19, 20}. This was the only treatment that increased the expression of this gene. Further research is warranted to determine if this cellular response is common across organisms exposed to AuNPs and to determine if NM-actin protein binding is a mechanism for cellular toxicity. Many other genes triggered by the ligand-NM combination were also triggered to a similar extent by the ligand alone. This may indicate potential opportunities to describe organism molecular response based on the ligand alone, however unique findings only triggered by the ligand-NM combination may downplay our ability to do this.

This research demonstrated that sub-lethal concentrations of positively and negatively charged AuNPs do not induce oxidative stress related pathways. The primary proposed mechanism for NM toxicity is oxidative stress. A previous study exploring the impact of positively and negatively charged AuNPs to the cells of the digestive tract of *D. magna* showed induction of oxidative stress related pathways with

exposure to positively charged particles²¹. In this study the whole organism gene expression response to functionalized AuNPs did not induce oxidative stress related pathways. It may be that oxidative stress is localized at the primary site of NM interaction within the organism and that harvesting the total RNA from the whole organism decreases my ability to detect the changes in oxidative stress related transcripts in the cells most likely to be exposed to NMs. In addition, it could be related to time as my exposures lasted 48 hours or 21 days and the aforementioned study assessed impacts after 24 hours.

In order to fully understand modes of action and mechanisms for NM toxicity, molecular level studies need to be linked to impacts on environmentally relevant endpoints. Studies thus far have primarily focused on oxidative stress related pathways; pathways that may not always be indicative of organism fitness or of potential for disruptions in organism populations. My study examined several other pathways besides oxidative stress, such as reproductive, cell maintenance and proteotoxic stress related pathways. My study demonstrated that it is possible to identify nanospecific induced organism gene expression responses. In addition, I was able to determine general trends in organism response to NM properties. While this study was informative, future studies are needed that address issues such as NM dose-response relationship with endpoints and molecular changes, issues of comparing aggregated systems to unaggregated systems and studies are needed that expand on the number of genes and pathways we investigate coupled with environmentally relevant endpoint impacts. Expanding on this understanding, exploring the molecular changes of organisms exposed to multiple well-tailored

hypothesis driven NMs will enable us to develop a suite of biomarkers that are important in predicting NM impacts based on their surface properties. Traditional biomarkers and novel biomarkers of toxicity for NMs may then be used in the development of high throughput screening assays and models that inform NM design.

Can altering the core chemical composition of multicomponent metal nanomaterials reduce impacts to molecular and apical endpoints?

In chapter four of this dissertation I determined nanospecific impacts caused by NMs and concluded that specific alterations in the chemical composition of multicomponent metal oxide NMs alleviates toxic impacts to *Daphnia* apical endpoints. In this study, I systematically identified the toxicity of two next generation battery materials, LCO and NMC, by assessing the toxicity of the individual ionic metal components and the dissolved metals in suspension. LCO and NMC are composed of lithium and cobalt and lithium, nickel, manganese and cobalt, respectively. The structure of NMC is 33% cobalt while the structure of LCO is 100% cobalt. Out of the ionic metals I tested, I determined cobalt to be the most toxic, potentially explaining the increase in toxicity observed for LCO NMs. After chronic exposure, LCO NMs impacted daphnid reproduction and survival to an equal extent as NMC but at concentrations four times lower. Dissolution studies revealed more cobalt dissolution occurred from LCO than NMC. Based on the dissolution of these materials in my media I determined that the metal levels in the background NM suspension could not explain the observed effects. Similarly the supernatant controls from NM suspensions that contained the mixture of dissolved metals could not account for the impacts to

daphnid reproduction and survival. Therefore I conclude that the effects I observed were specific to the NM. However, it is difficult to rule out whether NM dissolution at the contact site is the cause for toxicity as the particles adhered to the daphnid carapace and accumulated in the digestive tract, which potentially delivered a localized high concentration of dissolved metals.

Gene expression response of daphnids exposed to LCO or NMC materials showed significant down regulation of a suite of genes in a dose-dependent manner and could not be explained by the dissolved metals in solution which further supported my conclusion that LCO and NMC cause nanospecific effects. Daphnids exposed to LCO or NMC supernatants showed no significant changes in the expression of the genes I explored while LCO and NMC exposed daphnids showed significantly down regulated genes involved in cell maintenance, metal toxicity attenuation, reproduction, and oxidative stress. The impact to daphnid gene expression was reduced when daphnids were exposed to concentrations of LCO and NMC that caused no impacts to daphnid survival and reproduction. Interestingly, 18s rRNA was significantly down regulated for both treatments in a dose-dependent manner which could lead to impairment of protein production, as ribosomes are composed of complexes of RNAs. Expression of actin was also down regulated at concentrations that caused impacts to daphnid apical endpoints similar to my previous study with AuNPs. Overall the down regulation associated with these transcripts may indicate cellular damage when daphnids were exposed to these materials at high concentrations and might indicate impairment of metabolic functions. I hypothesize that cellular degeneration is occurring

in the gut epithelial cells of daphnids as has been observed with the hepatic caeca by previous studies upon examining daphnids exposed to toxic metallic compounds¹³.

This research demonstrates the ability to mitigate the toxicity of complex technologically relevant NMs by altering the NM core chemical structure through chemical substitution. Based on the literature, my hypothesis was proven correct in that replacing toxic metals with more benign metals in the core structure could reduce the toxicity of these materials. However, I was wrong when I assumed the up regulation of genes involved in metal detoxification and oxidative stress attenuation. More studies are needed in order to influence the design of technologically relevant materials to enable these considerations ahead of the production cycle. Previous studies have focused on simple metal oxides, which were justified by the use and demand for these materials in commercial applications and the ease of studying the simple nature of their chemical structures. As industry shifts from simple metal oxides to complex multicomponent metal oxides for use in additional applications and improved performance, we must shift our assessment of nanotoxicology to these more complex materials. Previously it was thought that dissolution of metals into the background solution dominated the toxicity of metallic NMs. My study demonstrates that a greater understanding is needed, as I have defined effects that are specific to the metallic NM itself and cannot be explained by the dissolved metals in solution. While the gene expression pattern I observed does not identify a clear mechanism for toxicity or mode of action, I believe it is possible to further elucidate the mechanism of toxicity of these materials by coupling this study with investigations using histological

approaches and better understanding the accumulation of these materials and their free metals in daphnid cells.

Future directions

At the moment, each NM has to be tested individually, which emphasizes the need to develop new and refine old approaches used to determine NM toxicity. It will be a tremendous undertaking to assess each NM type and their modifications as new NMs are incorporated into the market place; this would result in the testing of potentially tens of thousands of unique NMs. However, an alternative to assessing NMs individually would be through the use of a grouping approach. In this approach, biological effects would be assigned to NM physiochemical properties and then decisions based on those properties would be made. For example, decisions can be made on whether or not to continue more detailed testing based on measured or anticipated effects. While the nanotoxicology community has been working towards this goal, not one specific property has been identified as the best predictor for NM toxicity; rather several properties have been shown to be important and it may be that a combination is used for predicting toxicity. Proposed properties to be used for grouping include but are not limited to: surface chemistry, reactivity, size, shape, crystalline phase, core material, and solubility. Therefore, continuing to link properties to adverse outcomes would enhance our ability to group NMs and identify which NMs need detailed toxicity testing.

In order to better enable grouping and validate properties considered to be important, we need to begin testing more complex NMs that are representative of NMs

from the future nanotechnology marketplace. Nanomaterials today are becoming more diverse as we move from bare NMs and simple metal oxides to surface functionalized NMs and complex multicomponent metal oxides. Nanotoxicology studies have largely focused on testing commercially available and simple metal NMs, metal oxides and carbon NMs. The knowledge we have been able to obtain from past studies has been critical for enabling a better understanding of the impacts of NM size, core chemistry and dissolution to toxicity. While the study of these materials have been justified by their wide scale use and applications, these NMs do not reflect the complexity of emerging materials used in nanotechnologies. As previously mentioned, it is impossible to test all NM types and modifications. In order to develop a fundamental understanding of the properties that govern the toxicity of next generation NMs there is a need for studies that employ model NMs with fine scale alterations to their surface and core properties to test scientific hypotheses regarding NM toxicity. Testing hypothesis driven model NMs such as the materials presented in this dissertation and NMs with subtle alterations to their core structures, surface charge density, hydrophobicity or ligand composition will greatly improve our fundamental understanding of baseline factors for toxicity and will inform NM grouping efforts.

In order to effectively determine the environmental impacts of nanotechnology studies are needed that explore the impact of environmental factors on NM toxicity. It has been shown that environmental variables such as natural organic matter and water chemistry alter NM dispersion, deterioration and transformation. Information that would describe these impacts on toxicity and their environmental fate and transportation would be invaluable for better understanding realistic exposures of

organisms to NMs in the environment. Characterizing the effects of NMs in environmentally relevant media will enable the identification of worst-case scenarios and mitigative factors for toxicity. This will better inform models that predict toxicity, which would then be able to predict toxicity in various environmental scenarios. This information would be combined with the hazard data and incorporated into the grouping process to increase the accuracy and precision of our predictions based on NM properties.

The majority of existing approaches to toxicity assessment have been largely focused on *in vitro* studies, which do not represent the complexities associated with whole organisms and often do not provide clear extrapolation of effects to whole organisms. In order to use these assays to predict and screen for environmentally relevant *in vivo* effects they need to be validated and refined to encompass the issues associated with testing NMs. Pairing these studies with environmentally relevant whole organism studies will greatly improve the applicability of these assays. In addition, coupling apical endpoint effects to impacts at the molecular, cellular and tissue level will enable us to link properties to mechanisms and modes of action for NM toxicity. This information based on early biological effects will be important in developing adverse outcome pathways, which may be used in part of the grouping process.

Lastly, taking into consideration lessons learned from previous nanotoxicology investigations such as controlling for experimental artifacts, confounding factors and the importance of NM characterization will increase our ability to make meaningful conclusions regarding NM toxicity. Investigating NMs in this scope will enable us to

employ reliable and robust data in high throughput assays, models and the NM design process to assess current and develop new sustainable technologies.

REFERENCES:

1. B. Collin, E. Oostveen, O. V. Tsyusko and J. M. Unrine, *Environmental science & technology*, 2014, **48**, 1280-1289.
2. S. Bhattacharjee, L. H. de Haan, N. M. Evers, X. Jiang, A. T. Marcelis, H. Zuilhof, I. M. Rietjens and G. M. Alink, *Part Fibre Toxicol*, 2010, **7**, 1.
3. W.-K. Oh, S. Kim, M. Choi, C. Kim, Y. S. Jeong, B.-R. Cho, J.-S. Hahn and J. Jang, *Acs Nano*, 2010, **4**, 5301-5313.
4. A. Gitipour, S. W. Thiel, K. G. Scheckel and T. Tolaymat, *Science of the Total Environment*, 2016, **557**, 363-368.
5. C. M. Goodman, C. D. McCusker, T. Yilmaz and V. M. Rotello, *Bioconjugate chemistry*, 2004, **15**, 897-900.
6. B. J. Marquis, Z. Liu, K. L. Braun and C. L. Haynes, *Analyst*, 2011, **136**, 3478-3486.
7. Y. Ge, Y. Zhang, J. Xia, M. Ma, S. He, F. Nie and N. Gu, *Colloids and Surfaces B: Biointerfaces*, 2009, **73**, 294-301.
8. M. S. Goodrich, L. H. Dulak, M. A. Friedman and J. J. Lech, *Environmental toxicology and chemistry*, 1991, **10**, 509-515.
9. Y. Qiu, Y. Liu, L. Wang, L. Xu, R. Bai, Y. Ji, X. Wu, Y. Zhao, Y. Li and C. Chen, *Biomaterials*, 2010, **31**, 7606-7619.
10. A. Asati, S. Santra, C. Kaittanis and J. M. Perez, *ACS nano*, 2010, **4**, 5321-5331.
11. A. Petushkov, J. Intra, J. B. Graham, S. C. Larsen and A. K. Salem, *Chemical research in toxicology*, 2009, **22**, 1359-1368.
12. E. Fröhlich, *Int J Nanomedicine*, 2012, **7**, 5577-5591.
13. N. N. Smirnov, *Physiology of the Cladocera*, Academic Press, 2013.
14. R. G. Clements, J. Nabholz and M. Zeeman, 1994.
15. R. Klaper, D. Arndt, J. Bozich and G. Dominguez, *Analyst*, 2014, **139**, 882-895.
16. L. Yang, G. Sundaresan, M. Sun, P. Jose, D. Hoffman, P. R. McDonagh, N. Lamichhane, C. S. Cutler, J. M. Perez and J. Zweit, *Journal of Materials Chemistry B*, 2013, **1**, 1421-1431.
17. Y. Zhang, H. Pan, P. Zhang, N. Gao, Y. Lin, Z. Luo, P. Li, C. Wang, L. Liu and D. Pang, *Nanoscale*, 2013, **5**, 5919-5929.
18. M. Ehrenberg and J. L. McGrath, *Acta biomaterialia*, 2005, **1**, 305-315.
19. P. Ruenraroengsak and A. T. Florence, *Journal of drug targeting*, 2010, **18**, 803-811.
20. V. G. Walker, Z. Li, T. Hulderman, D. Schwegler-Berry, M. L. Kashon and P. P. Simeonova, *Toxicology and applied pharmacology*, 2009, **236**, 319-328.
21. G. A. Dominguez, S. E. Lohse, M. D. Torelli, C. J. Murphy, R. J. Hamers, G. Orr and R. D. Klaper, *Aquat Toxicol*, 2015, **162**, 1-9.

CURRICULUM VITAE

Jared Bozich

Place of birth: Milwaukee, WI

Education

B.S., University of Wisconsin-Milwaukee, August 2012
Major: Conservation and Environmental Sciences

Dissertation Title: The Impact of Nanomaterial Functionalization and Core Chemical Composition on Toxicity to *Daphnia magna*

Publications:

J.S. Bozich, S. Bowman. 2015. Internet-Based Platforms for Science Communication. Integrated Environmental Assessment and Management: Learned Discourse. IEAM 11(3).

J.S. Bozich, T.A. Qiu, et al. 2015. Gene expression as an indicator of the molecular response and toxicity of the Gram-negative bacterium *Shewanella oneidensis* and the water flea *Daphnia magna* exposed to positively and negatively surface functionalized gold nanoparticles. *Environmental Science: Nano*.

J.S. Bozich, S.E. Lohse, M.D. Torelli, C.J. Murphy, R.J. Hamers, R.D. Klaper. 2014. Surface chemistry, charge and ligand type impact the toxicity of gold nanoparticles to *Daphnia magna*. *Environmental Science: Nano* 1:260-270.

R. Klaper, D. Arndt, **J. Bozich**, G. Dominguez. 2014. Molecular interactions of nanomaterials and organisms: defining biomarkers for toxicity and high-throughput screening using traditional and next-generation sequencing approaches. *Analyst* 139(5):882-95.